

Search for Muon to Electron Conversion in a Muonic Atom

Search for Muon to Electron Conversion in a Muonic Atom

Yoshitaka KUNO
RCNP, Osaka University
April 20th, 2024

Workshop on Muon Physics at the Intensity and Precision
Frontier (MIP2024)
PKU, Beijing, China



MIP 2024

Workshop on Muon Physics at the Intensity and Precision Frontiers

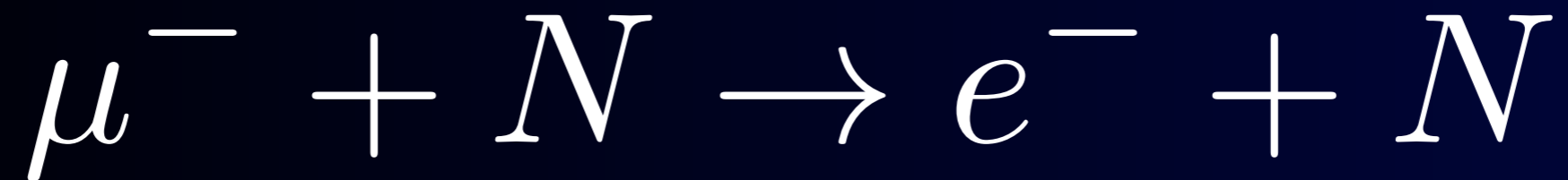
Apr 19–22, 2024 W301, School of Physics, PKU

Outline



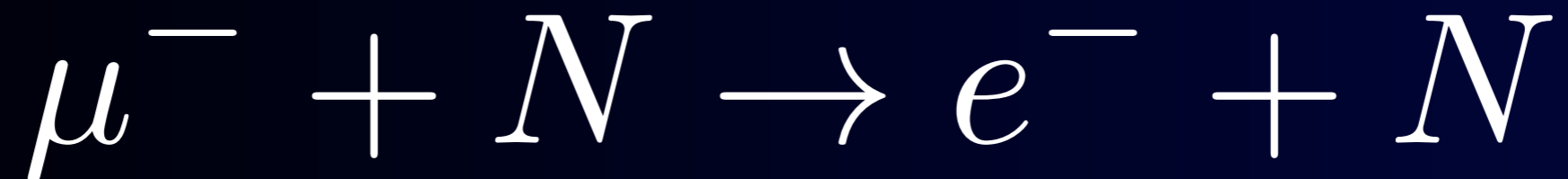
Outline

muon to electron conversion in a muonic atom



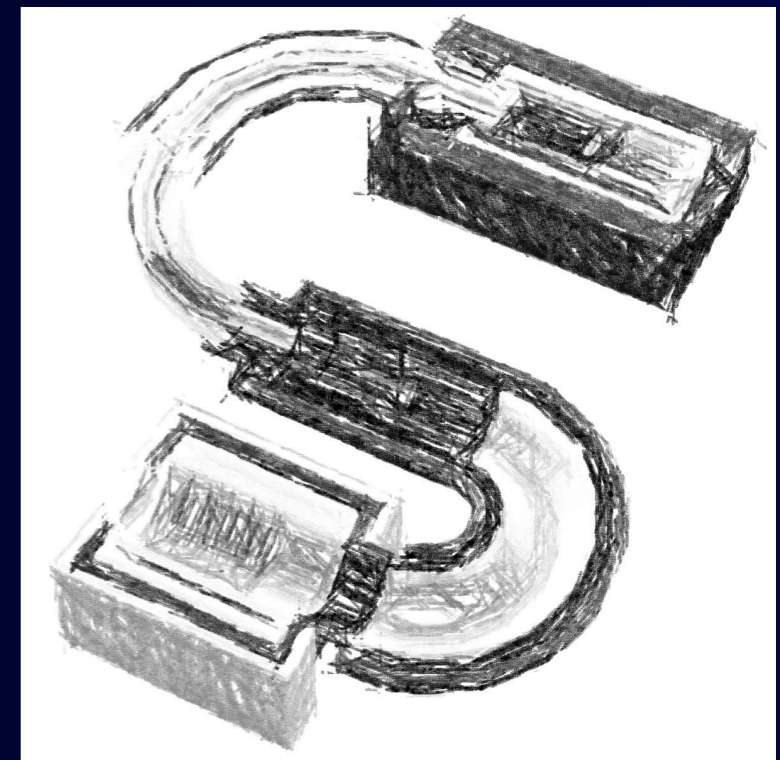
Charged Lepton Flavour Violation (CLFV)

muon to electron conversion in a muonic atom



Charged Lepton Flavour Violation (CLFV)

- Physics Motivation
- Recent Experimental Status (COMET)
- Related Rare Processes
- Future Prospects

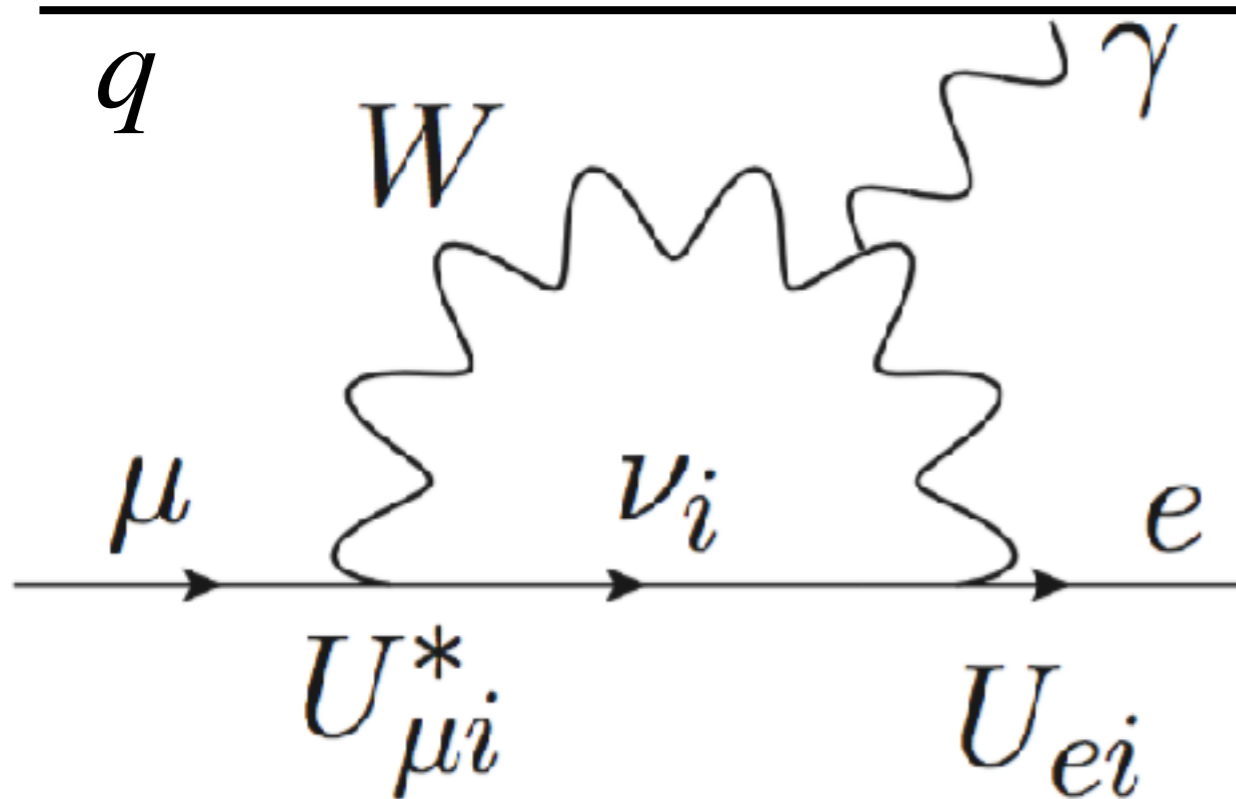


Physics and Phenomenology of Charged Lepton Flavour Violation (CLFV)



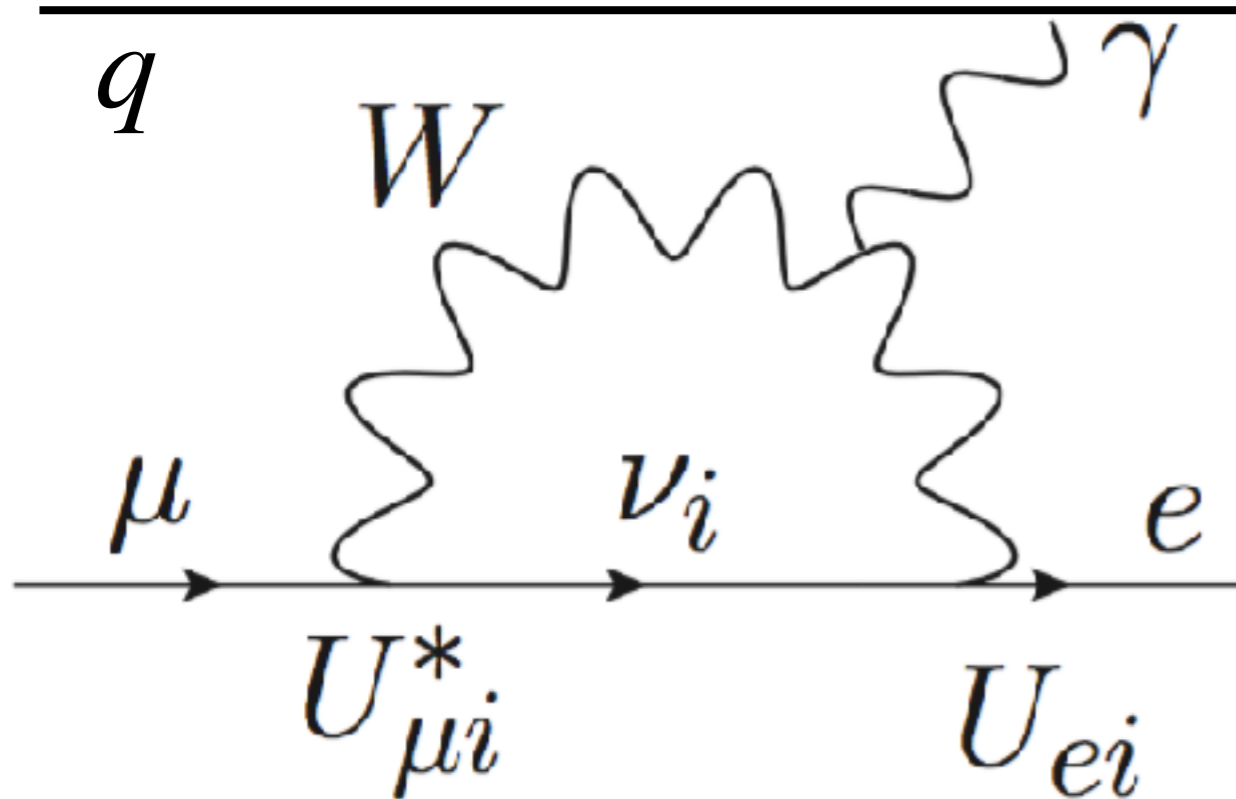
CLFV in the Standard Model (SM)

CLFV in the Standard Model (SM)



$$B(\mu \rightarrow e\gamma) = \frac{3\alpha}{32\pi} \left| \sum_{i=2,3} U_{\mu i}^* U_{ei} \frac{\Delta m_{1i}^2}{m_W^2} \right|^2$$

CLFV in the Standard Model (SM)



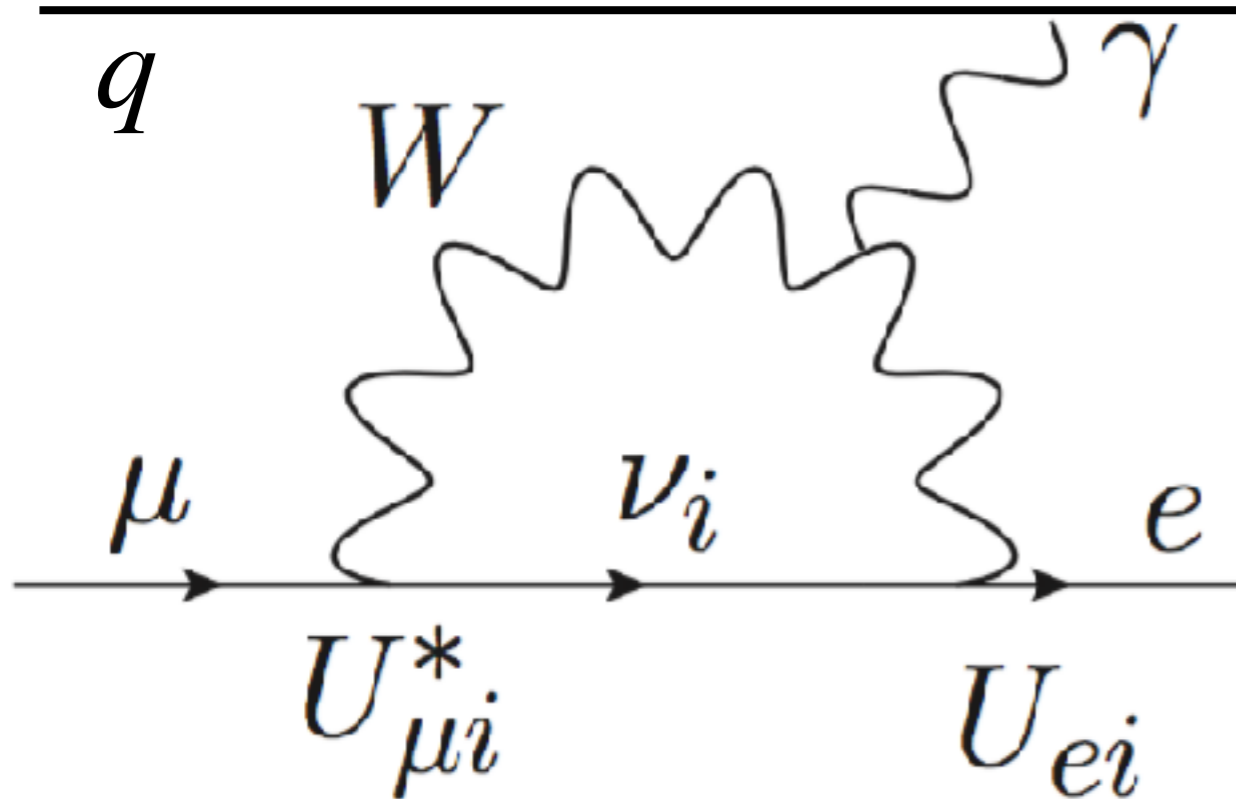
BR ~ O(10⁻⁵⁴)

$$\left(\left| \frac{\Delta m_\nu^2}{m_W^2} \right|^2 \rightarrow 10^{-50} \right)$$

$$B(\mu \rightarrow e\gamma) = \frac{3\alpha}{32\pi} \left| \sum_{i=2,3} U_{\mu i}^* U_{ei} \frac{\Delta m_{1i}^2}{m_W^2} \right|^2$$

S.T. Petcov, Sov.J. Nucl. Phys. 25 (1977) 340
 W.J. Marciano et al., Phys. Lett. B 67 (1977) 303
 B.W. Lee, et al., Phys. Rev. Lett. 38 (1977) 937
 B.W. Lee et al., Phys. Rev. D 16 (1977) 1444.

CLFV in the Standard Model (SM)



$$\text{BR} \sim \mathcal{O}(10^{-54})$$

$$\left(\left| \frac{\Delta m_\nu^2}{m_W^2} \right|^2 \rightarrow 10^{-50} \right)$$

$$B(\mu \rightarrow e\gamma) = \frac{3\alpha}{32\pi} \left| \sum_{i=2,3} U_{\mu i}^* U_{ei} \frac{\Delta m_{1i}^2}{m_W^2} \right|^2$$

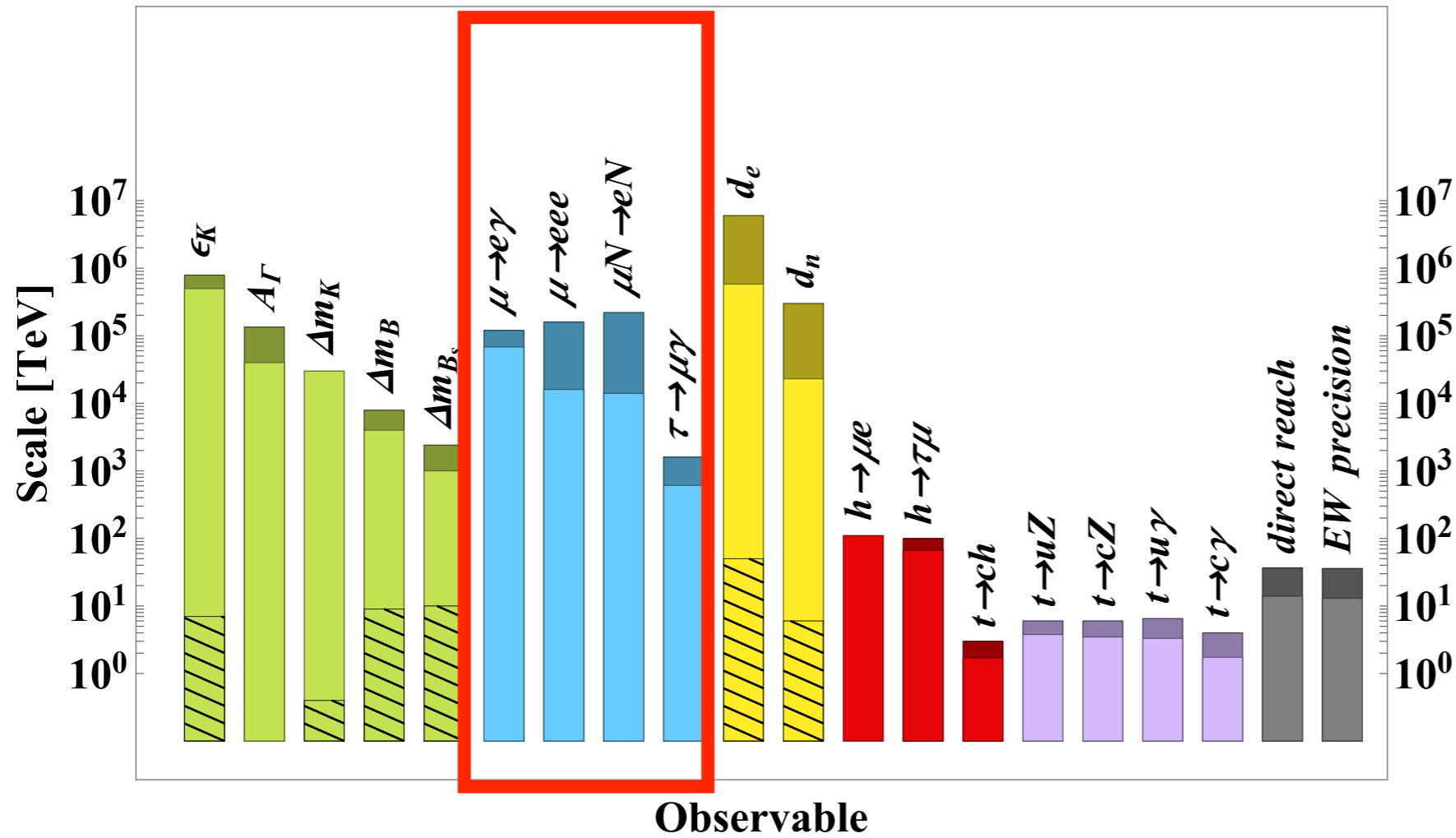
S.T. Petcov, Sov.J. Nucl. Phys. 25 (1977) 340
 W.J. Marciano et al., Phys. Lett. B 67 (1977) 303
 B.W. Lee, et al., Phys. Rev. Lett. 38 (1977) 937
 B.W. Lee et al., Phys. Rev. D 16 (1977) 1444.

1 CLFV has clear signature of BSM **w/o SM backgrounds.**



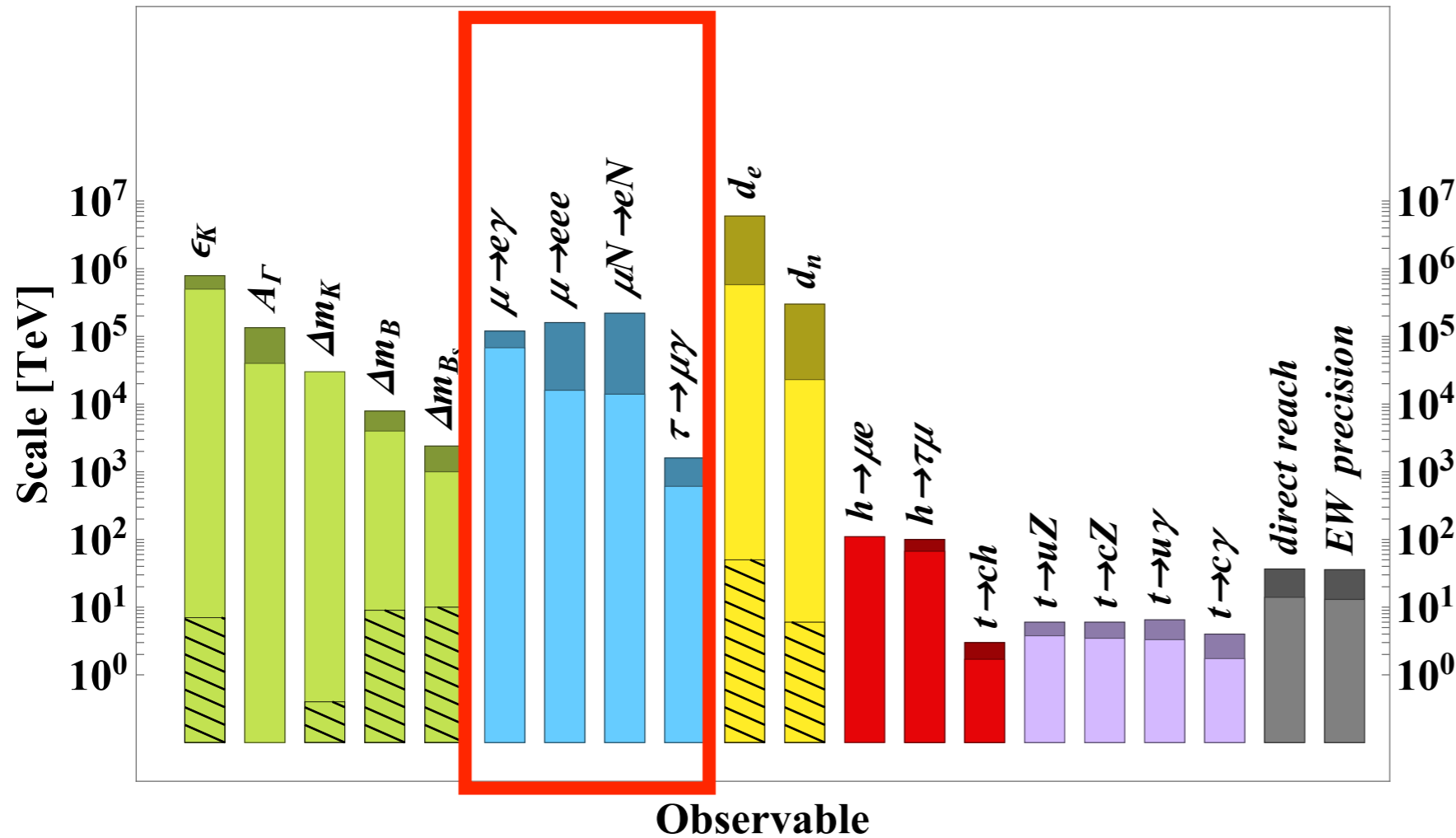
CLFV Sensitivity to BSM in EFT

CLFV Sensitivity to BSM in EFT



light colour: present, dark colour: future prospect
 from European particle Physics Strategy Update (2019)

CLFV Sensitivity to BSM in EFT



light colour: present, dark colour: future prospect
 from European particle Physics Strategy Update (2019)

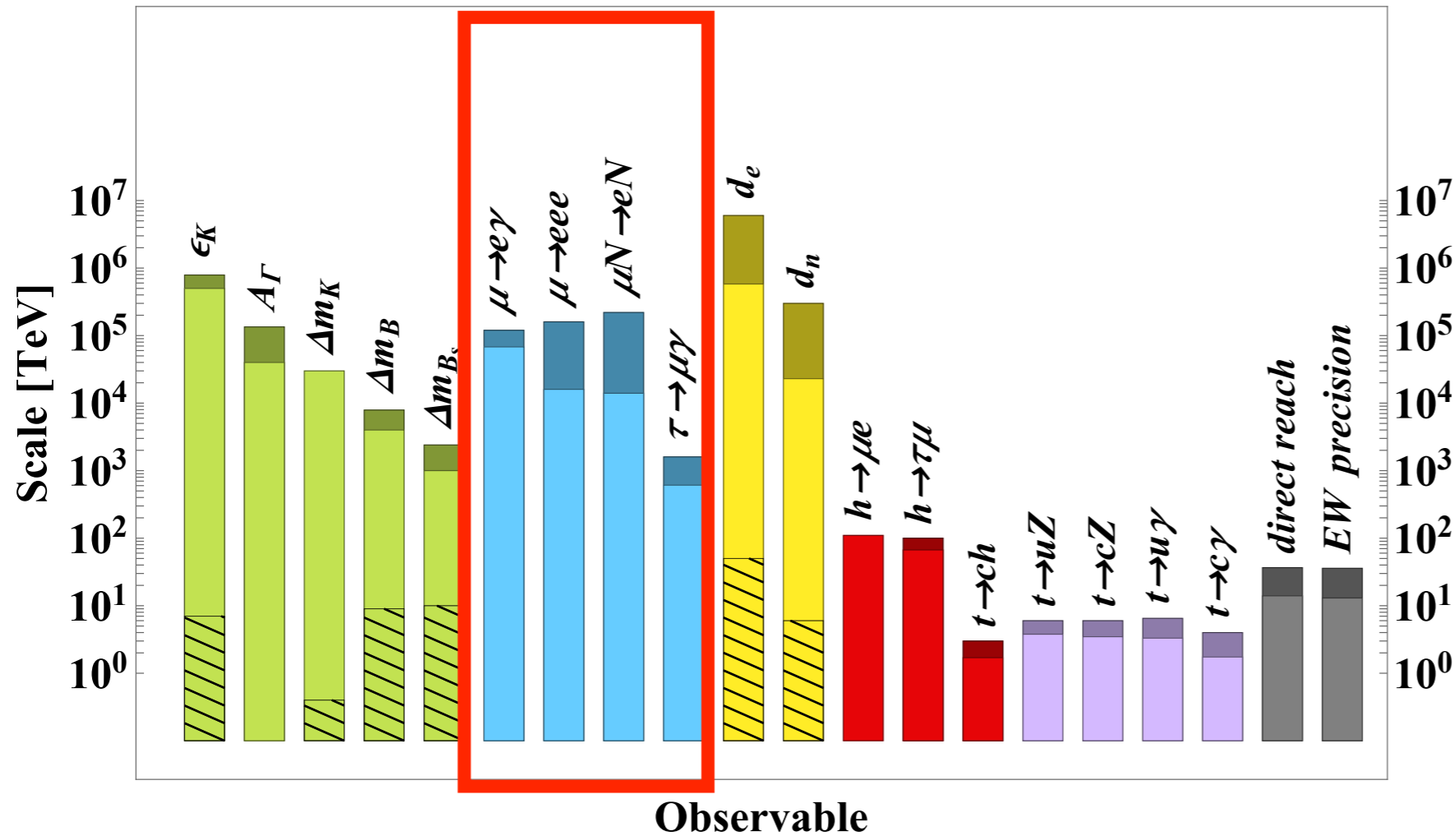
$$\mathcal{L}_{\text{CLFV}} \approx \frac{C}{\Lambda^2} O^{(6)}$$

dimension 6

$$\text{Rate} \propto \frac{C^2}{\Lambda^4}$$

10 times in $\Lambda \rightarrow$
 Experimental
 Improvements:
 aimed as $\times 10^4$

CLFV Sensitivity to BSM in EFT



light colour: present, dark colour: future prospect
 from European particle Physics Strategy Update (2019)

$$\mathcal{L}_{\text{CLFV}} \approx \frac{C}{\Lambda^2} O^{(6)}$$

dimension 6

$$\text{Rate} \propto \frac{C^2}{\Lambda^4}$$

10 times in $\Lambda \rightarrow$
 Experimental
 Improvements:
 aimed as $\times 10^4$

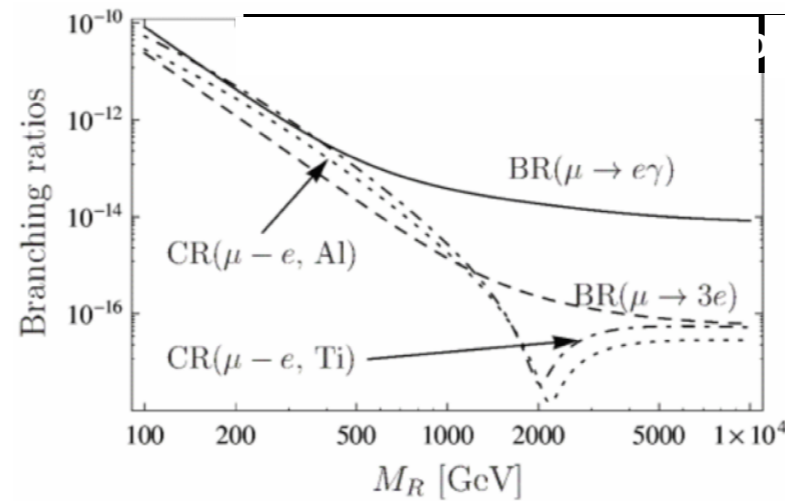


Model Dependent CLFV Predictions

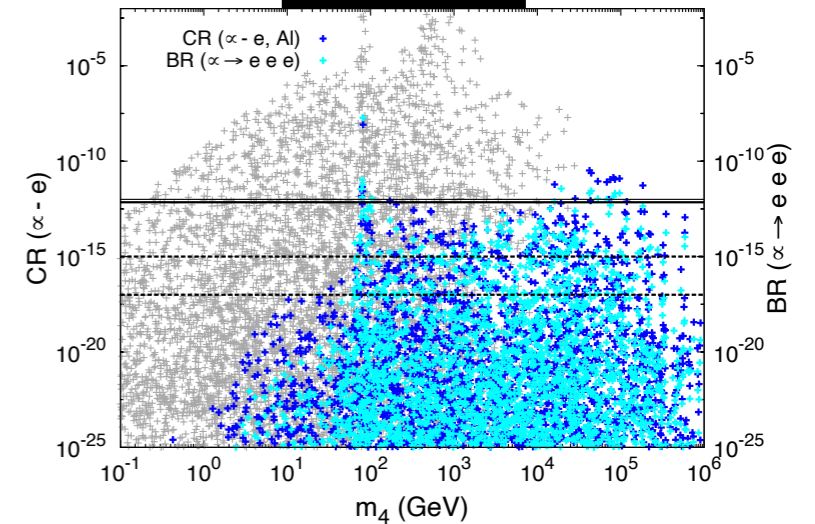
Model Dependent CLFV Predictions

only some examples

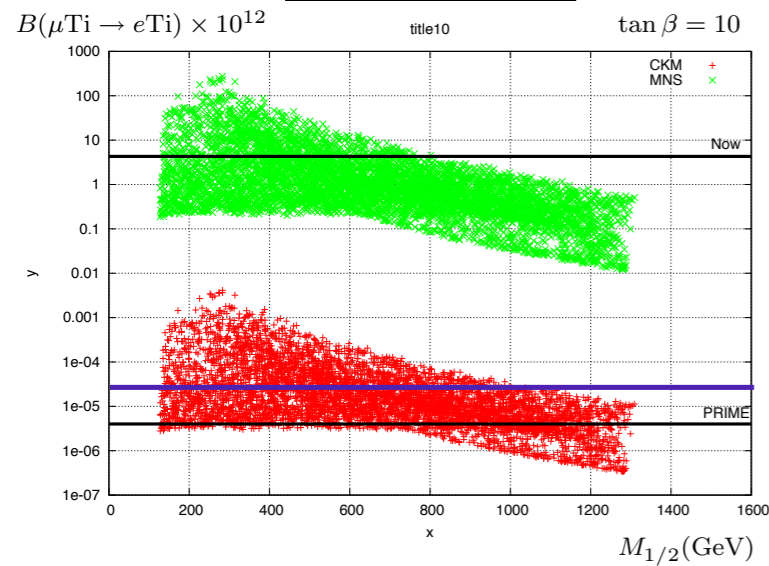
SUSY: Heavy RH Neutrino



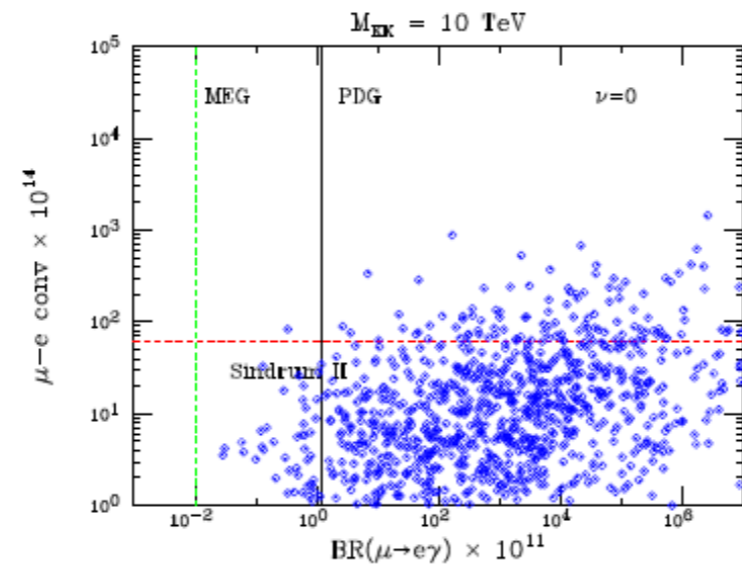
SM+HNL



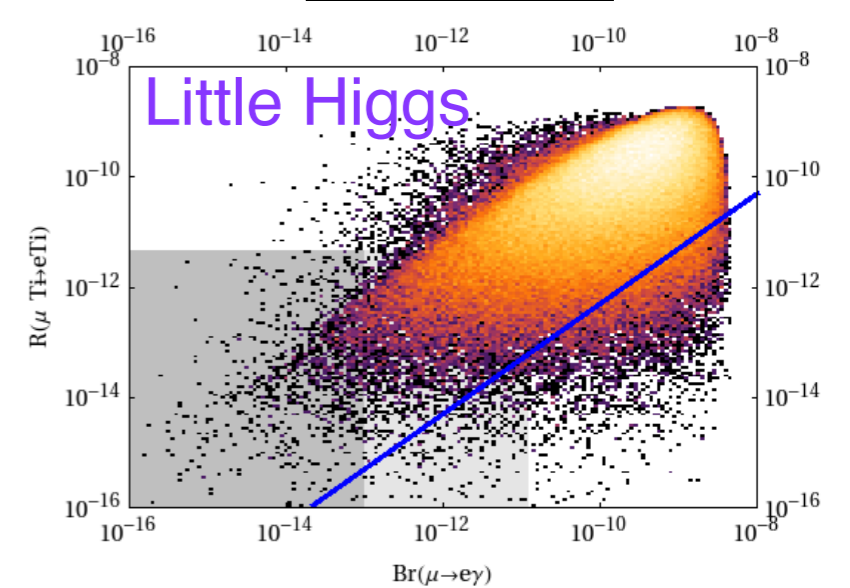
SUSY-GUT



extra dimension model



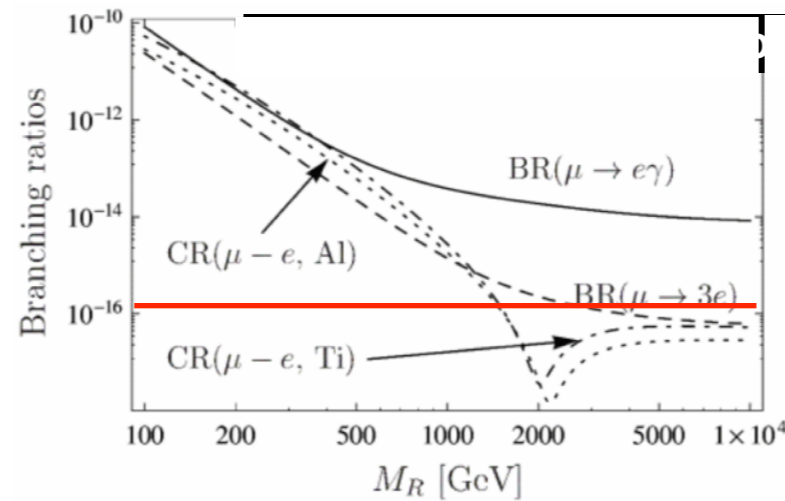
Little Higgs



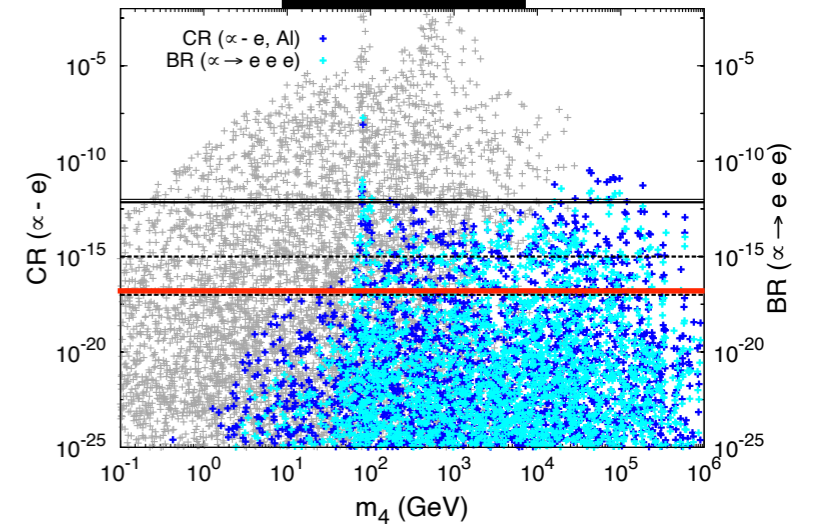
Model Dependent CLFV Predictions

only some examples

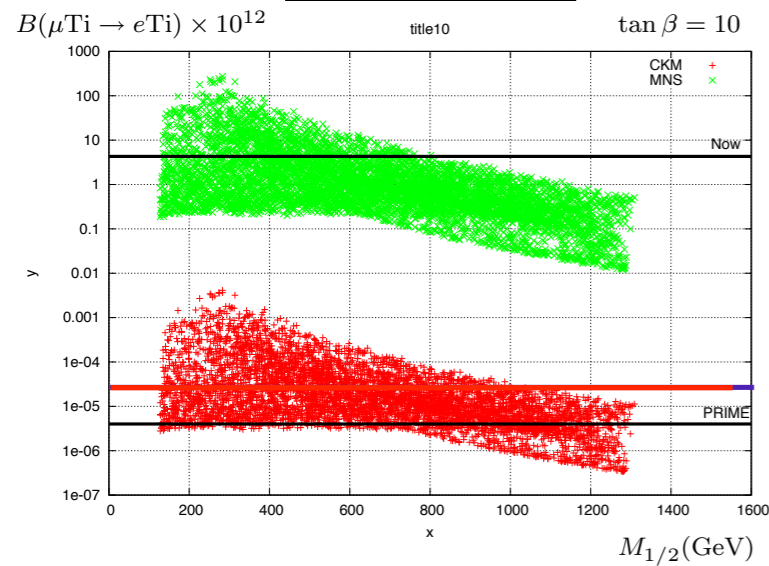
SUSY: Heavy RH Neutrino



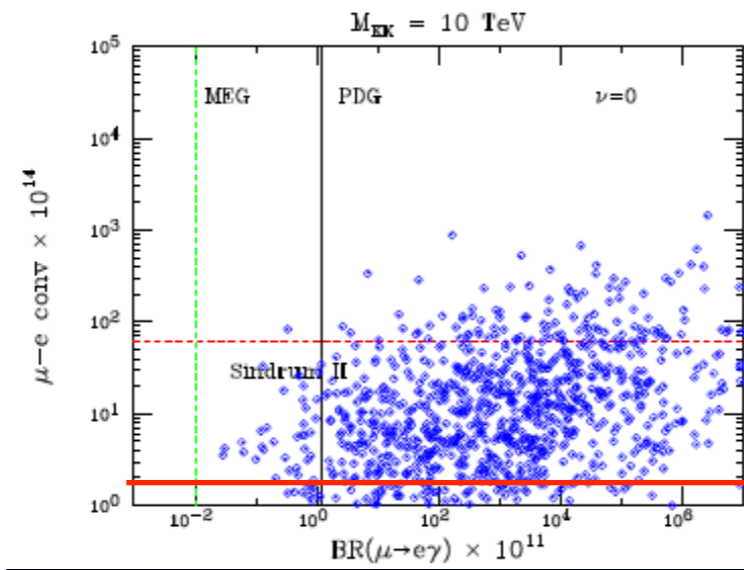
SM+HNL



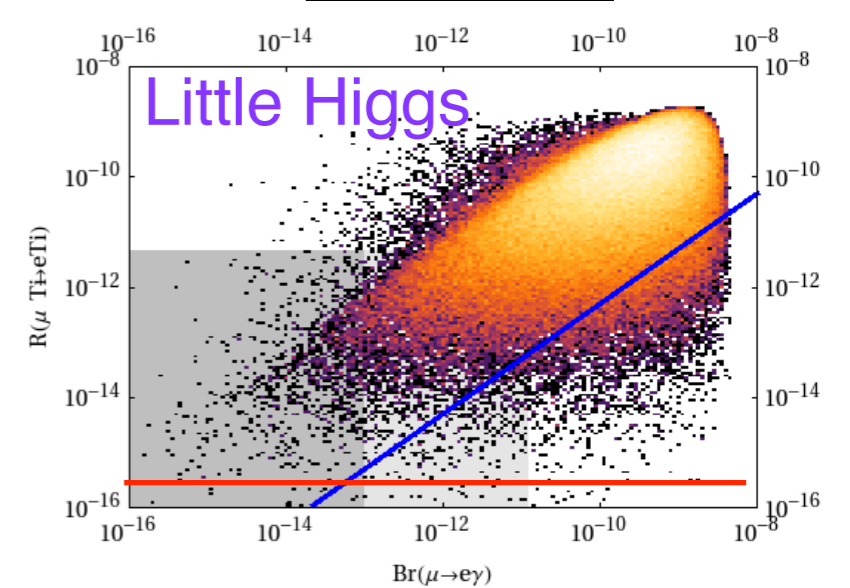
SUSY-GUT



extra dimension model



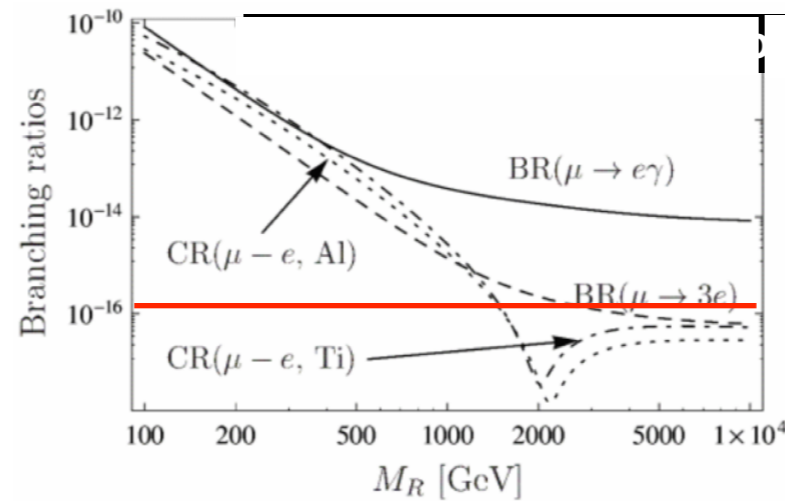
Little Higgs



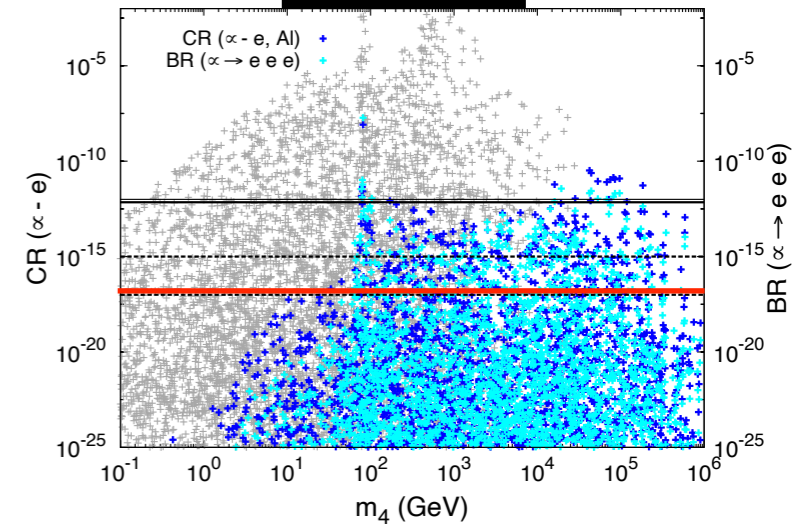
Model Dependent CLFV Predictions

only some examples

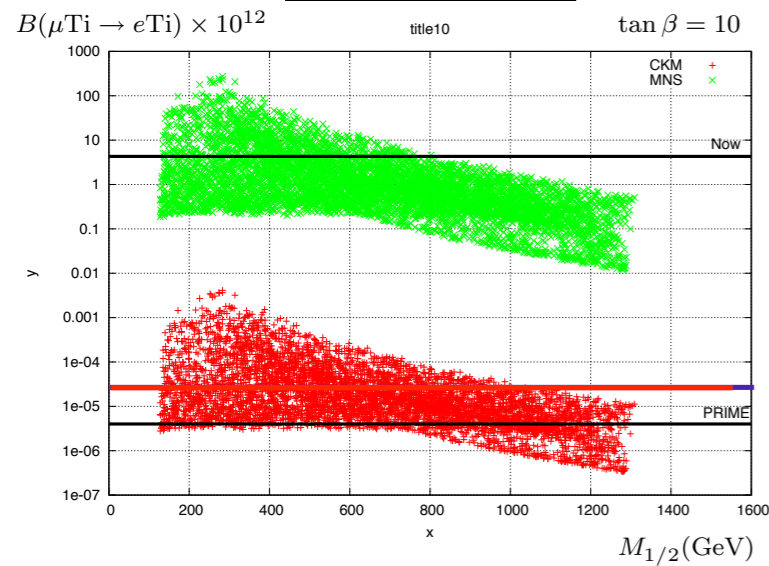
SUSY: Heavy RH Neutrino



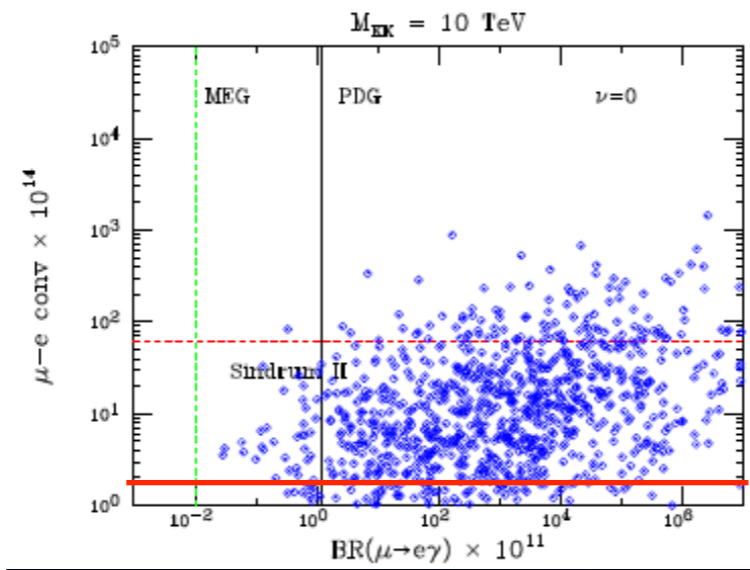
SM+HNL



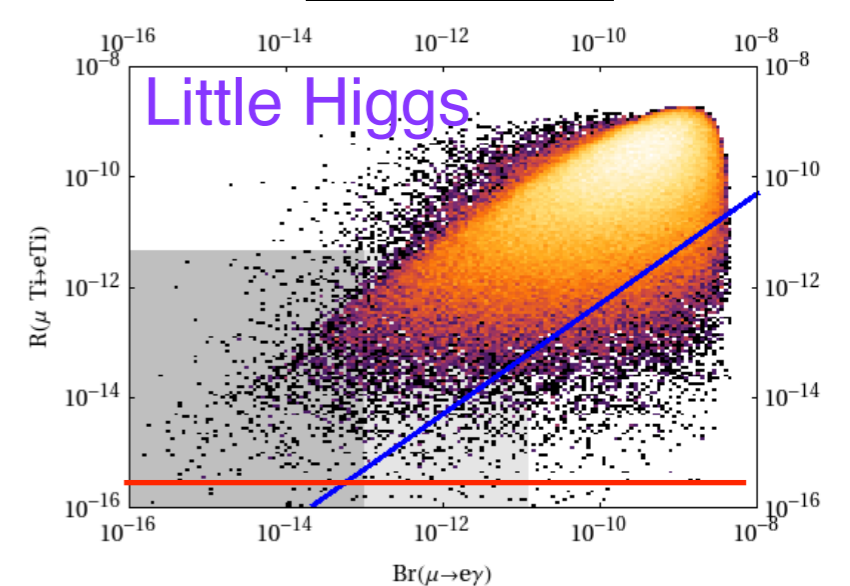
SUSY-GUT



extra dimension model



Little Higgs



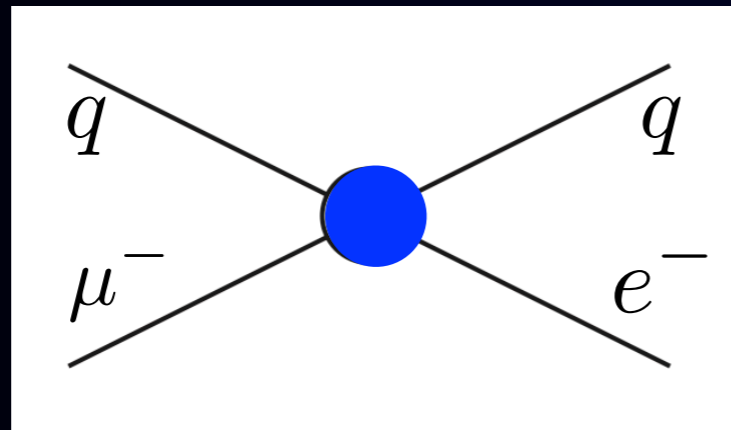
3 Many BSM models predict sizable CLFV rates.

$\mu^- \rightarrow e^-$ Conversion in EFT



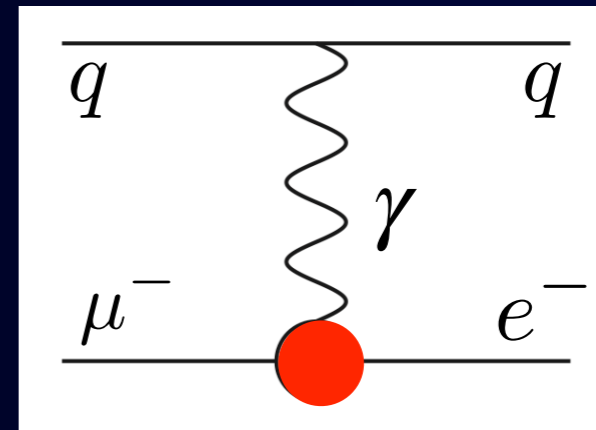
$\mu^- \rightarrow e^-$ Conversion in EFT

Contact Interaction



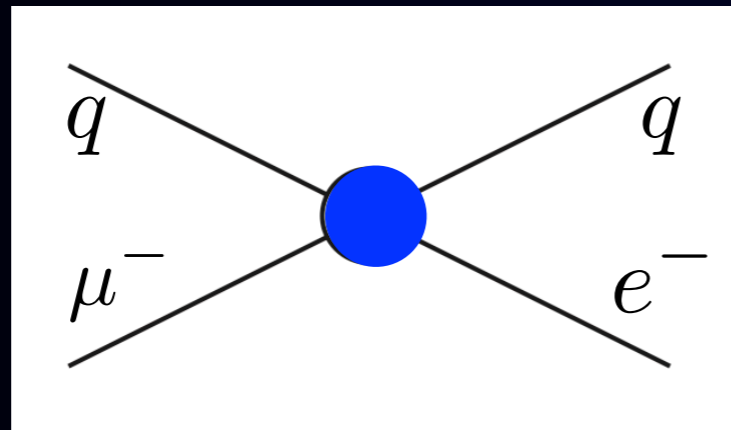
+

Photonic Interaction



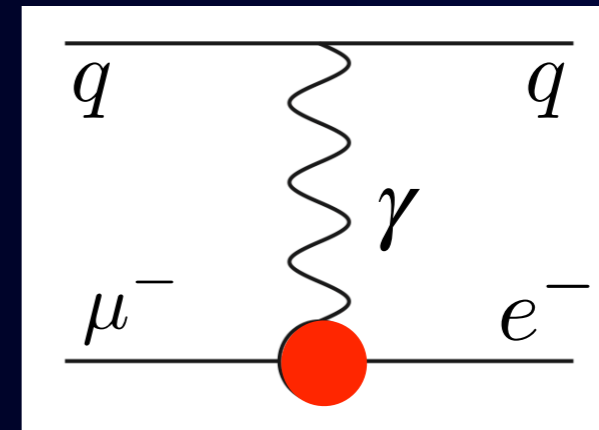
$\mu^- \rightarrow e^-$ Conversion in EFT

Contact Interaction



+

Photonic Interaction

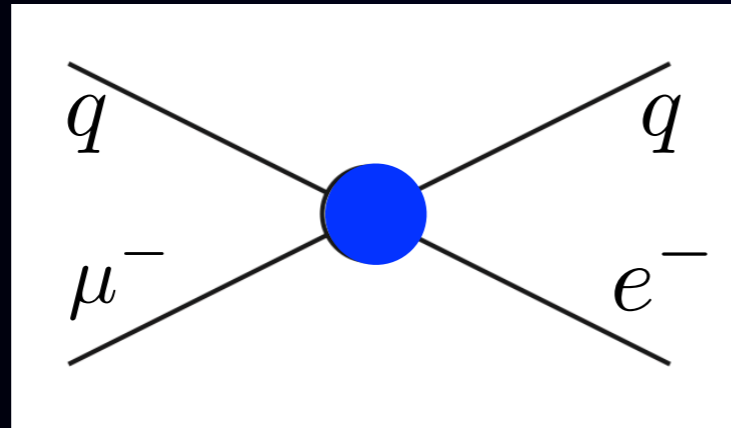


- dipole (L/R) (spin independent)
- di-photons (L/R) $\mu e F F$

S. Davidson, YK, Y. Uesaka, M. Yamanaka,
Phys. Rev. D102, 11504 (2020)

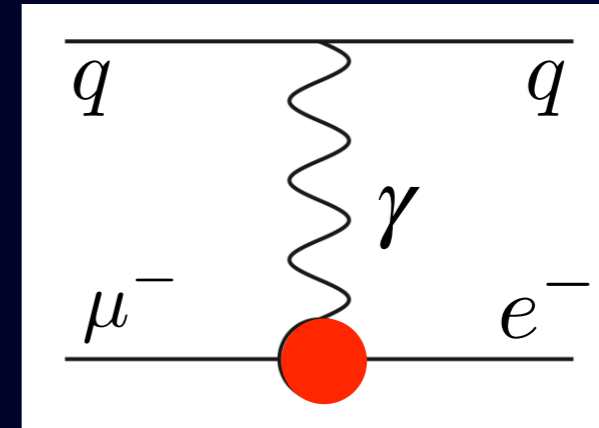
$\mu^- \rightarrow e^-$ Conversion in EFT

Contact Interaction



+

Photonic Interaction



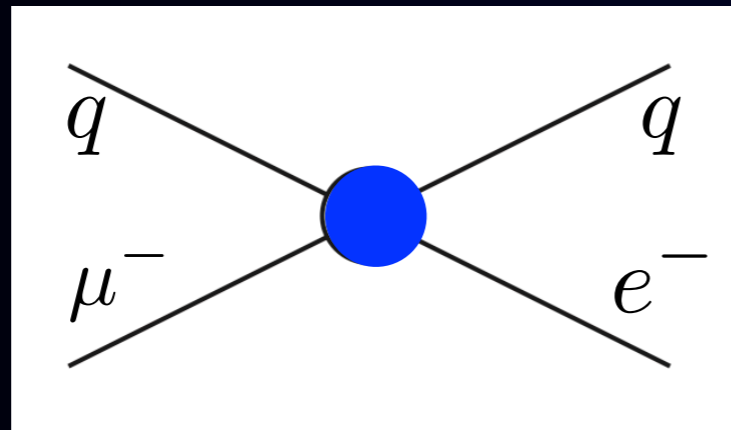
- dipole (L/R) (spin independent)
- di-photons (L/R) $\mu e F F$

S. Davidson, YK, Y. Uesaka, M. Yamanaka,
Phys. Rev. D102, 11504 (2020)

analogy to
DM scattering

$\mu^- \rightarrow e^-$ Conversion in EFT

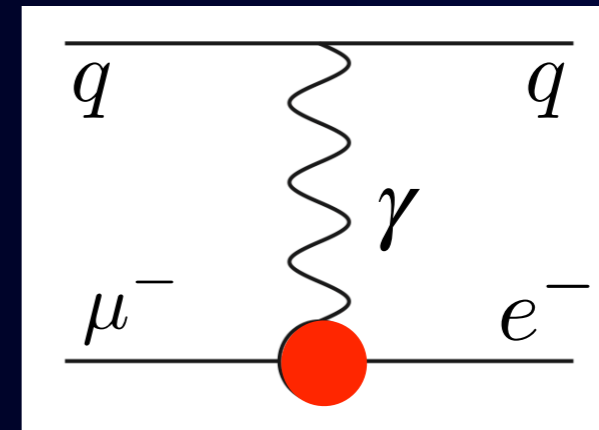
Contact Interaction



analogy to
DM scattering

- scalar (L/R) (spin independent)
- vector (L/R) (spin independent)
- pseudoscalar (L/R) (spin dependent)
- axial vector (L/R) (spin dependent)
- tensor (L/R) (spin dependent)

Photonic Interaction



- dipole (L/R) (spin independent)
- di-photons (L/R) $\mu e F F$

S. Davidson, YK, Y. Uesaka, M. Yamanaka,
Phys. Rev. D102, 11504 (2020)

V. Cirigliano, S. Davidson, YK, Phys. Lett. B 771 (2017) 242

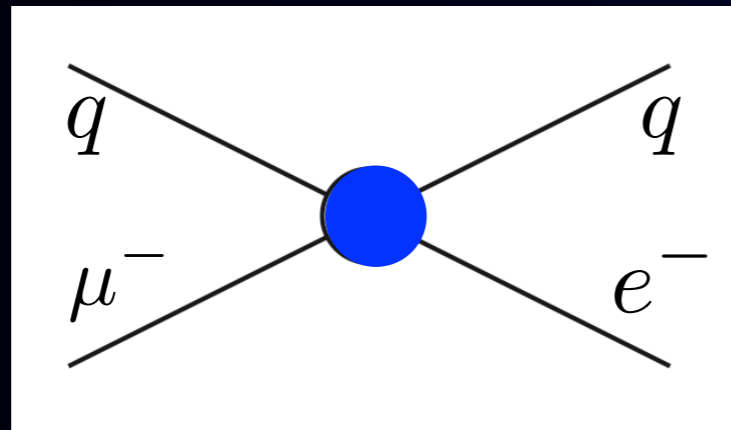
S. Davidson, YK, A. Saporta, Eur. Phys. J. C78 (2018) 109

E. Rule, W.C. Haxton, K. McElvain, Phys. Rev. Lett. 130 131901 (2023)

M. Hoferichter, J. Menendez and F. Noel, Phys. Rev. Lett. 130, 131902 (2023)

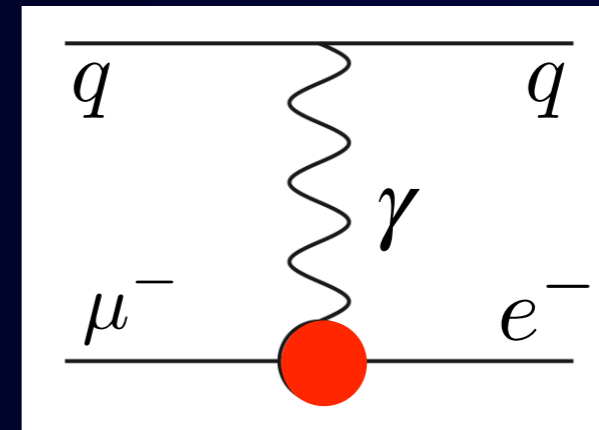
$\mu^- \rightarrow e^-$ Conversion in EFT

Contact Interaction



+

Photonic Interaction



analogy to DM scattering

- scalar (L/R) (spin independent)
- vector (L/R) (spin independent)
- pseudoscalar (L/R) (spin dependent)
- axial vector (L/R) (spin dependent)
- tensor (L/R) (spin dependent)

- dipole (L/R) (spin independent)
- di-photons (L/R) $\mu e F F$

S. Davidson, YK, Y. Uesaka, M. Yamanaka, Phys. Rev. D102, 11504 (2020)

V. Cirigliano, S. Davidson, YK, Phys. Lett. B 771 (2017) 242

S. Davidson, YK, A. Saporta, Eur. Phys. J. C78 (2018) 109

E. Rule, W.C. Haxton, K. McElvain, Phys. Rev. Lett. 130 131901 (2023)

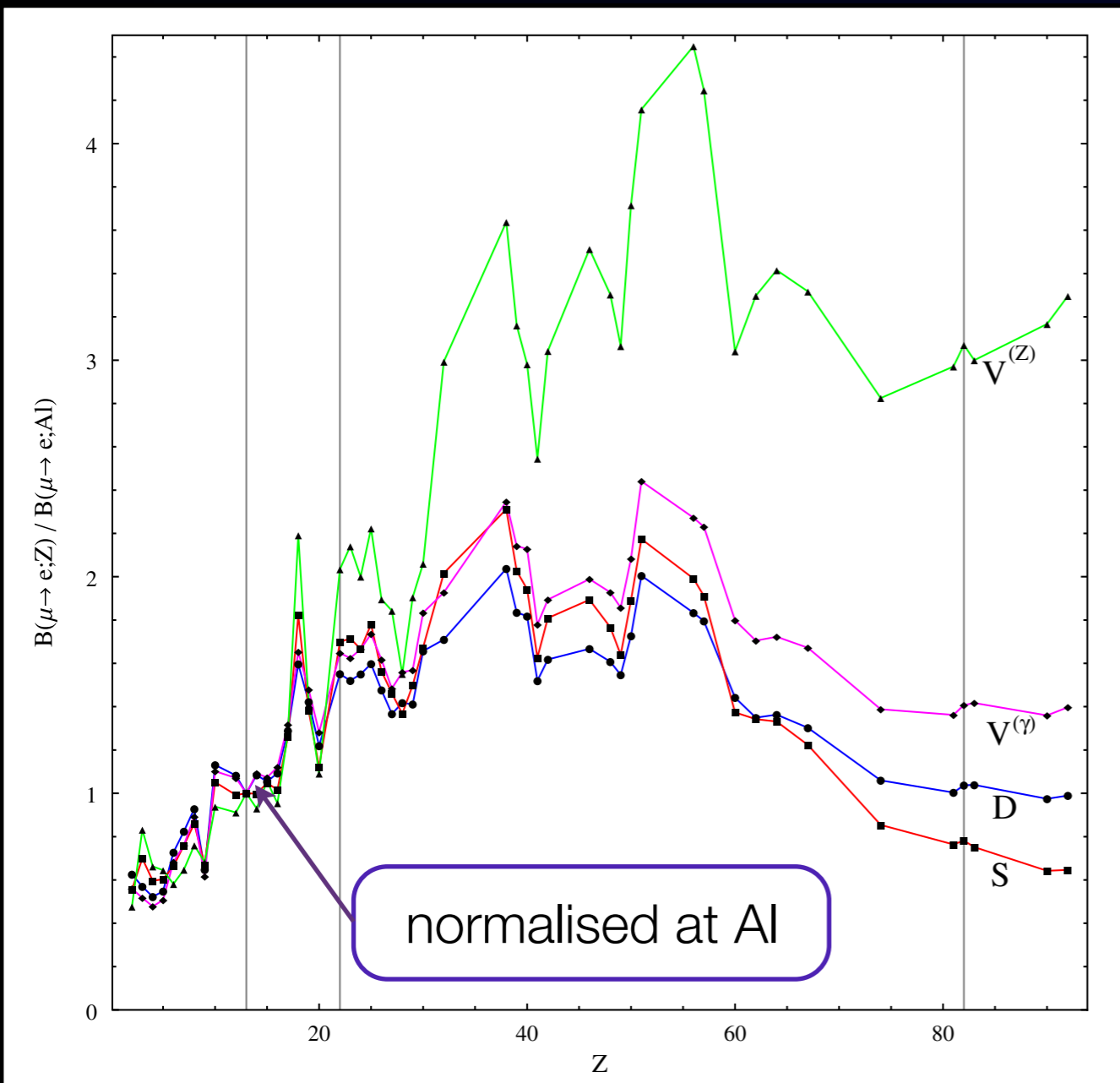
M. Hoferichter, J. Menendez and F. Noel, Phys. Rev. Lett. 130, 131902 (2023)

different for protons and neutrons \rightarrow target dependence

$\mu \rightarrow e$ Conversion Rates for Different Target Material



$\mu \rightarrow e$ Conversion Rates for Different Target Material

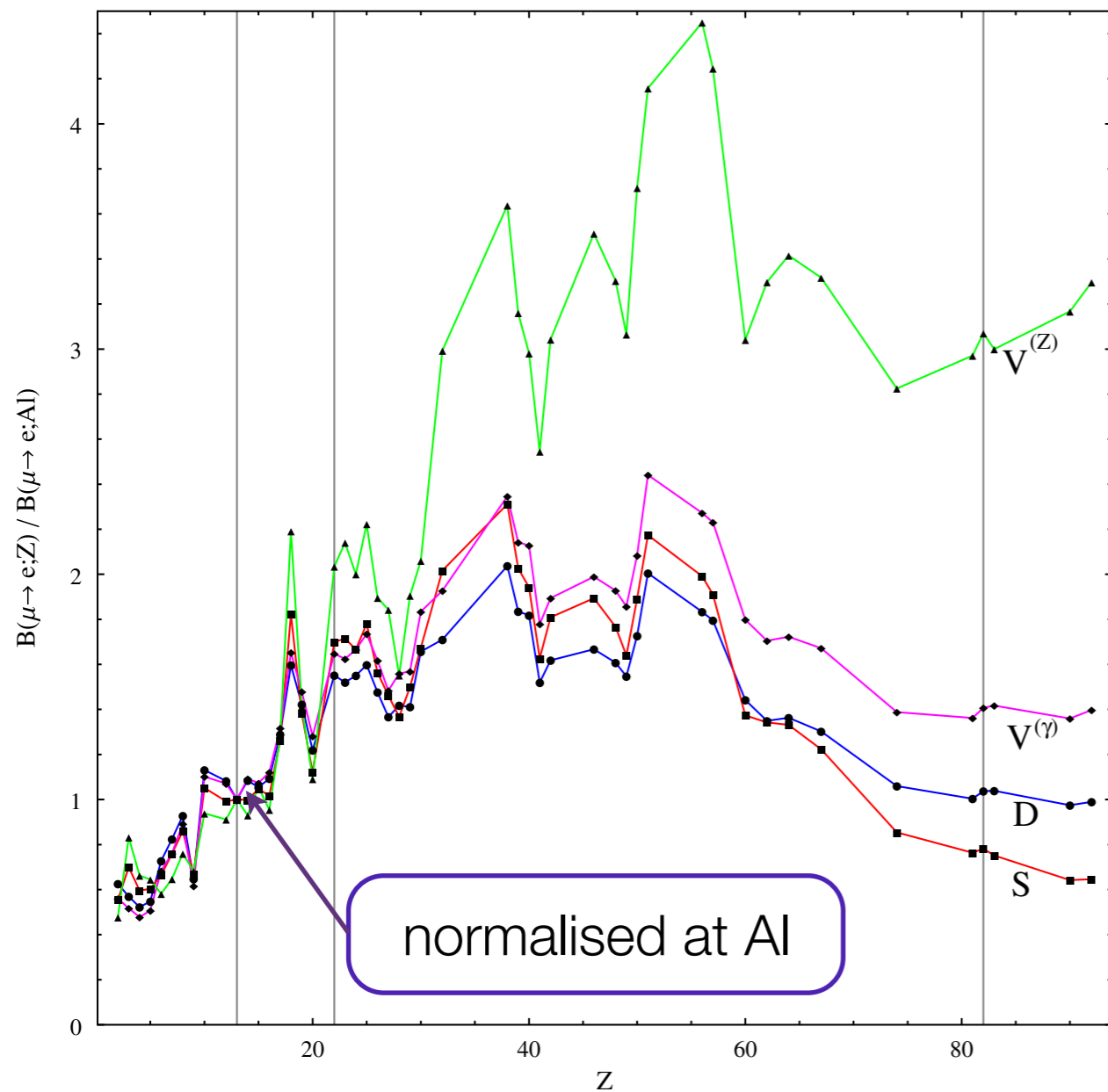


R. Kitano, M. Koike and Y. Okada, Phys.Rev. D66 (2002) 096002; D76 (2007) 059902
V. Cirigliano, R. Kitano, Y. Okada, and P. Tuzon, Phys. Rev. D80 (2009) 013002
S. Davidson, YK, M. Yamanaka, Phys. Lett. B790 (2019) 380-388

$\mu \rightarrow e$ Conversion Rates for Different Target Material



one interaction at a time



vector interaction
(with Z boson)

with Z penguin

vector interaction
(with photon
-charge radius)

left-right models

dipole interaction

SUSY-GUT

scalar interaction

SUSY seesaw

R. Kitano, M. Koike and Y. Okada, Phys.Rev. D66 (2002) 096002; D76 (2007) 059902

V. Cirigliano, R. Kitano, Y. Okada, and P. Tuzon, Phys. Rev. D80 (2009) 013002

S. Davidson, YK, M. Yamanaka, Phys. Lett. B790 (2019) 380-388

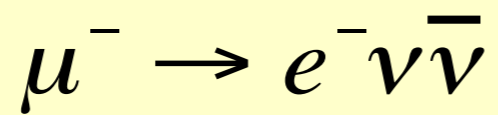
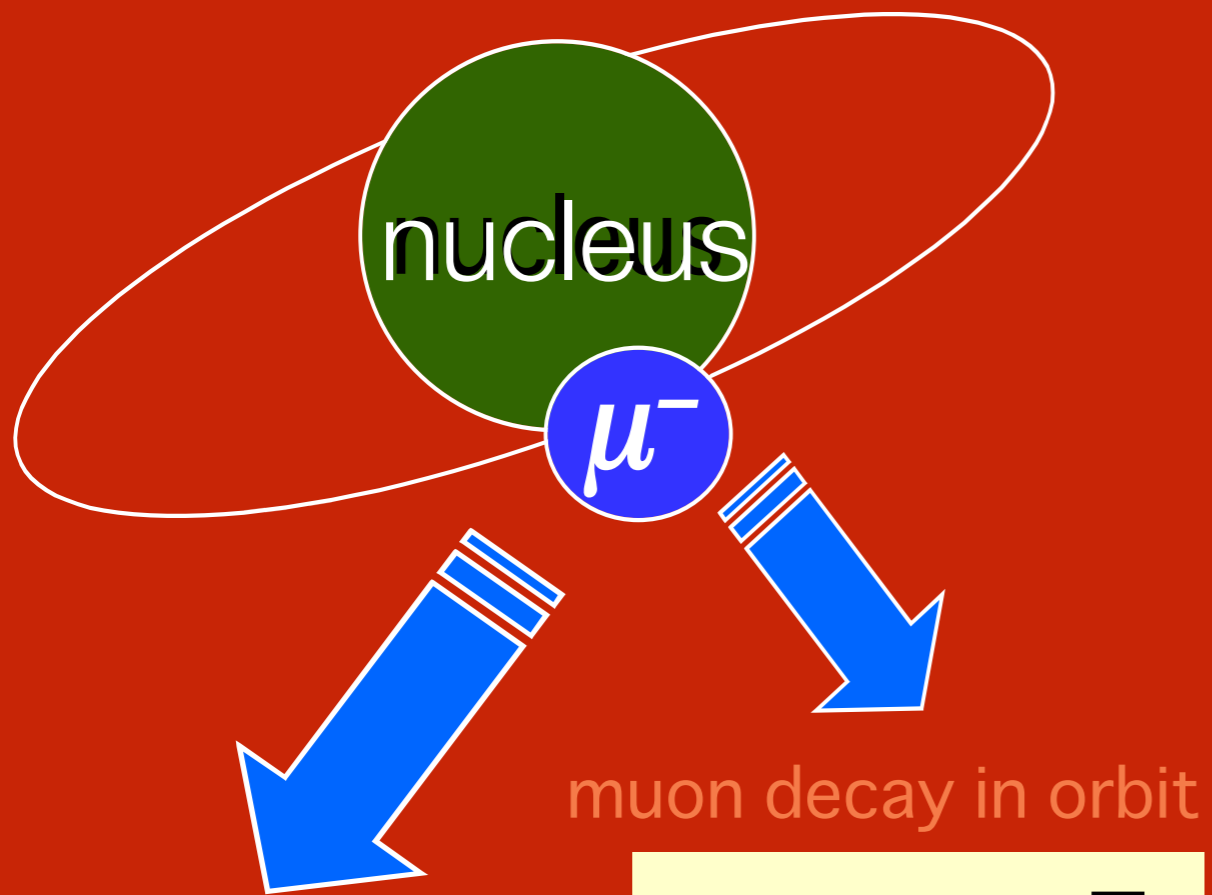
What is $\mu \rightarrow e$ conversion ?



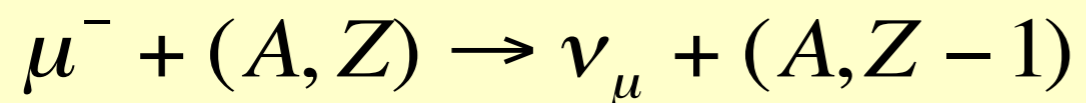
$\mu \rightarrow e$ Conversion in a muonic atom

$\mu \rightarrow e$ Conversion in a muonic atom

1s state in a muonic atom



nuclear muon capture

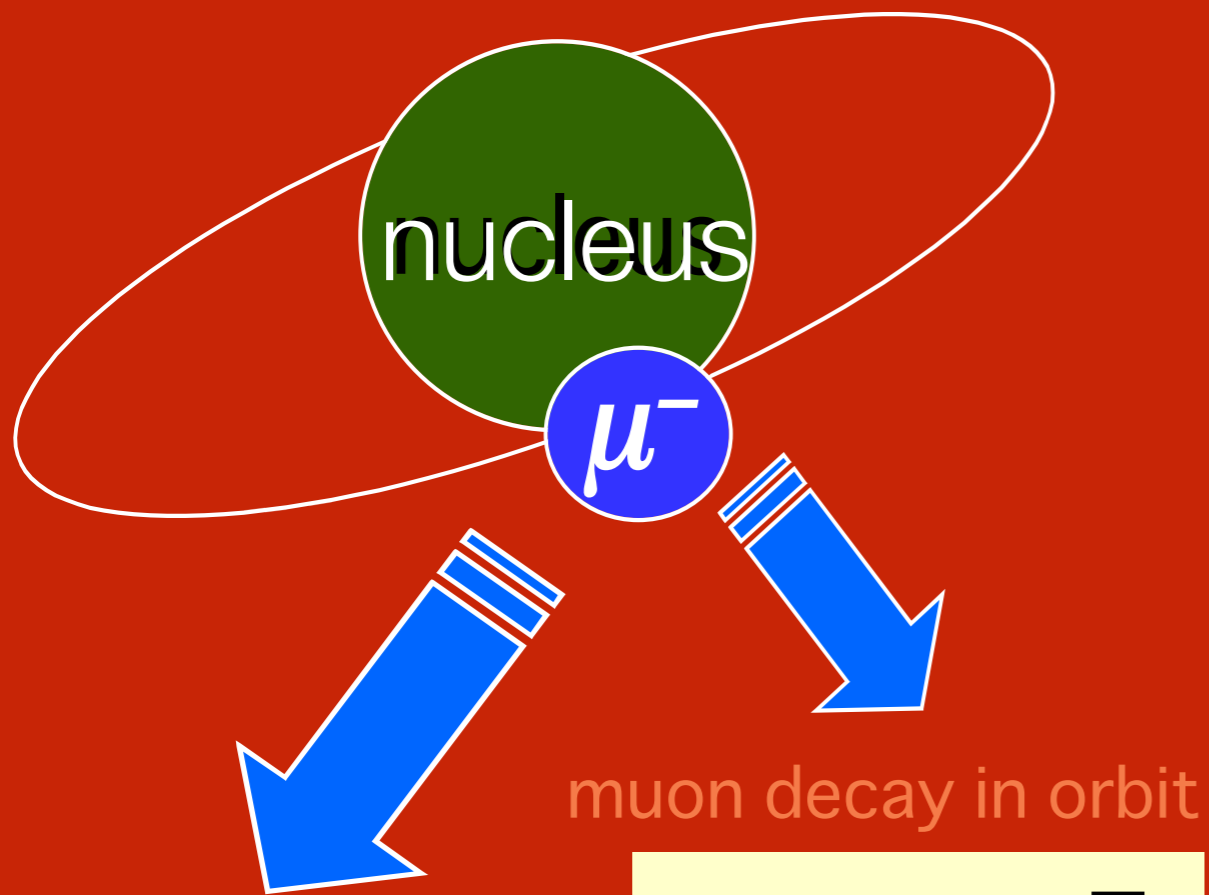


$$CR(\mu^-N \rightarrow e^-N) \equiv \frac{\Gamma(\mu^-N \rightarrow e^-N)}{\Gamma(\mu^-N \rightarrow \text{all})}$$

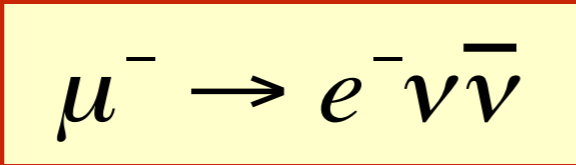


$\mu \rightarrow e$ Conversion in a muonic atom

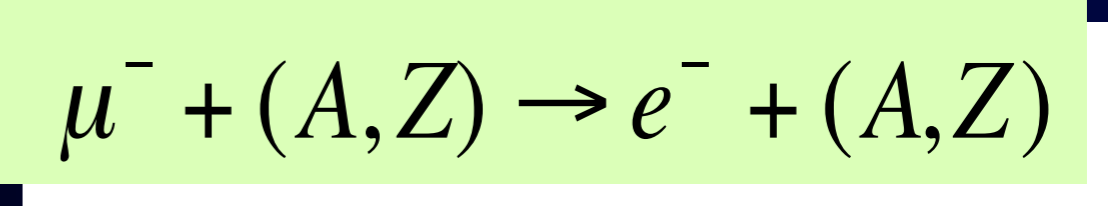
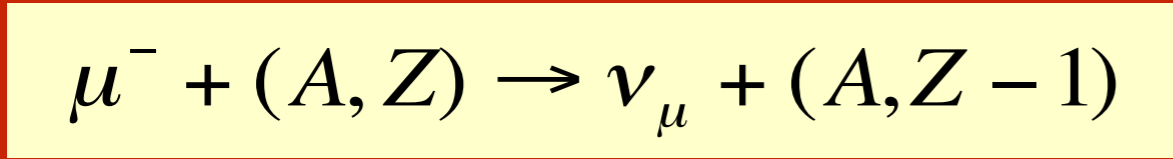
1s state in a muonic atom



muon decay in orbit



nuclear muon capture



Event Signature :

a single mono-energetic electron of 105 MeV

Backgrounds:

- (1) physics backgrounds
- (2) beam-related backgrounds
- (3) cosmic rays, false tracking

	Z	CR limit
sulfur	16	$<7 \times 10^{-11}$
titanium	22	$<4.3 \times 10^{-12}$
copper	39	$<1.6 \times 10^{-8}$
gold	79	$<7 \times 10^{-13}$
lead	82	$<4.6 \times 10^{-11}$

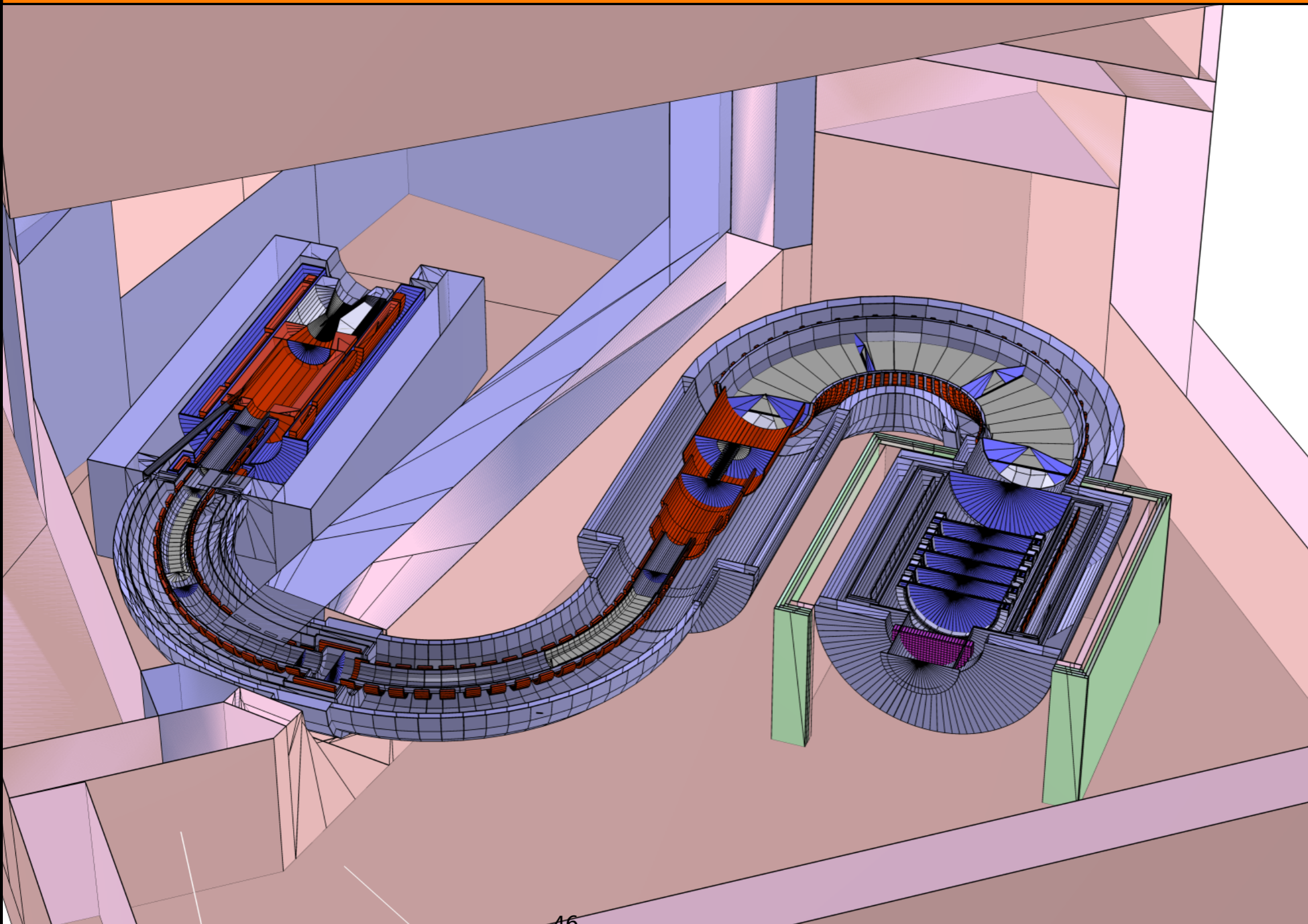
COMET at J-PARC

COMET=COherent Muon to Electron Transition

COMET

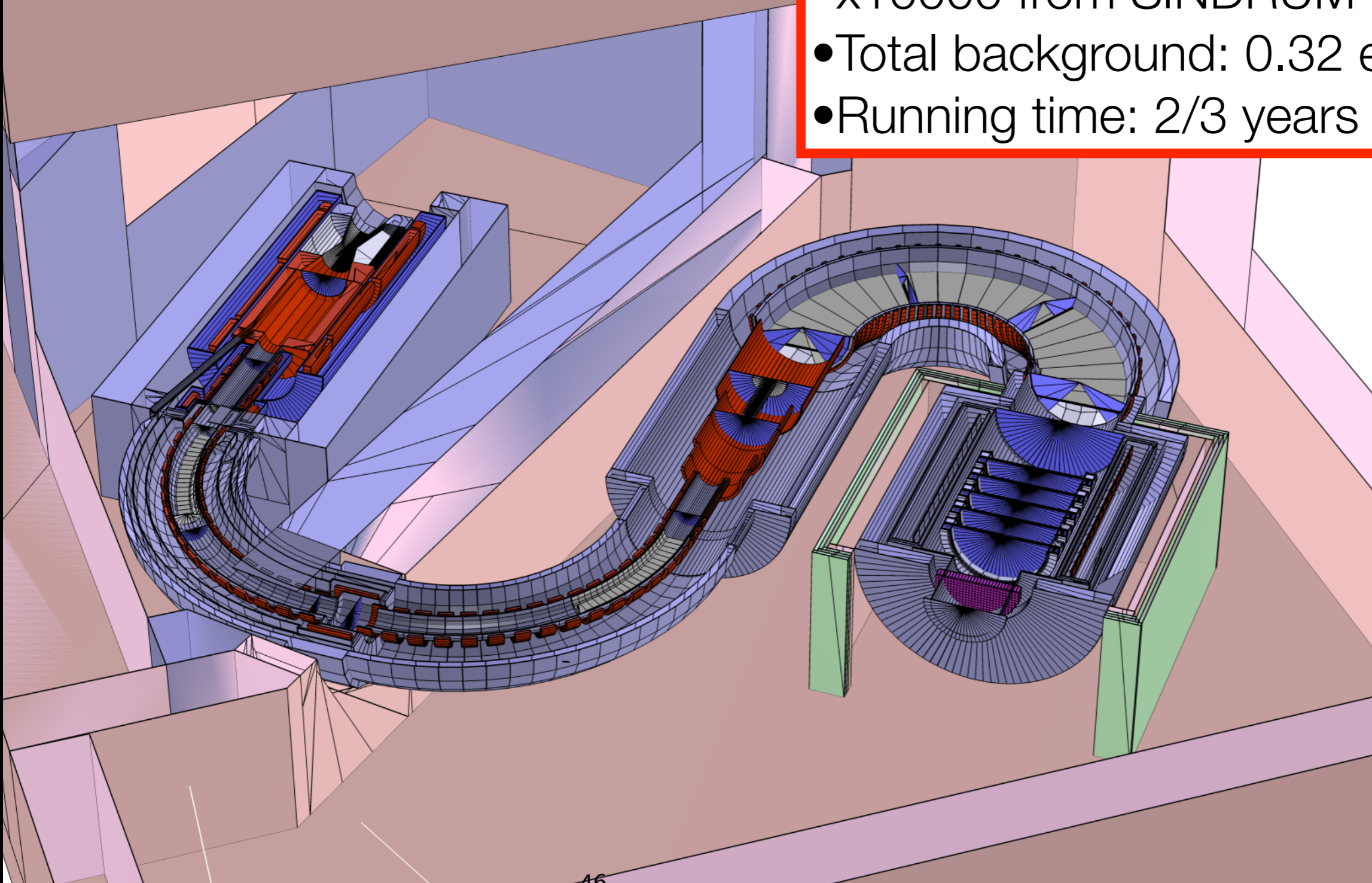


COMET



COMET

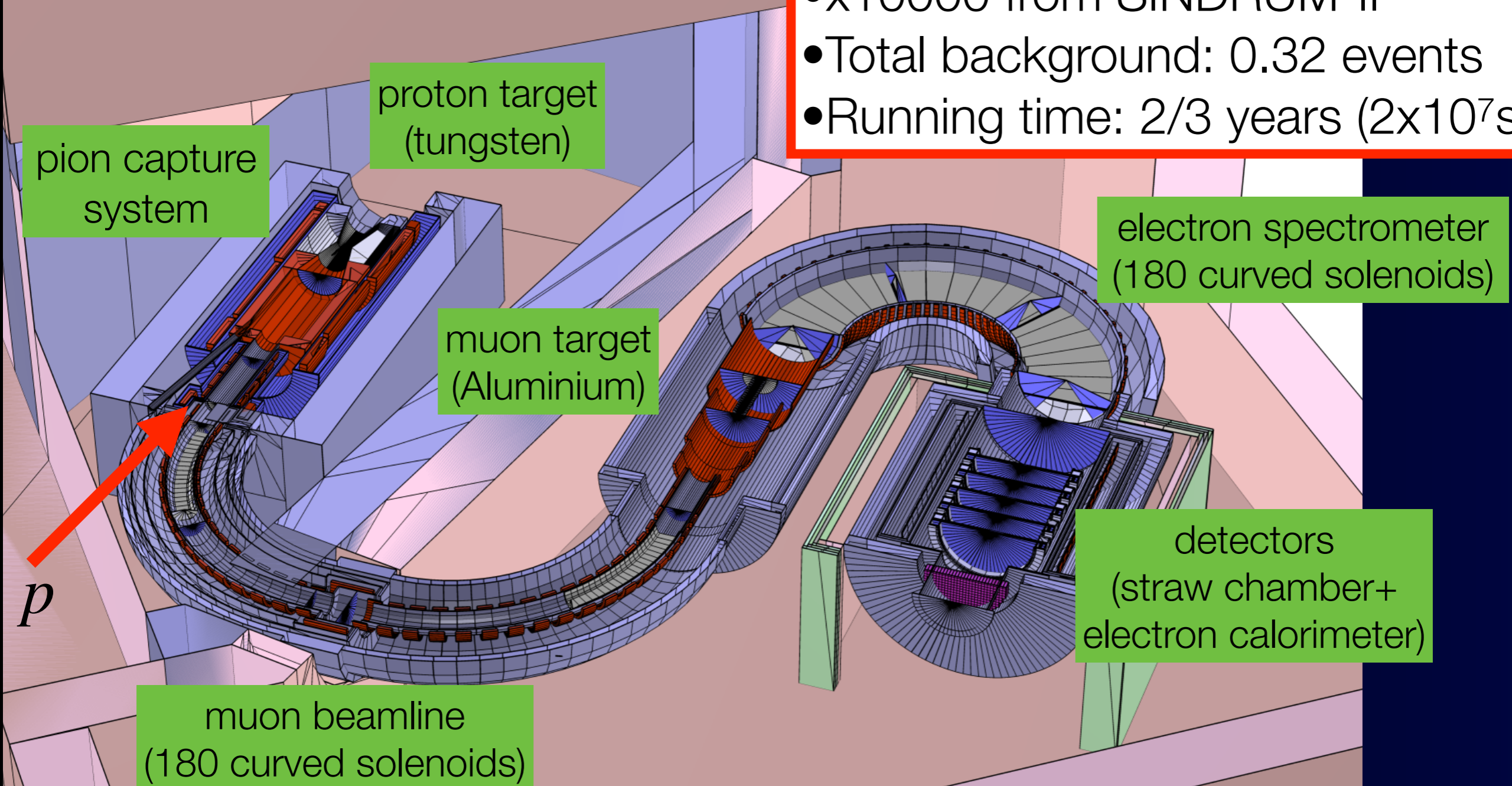
- Proton beam, 8 GeV, 56kW
- 5×10^{10} stopped muons/s
- Single event sensitivity : 1.4×10^{-17}
- 90% CL limit : $< 3.2 \times 10^{-17}$
- x10000 from SINDRUM-II
- Total background: 0.32 events
- Running time: 2/3 years (2×10^7 sec)



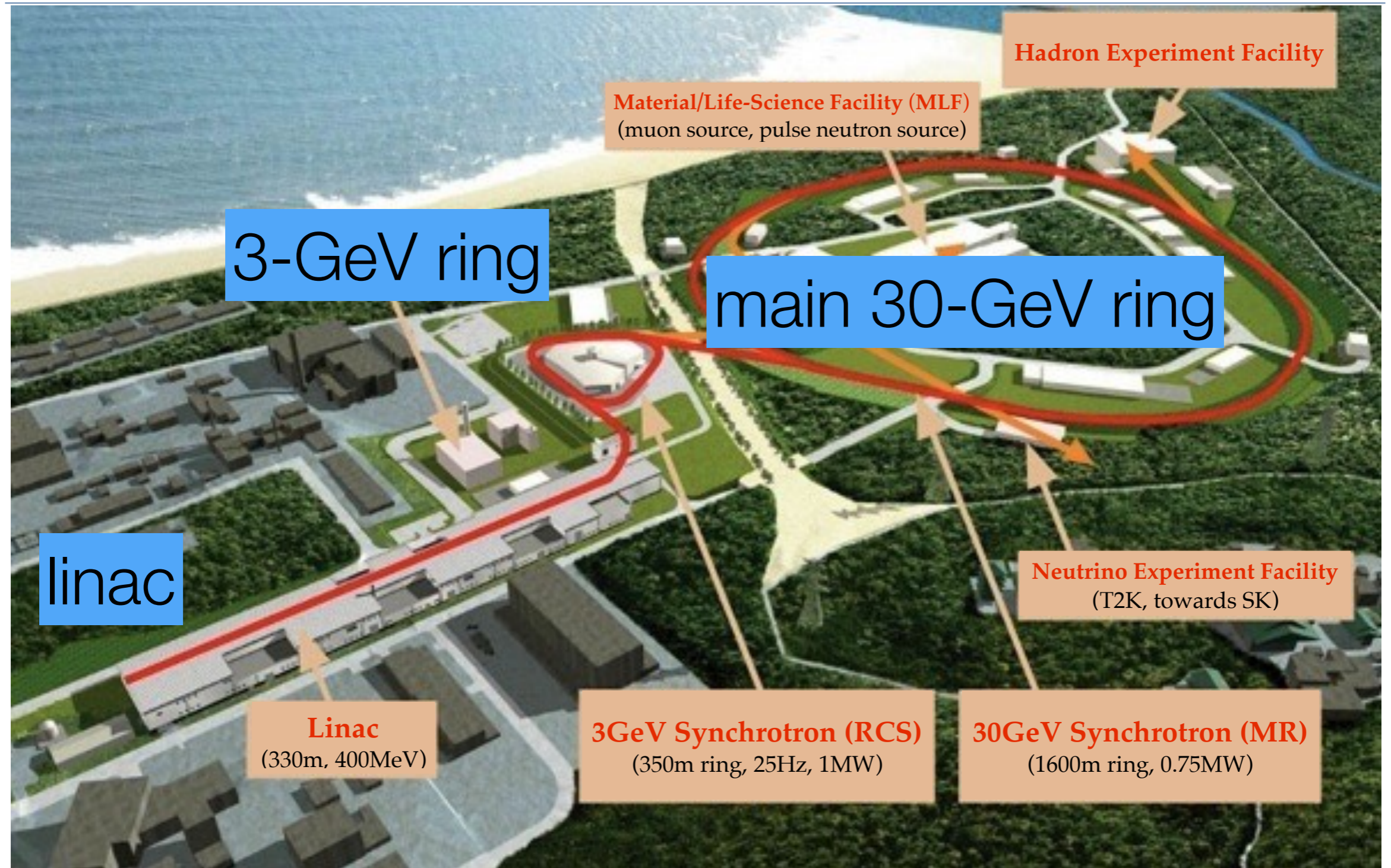
COMET

- Proton beam, 8 GeV, 56kW
- 5×10^{10} stopped muons/s

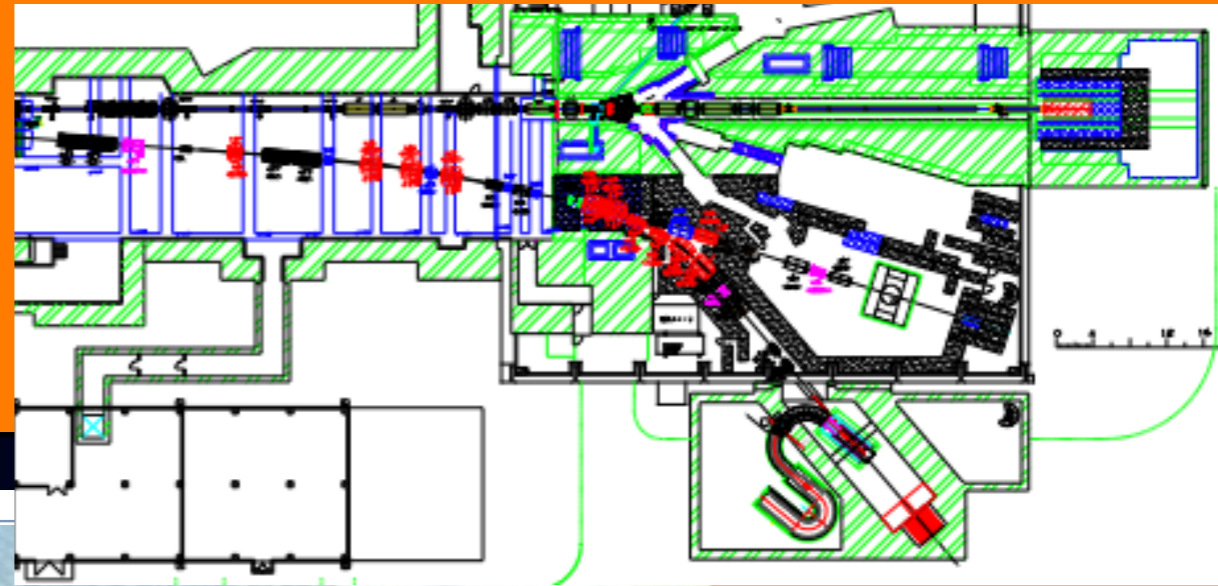
- Single event sensitivity : 1.4×10^{-17}
- 90% CL limit : $< 3.2 \times 10^{-17}$
- x10000 from SINDRUM-II
- Total background: 0.32 events
- Running time: 2/3 years (2×10^7 sec)



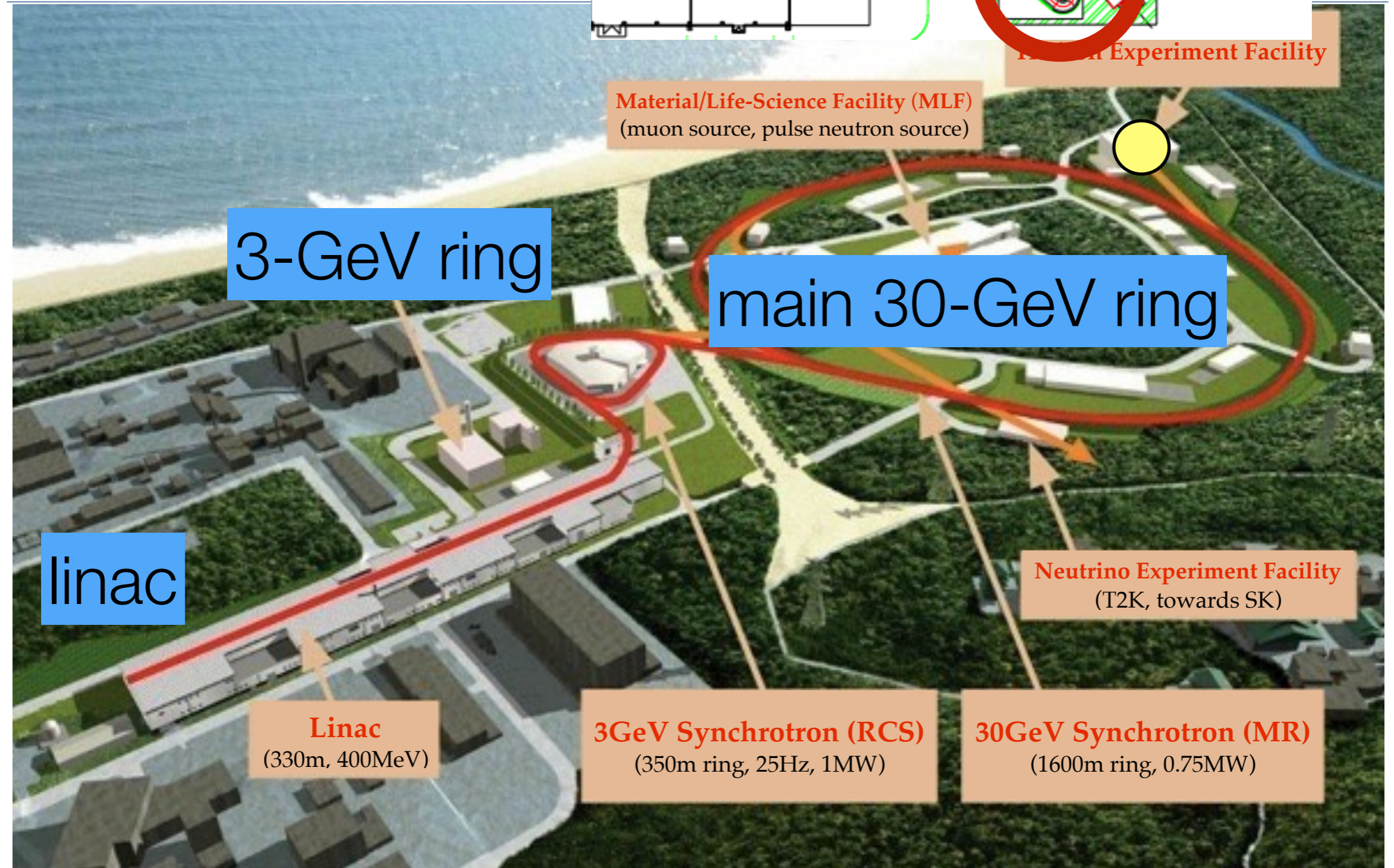
Proton Accelerator J-PARC



Proton Accelerator J-PARC



Proton Accelerator J-PARC



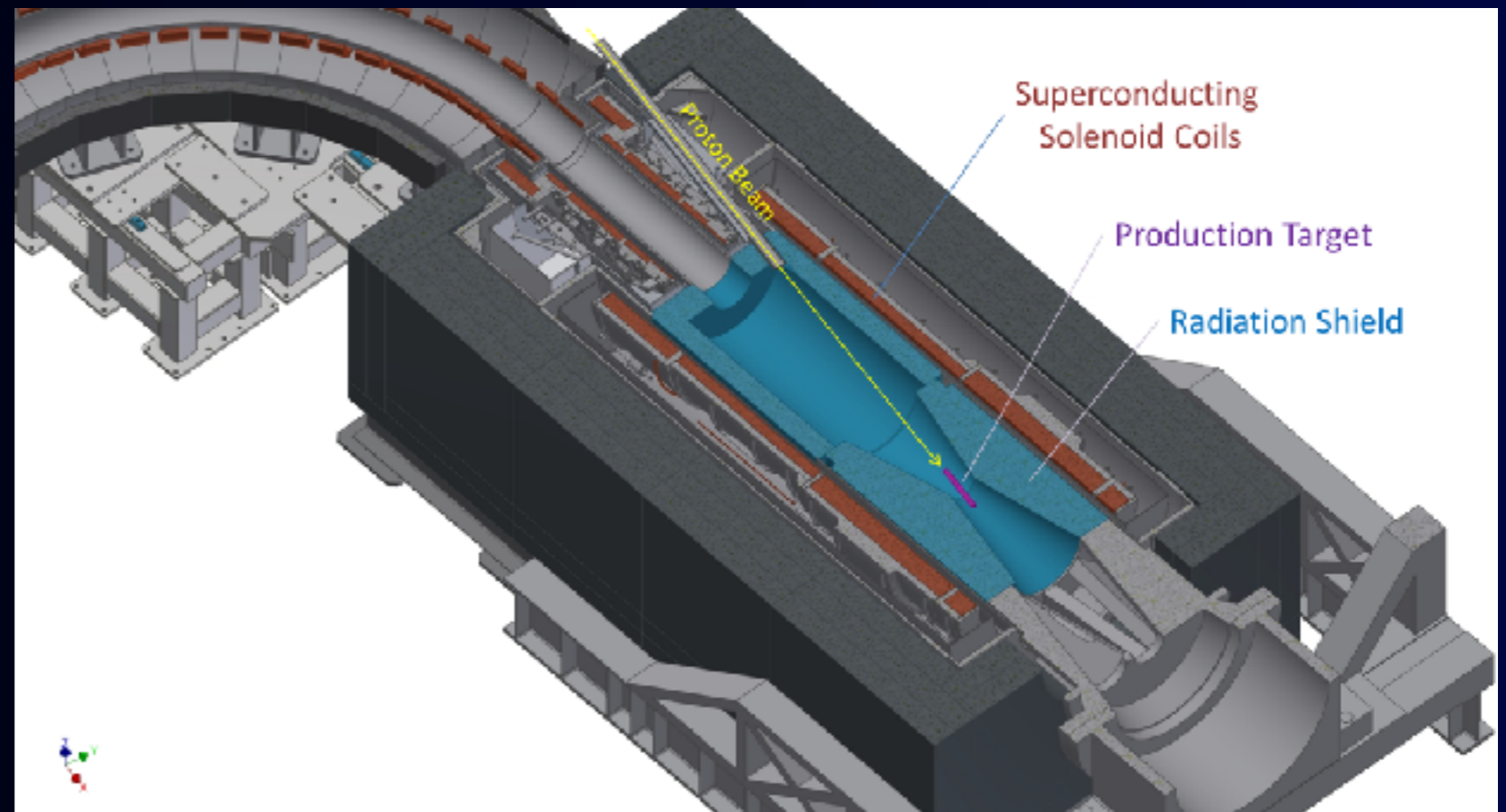


Improvements for Signal Sensitivity

Improvements for Signal Sensitivity

Pion Capture System

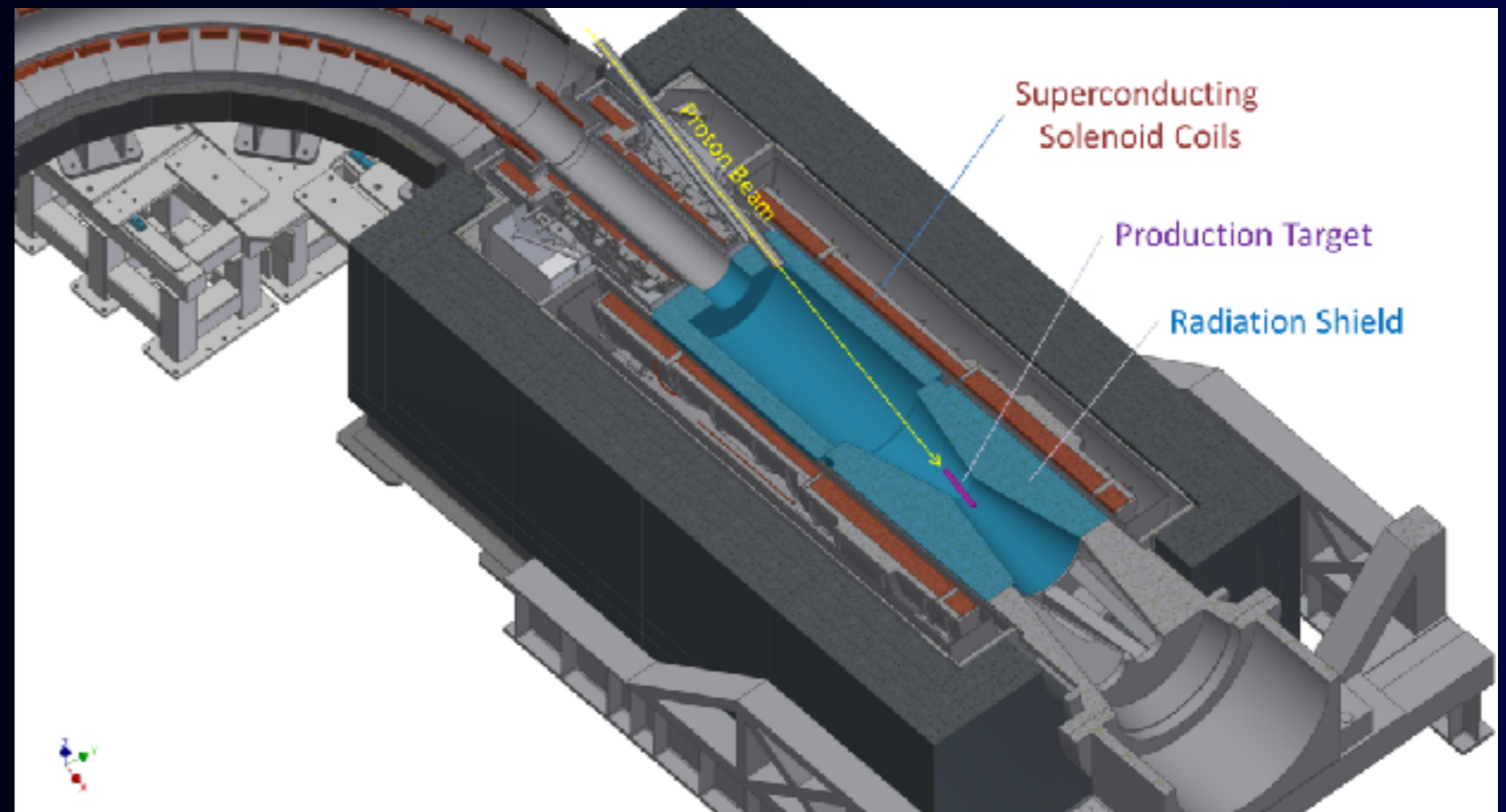
Pions and muons are captured and transported by high field SC solenoids.



Improvements for Signal Sensitivity

Pion Capture System

Pions and muons are captured and transported by high field SC solenoids.

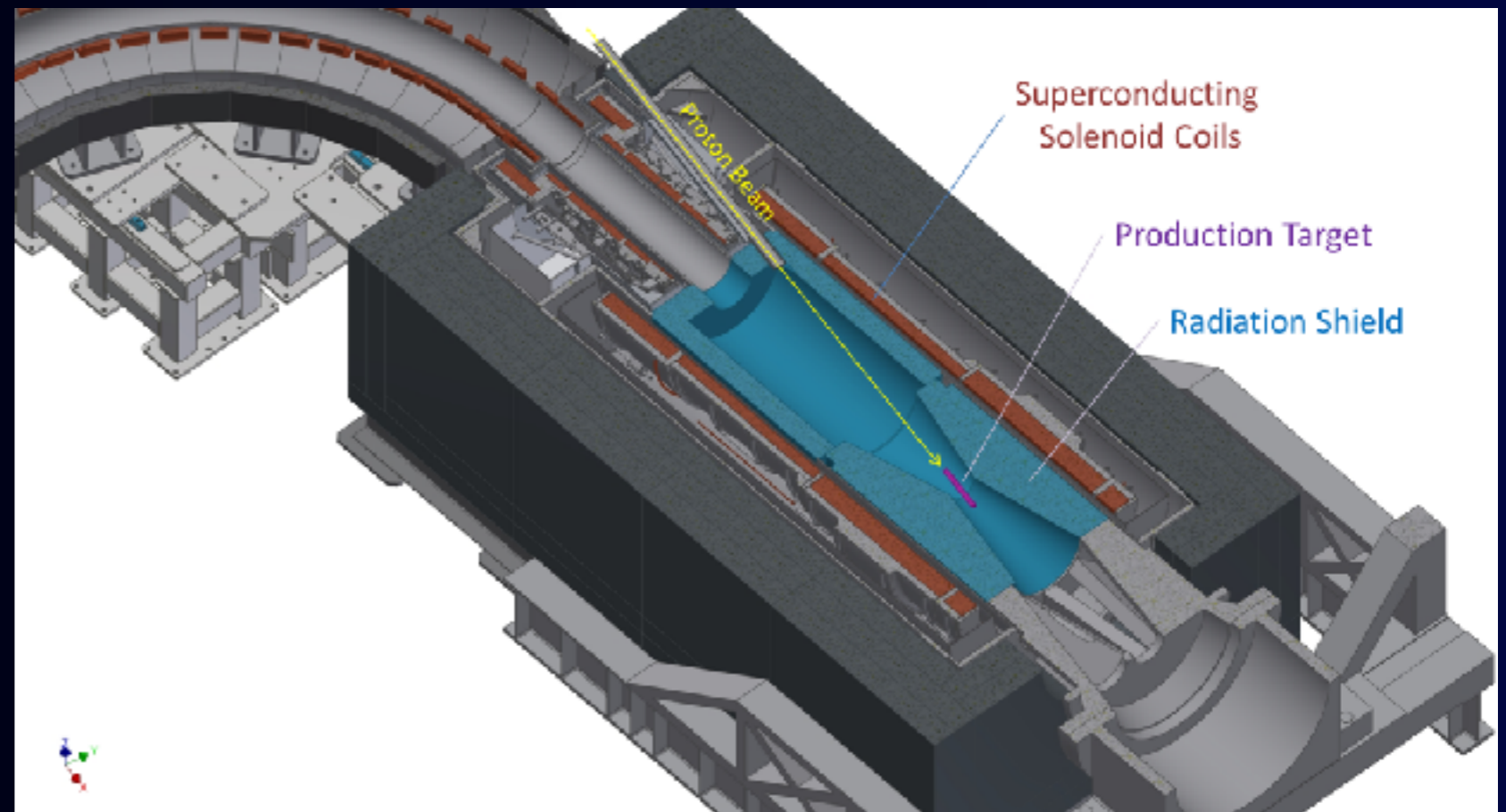


$10^{11} \mu/s$ for 50 kW proton beam power
or 10^{18} muons in total

Improvements for Signal Sensitivity

Pion Capture System

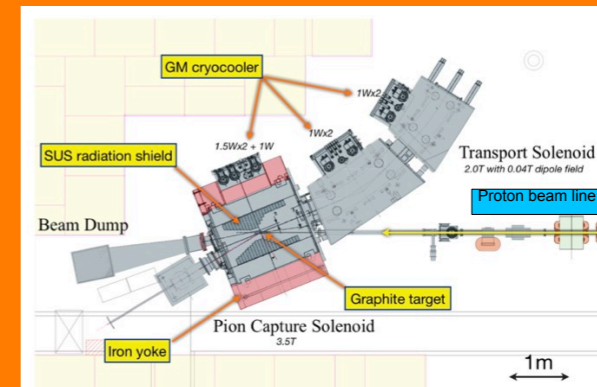
Pions and muons are captured and transported by high field SC solenoids.



$10^{11} \mu/s$ for 50 kW proton beam power
or 10^{18} muons in total

The previous experiment used 10^{14} muons.

MuSIC at RCNP, Osaka University (2011 -)

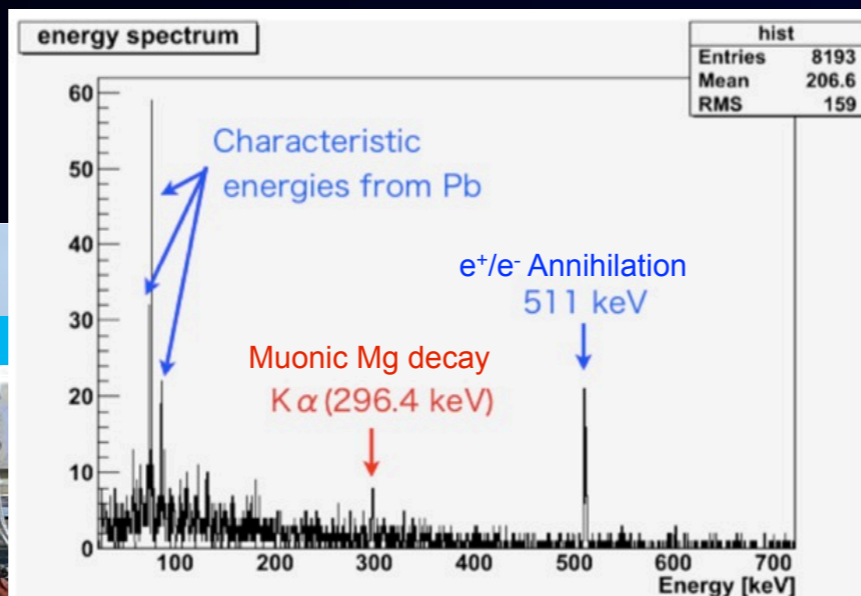
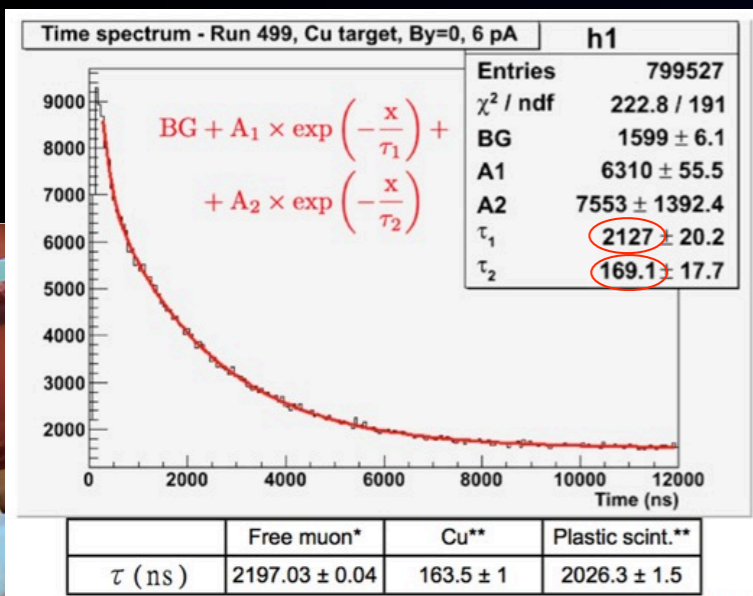
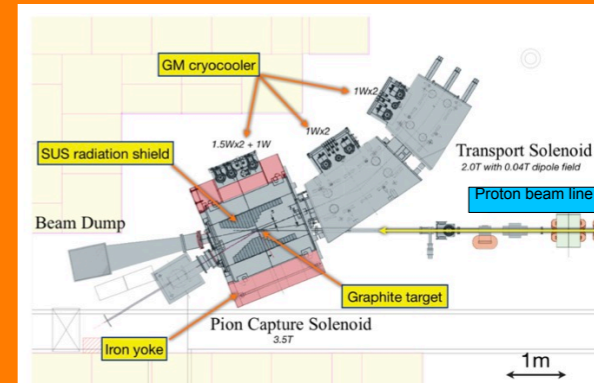


Science

3.5T and graphite
proton target

素粒子の一つであるミューオンを世界最高の効率で生成する装置「MuSIC」。宇宙の始まりに何が起こったのか、宇宙はどのような法則で成り立っているのかを、大量のミューオンと最新技術を駆使して研究する

MuSIC at RCNP, Osaka University (2011 -)



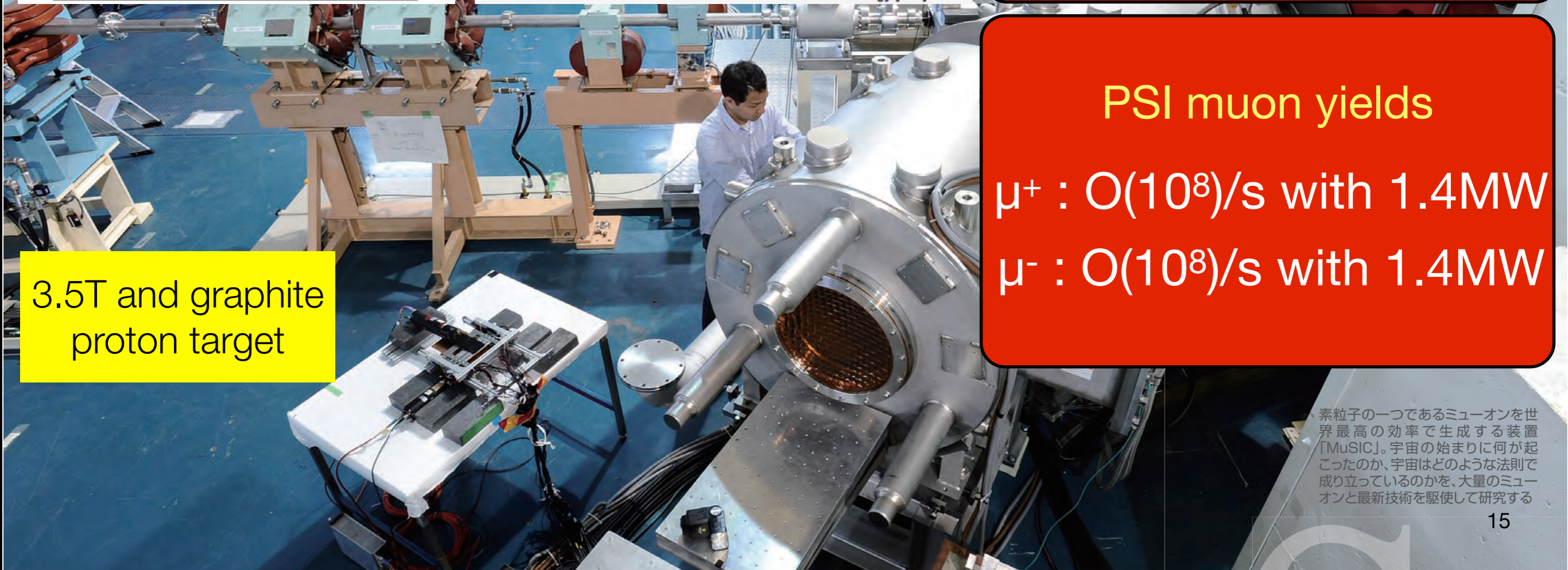
MuSIC muon yields

μ^+ : $3 \times 10^8 / \text{s}$ with 400W
 μ^- : $1 \times 10^8 / \text{s}$ with 400W

PSI muon yields

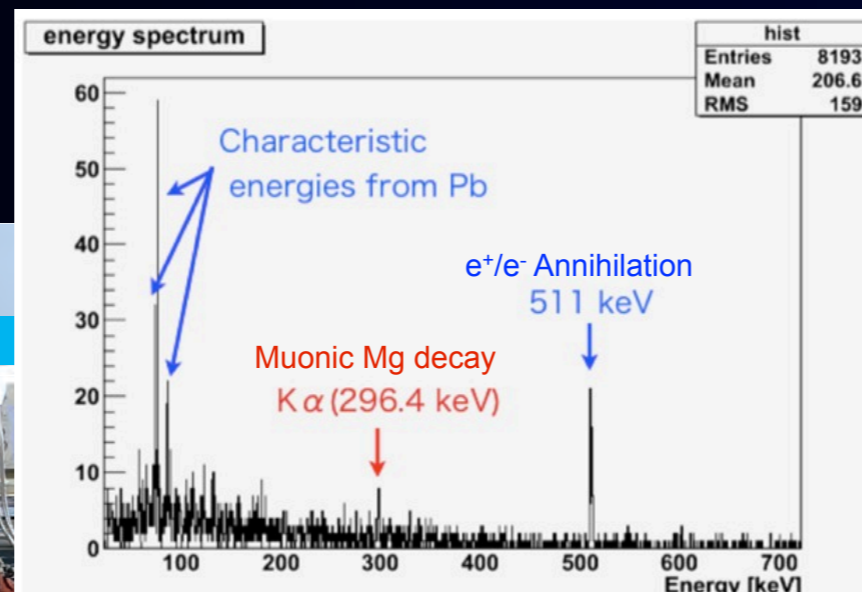
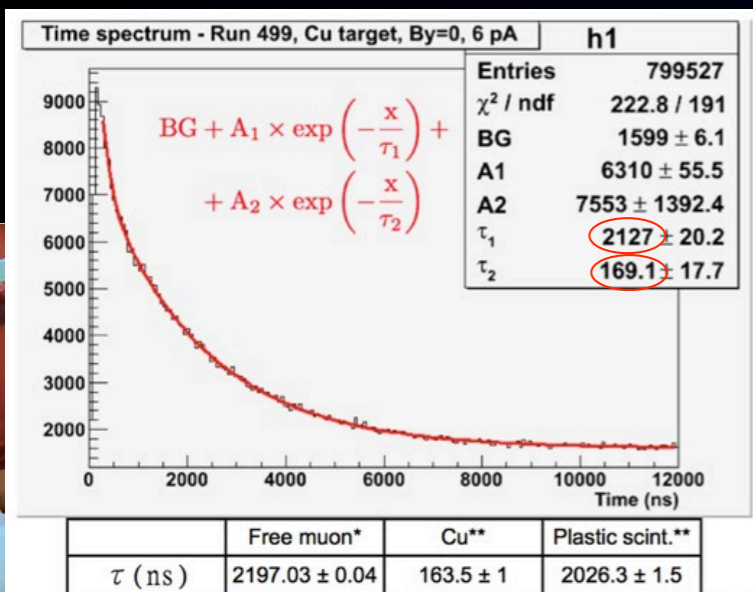
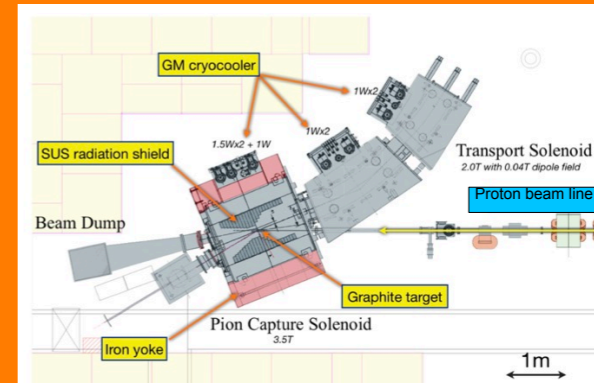
μ^+ : $O(10^8) / \text{s}$ with 1.4MW
 μ^- : $O(10^8) / \text{s}$ with 1.4MW

3.5T and graphite proton target



素粒子の一つであるミューオンを世界最高の効率で生成する装置「MuSIC」。宇宙の始まりに何が起こったのか、宇宙はどのような法則で成り立っているのかを、大量のミューオンと最新技術を駆使して研究する

MuSIC at RCNP, Osaka University (2011 -)

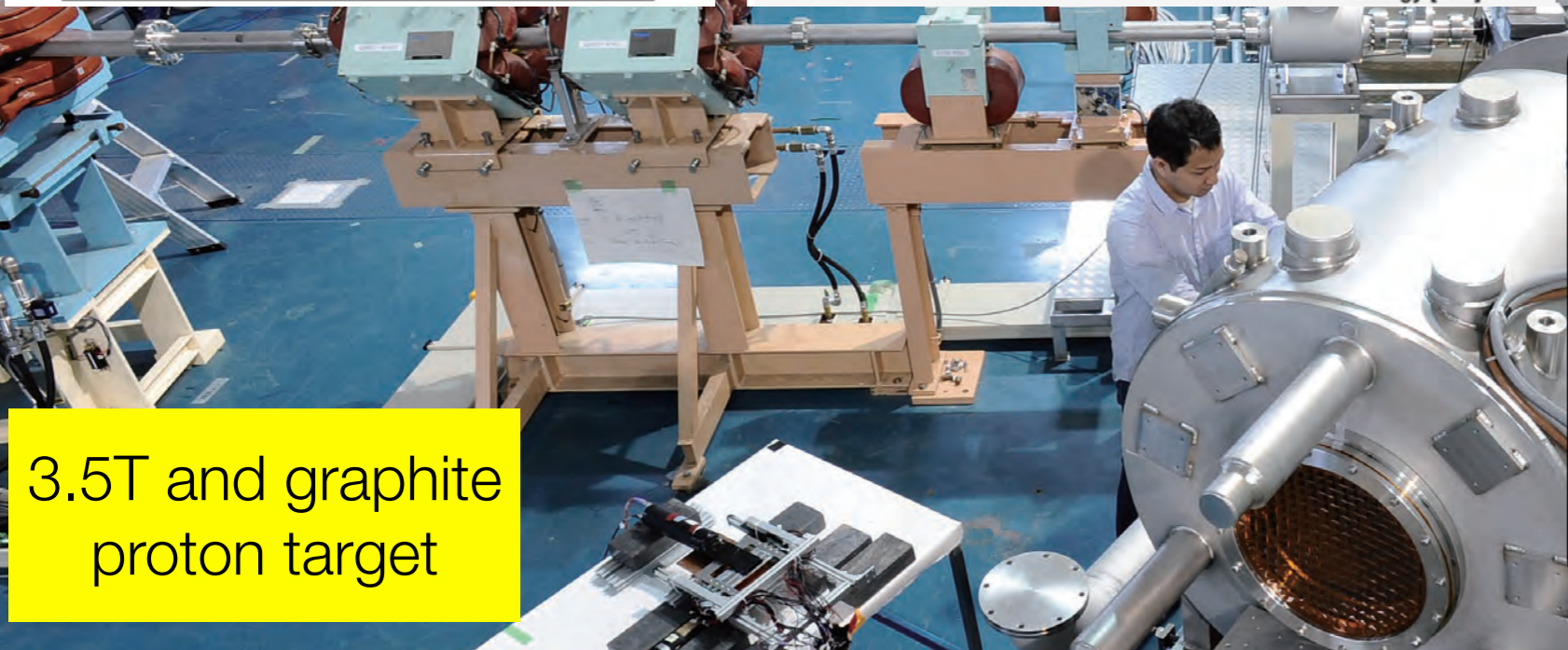


MuSIC muon yields

μ^+ : $3 \times 10^8 / \text{s}$ with 400W
 μ^- : $1 \times 10^8 / \text{s}$ with 400W

PSI muon yields

μ^+ : $O(10^8) / \text{s}$ with 1.4MW
 μ^- : $O(10^8) / \text{s}$ with 1.4MW



3.5T and graphite proton target

$10^{11} / \text{s}$ with 50 kW, possible!

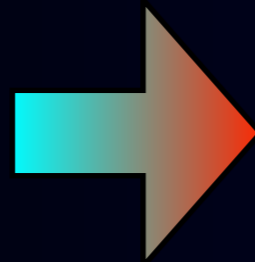
世界
装置
が起
則で
ユ一
する



Improvements of Background Rejection

Improvements of Background Rejection

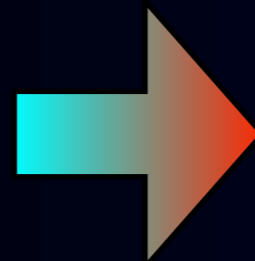
Muon DIO background



Low-mass trackers in vacuum & thin target

improve electron energy resolution

Beam-related backgrounds

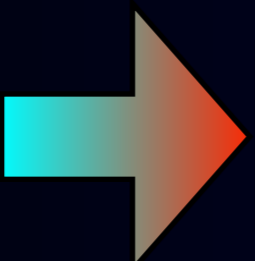


Beam pulsing with separation of 1 μsec

measured between beam pulses

proton extinction = #protons between pulses/#protons in a pulse $< 10^{-10}$

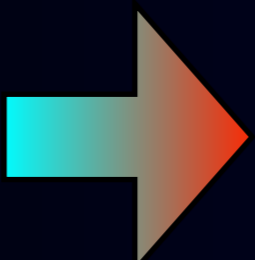
Decay in flight background



Curved solenoids for momentum selection

eliminate energetic muons (>75 MeV/c)

Cosmic ray background

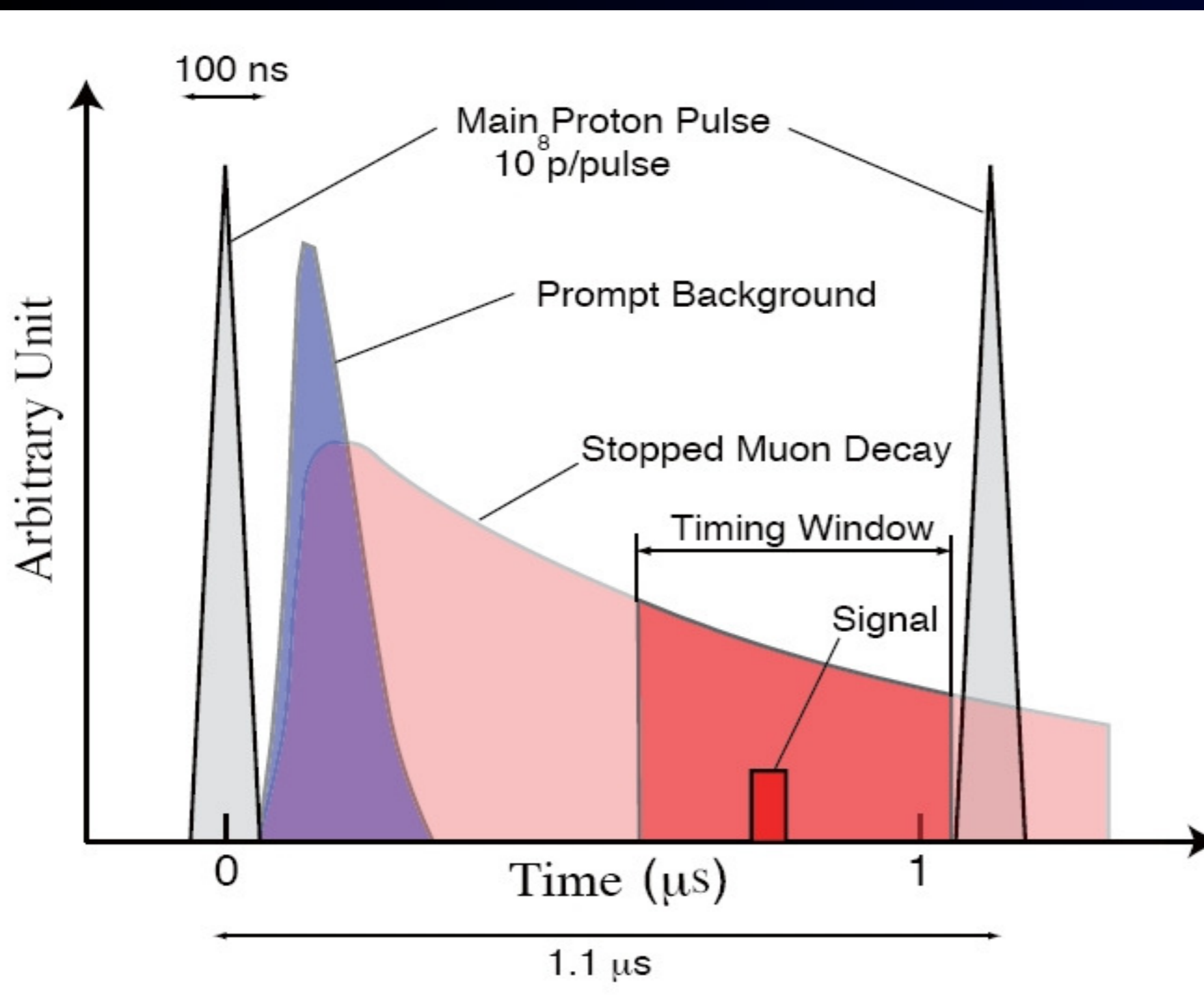
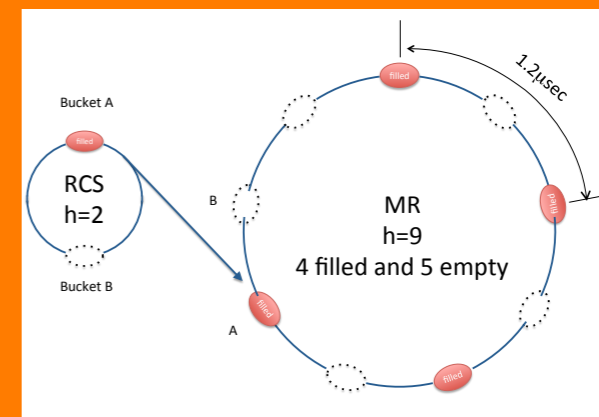


Cosmic ray active veto system

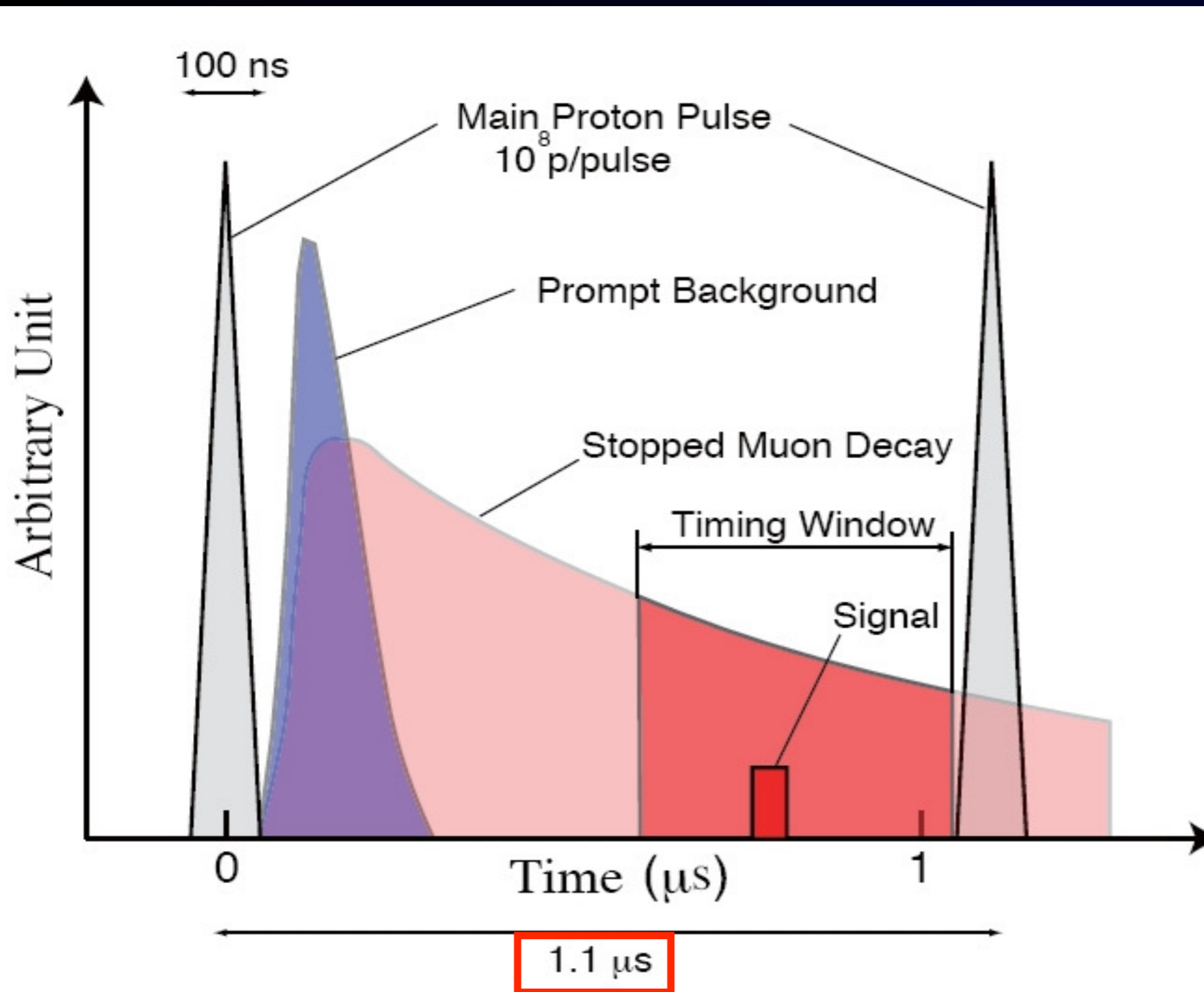
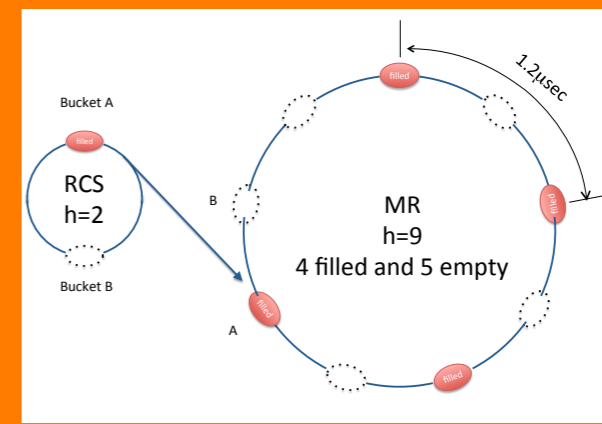
Pulsed Proton Beam Time Structure at J-PARC



Pulsed Proton Beam Time Structure at J-PARC

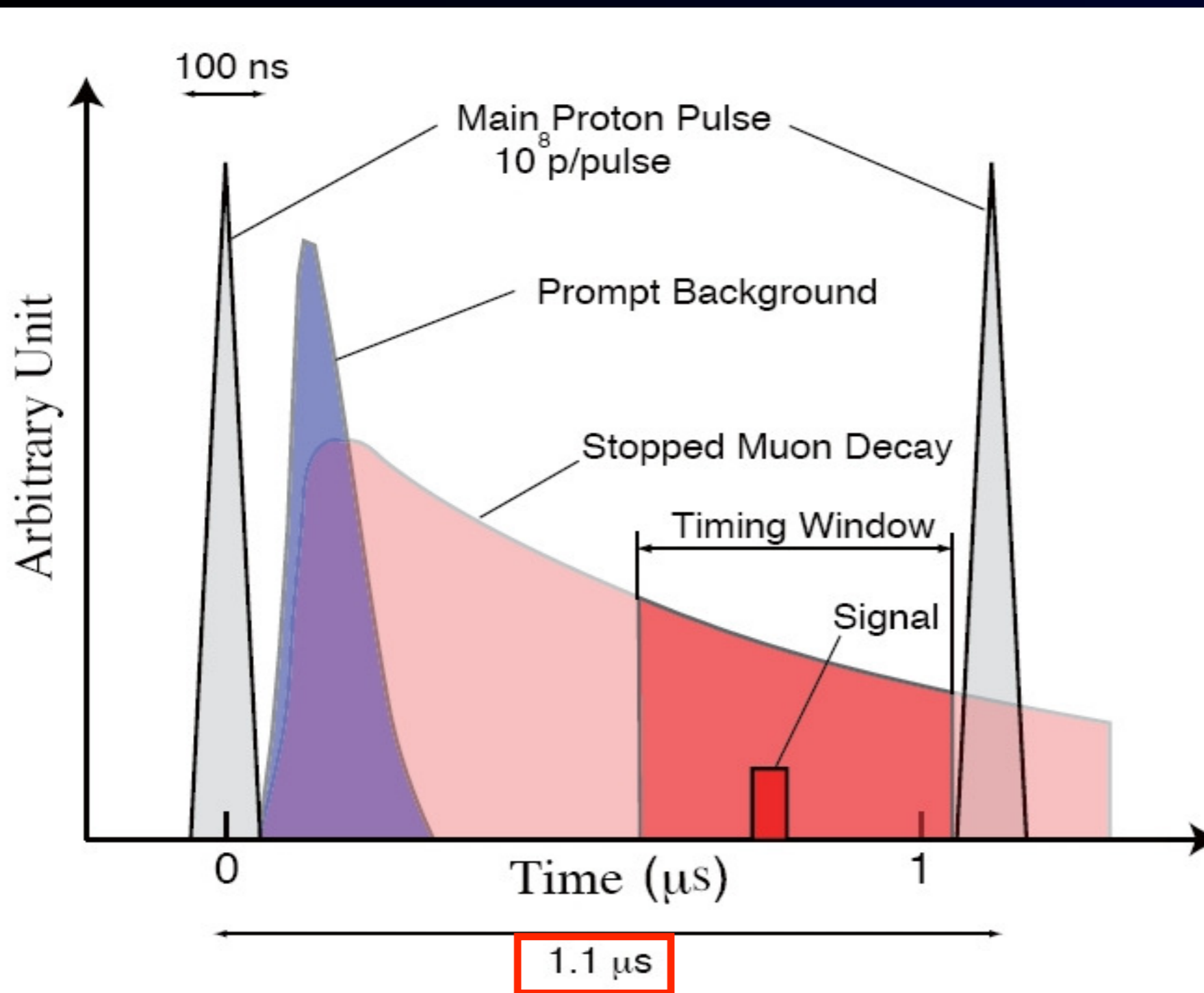
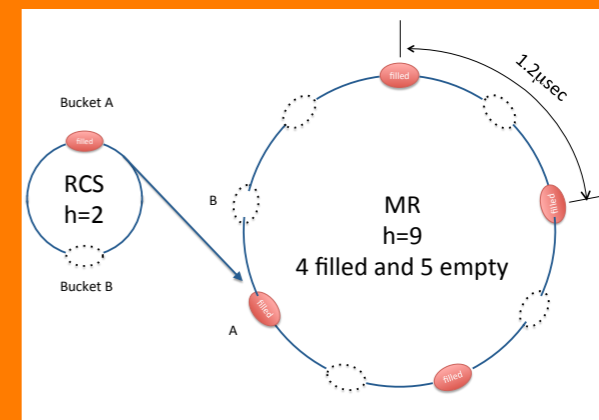


Pulsed Proton Beam Time Structure at J-PARC



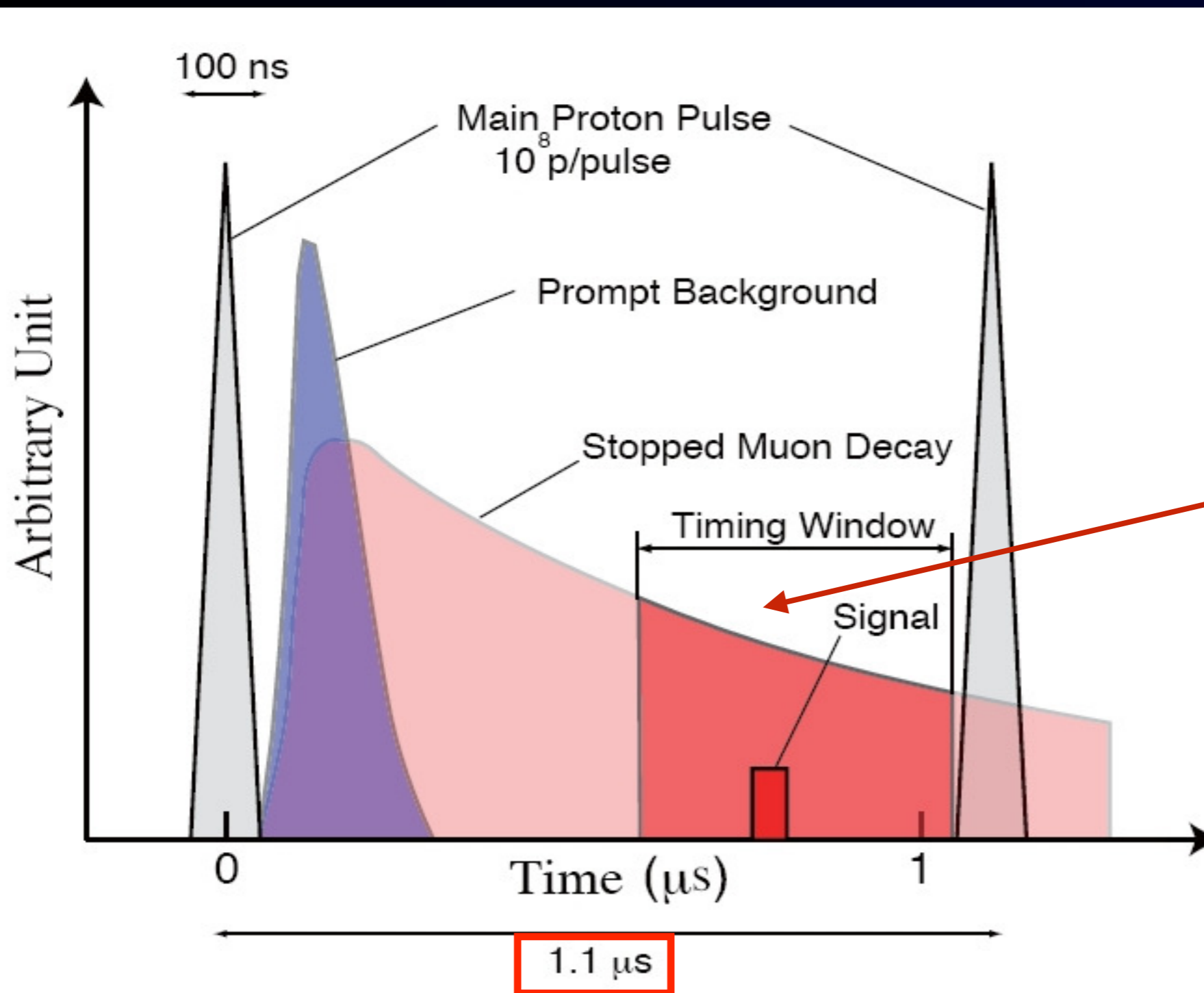
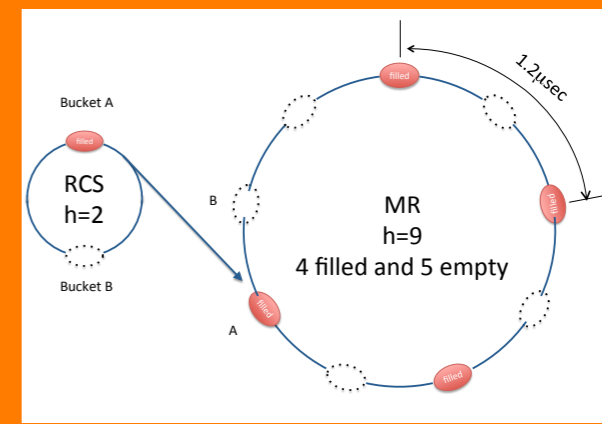
Bunched slow extraction with every other RF bunch filled by protons.

Pulsed Proton Beam Time Structure at J-PARC



Aluminum muon target (muonic atom lifetime of 864 ns is good for 1.1 μs repetition.)

Pulsed Proton Beam Time Structure at J-PARC

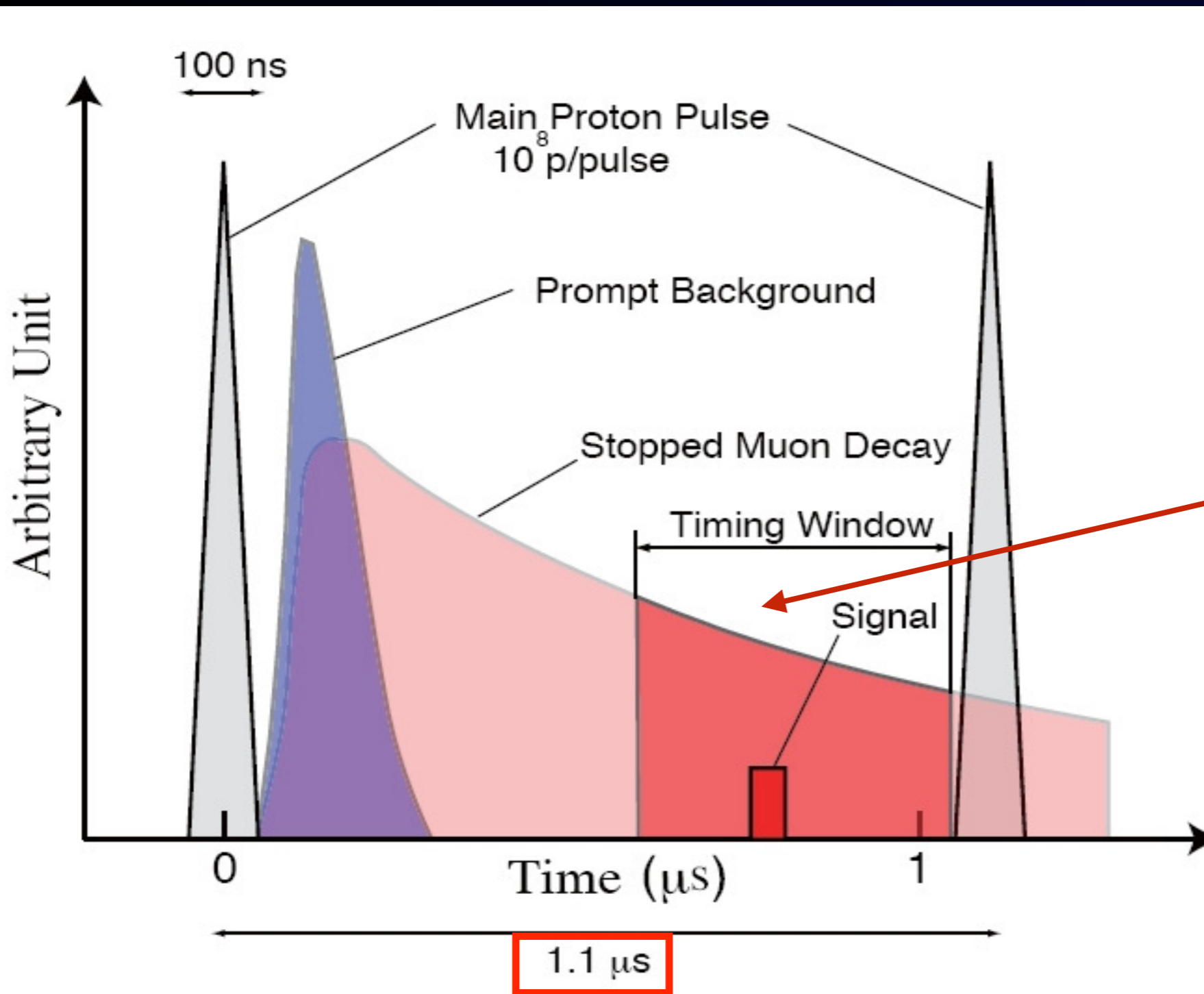
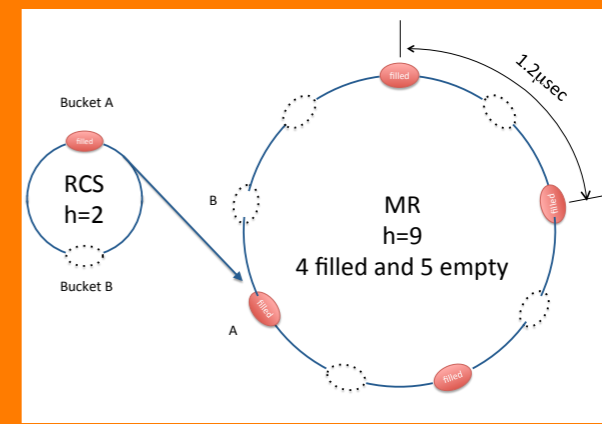


Aluminum muon target (muonic atom lifetime of 864 ns is good for 1.1 μs repetition.)

Delayed time window to avoid beam background, like pions. (from 700 ns to 1.1 μs)

Bunched slow extraction with every other RF bunch filled by protons.

Pulsed Proton Beam Time Structure at J-PARC

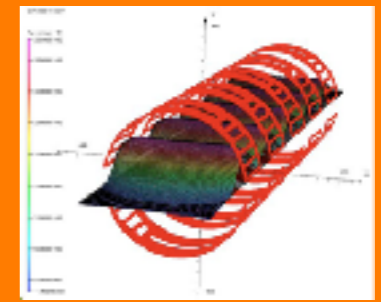


Aluminum muon target (muonic atom lifetime of 864 ns is good for 1.1 μs repetition.)

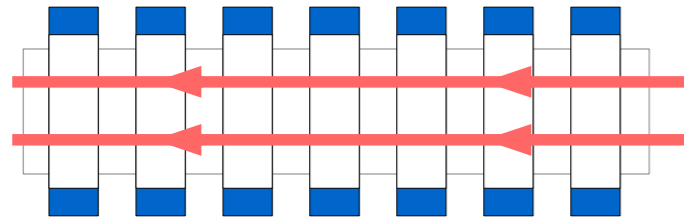
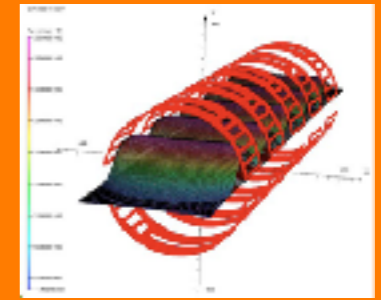
Delayed time window to avoid beam background, like pions. (from 700 ns to 1.1 μs)

Proton extinction factor (proton leakage between pulses) $\sim 10^{-10}$

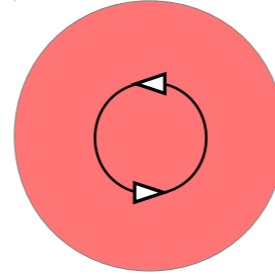
Curved Solenoids with Dipole field in COMET



Curved Solenoids with Dipole field in COMET

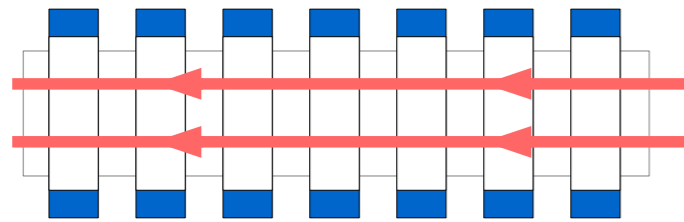
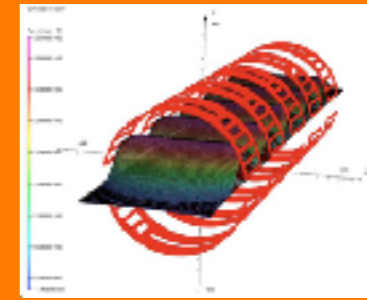


- Uniform B field
- Linear field lines

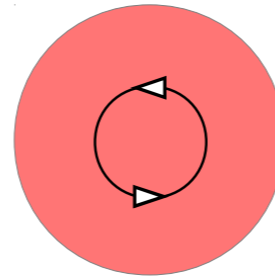


Helical motion
about field lines

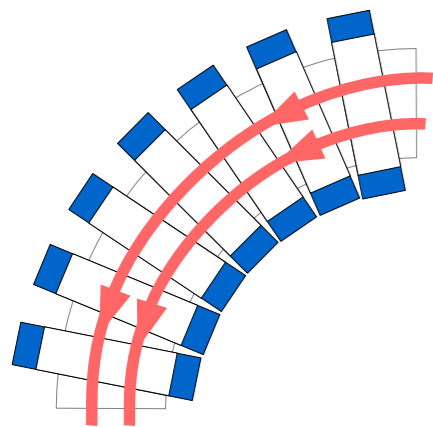
Curved Solenoids with Dipole field in COMET



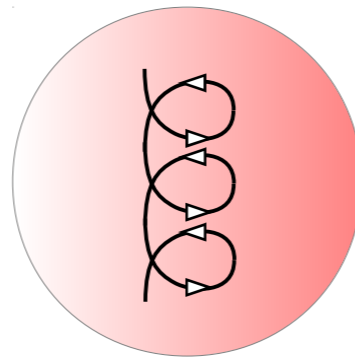
- Uniform B field
- Linear field lines



Helical motion about field lines



- Radial gradient in magnetic field
- Cylindrical field lines



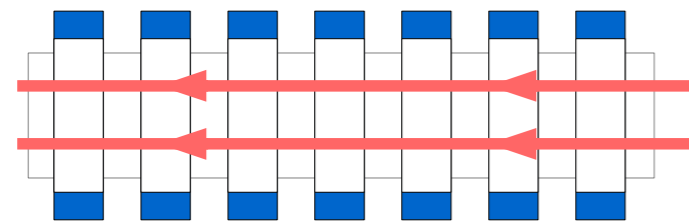
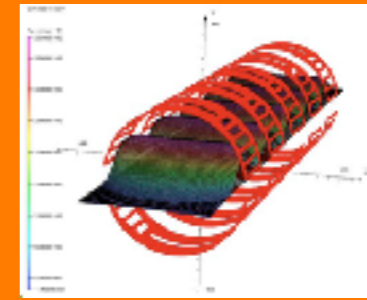
Helical motion about a drifting centre

$$D_{\text{drift}} \propto \frac{p}{qB} \frac{s}{R}$$

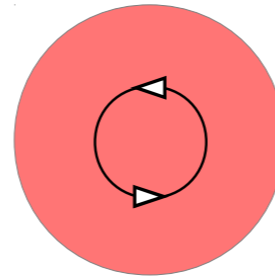
$$D = \frac{1}{qB} \left(\frac{s}{R} \right) \frac{p_L^2 + \frac{1}{2}p_T^2}{p_L},$$

$$= \frac{1}{qB} \left(\frac{s}{R} \right) \frac{p}{2} \left(\cos \theta + \frac{1}{\cos \theta} \right)$$

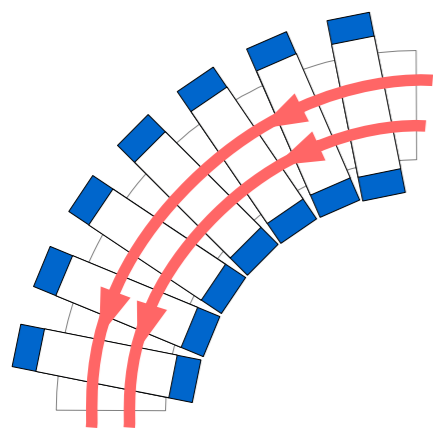
Curved Solenoids with Dipole field in COMET



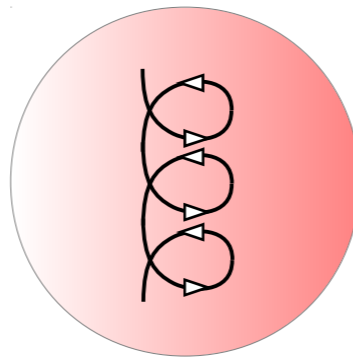
- Uniform B field
- Linear field lines



Helical motion about field lines

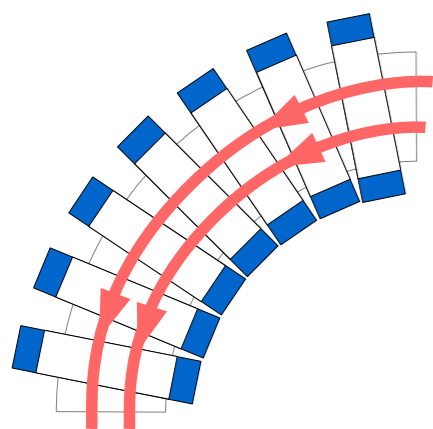


- Radial gradient in magnetic field
- Cylindrical field lines

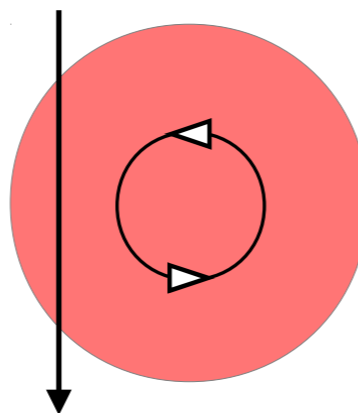


Helical motion about a drifting centre

$$D_{\text{drift}} \propto \frac{p}{qB} \frac{s}{R}$$



- Radial gradient in magnetic field
- Cylindrical field lines
- dipole field normal to the bending plane



Helical motion of selected momentum p_0 staying in the bending plane

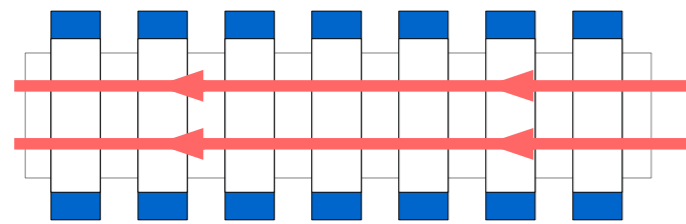
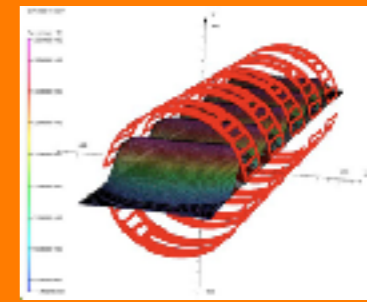
$$B_{\text{dipole}} \propto \frac{p_0}{qR}$$

$$D = \frac{1}{qB} \left(\frac{s}{R} \right) \frac{p_L^2 + \frac{1}{2}p_T^2}{p_L},$$

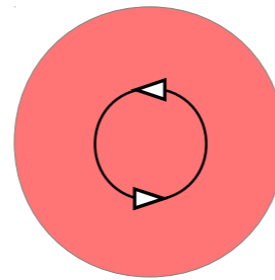
$$= \frac{1}{qB} \left(\frac{s}{R} \right) \frac{p}{2} \left(\cos \theta + \frac{1}{\cos \theta} \right)$$

$$B_{\text{comp}} = \frac{1}{qR} \frac{p_0}{2} \left(\cos \theta_0 + \frac{1}{\cos \theta_0} \right)$$

Curved Solenoids with Dipole field in COMET

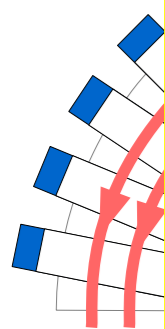


- Uniform B field
- Linear field lines

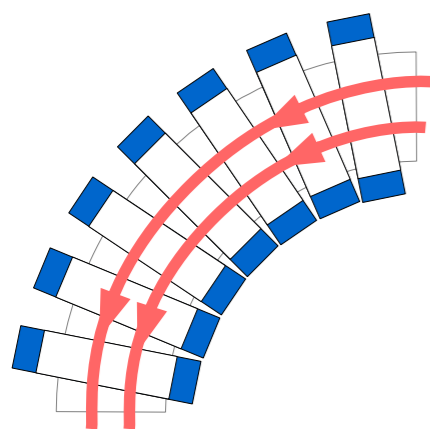


Helical motion about field lines

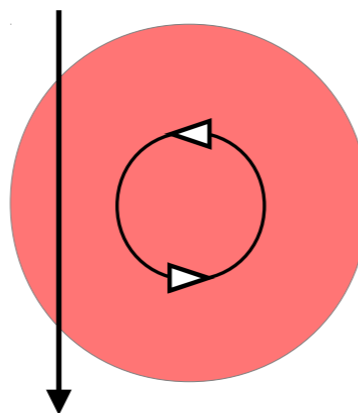
Advantages:



- The second curved solenoid with opposite bending is not needed.
- The diameter of curved solenoids gets smaller.
- Muon beam is momentum-dispersive at the end.



- Radial gradient in magnetic field
- Cylindrical field lines
- dipole field normal to the bending plane



Helical motion of selected momentum p_0 staying in the bending plane

$$B_{\text{dipole}} \propto \frac{p_0}{qR}$$

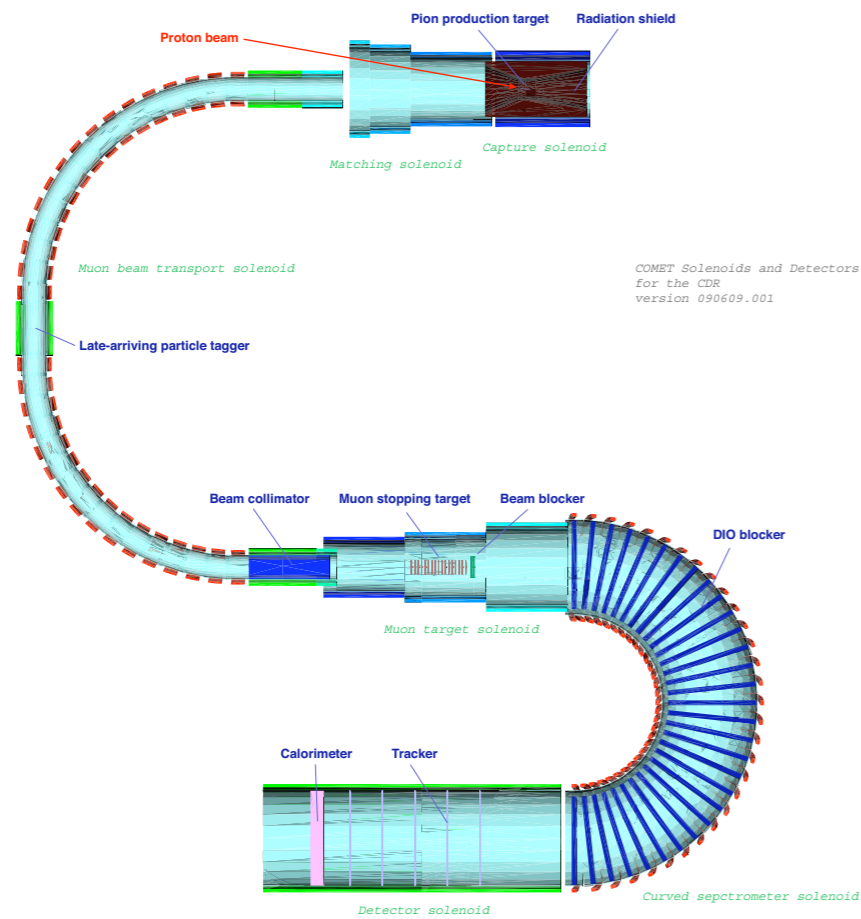
$$B_{\text{comp}} = \frac{1}{qR} \frac{p_0}{2} \left(\cos \theta_0 + \frac{1}{\cos \theta_0} \right)$$

$$\frac{1}{2} p_T^2, \left(\cos \theta + \frac{1}{\cos \theta} \right)$$

COMET Features



COMET Features



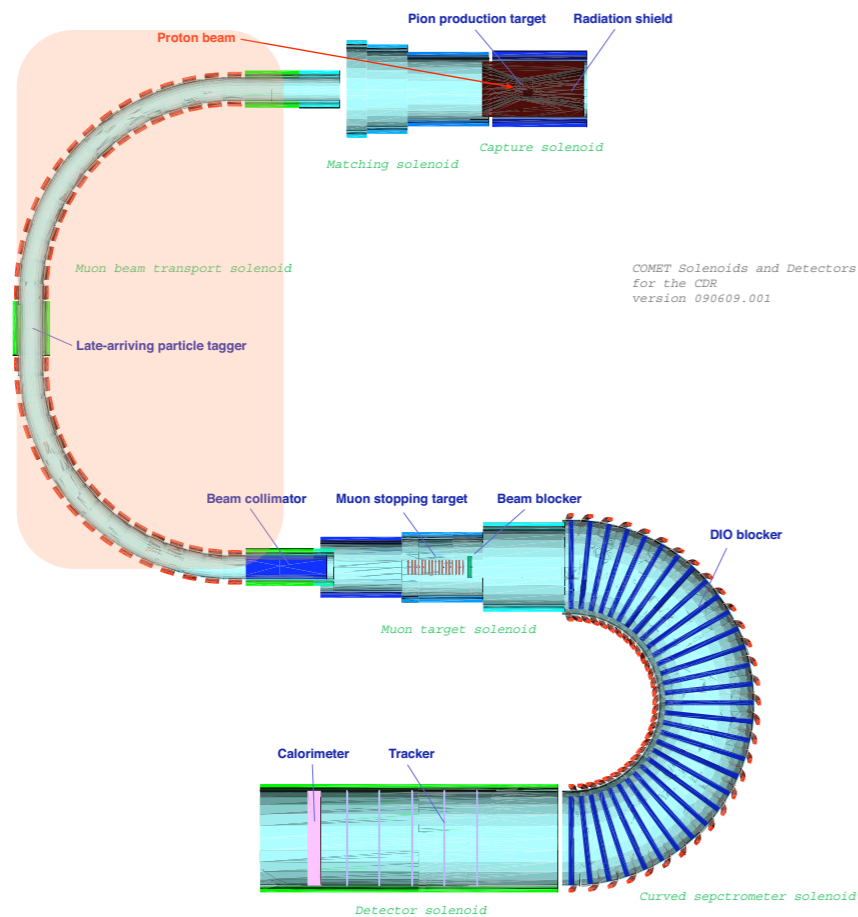
muon
beam line

2x 90° bend
(same direction)

electron
spectrometer

180° bend
curved solenoids

COMET Features



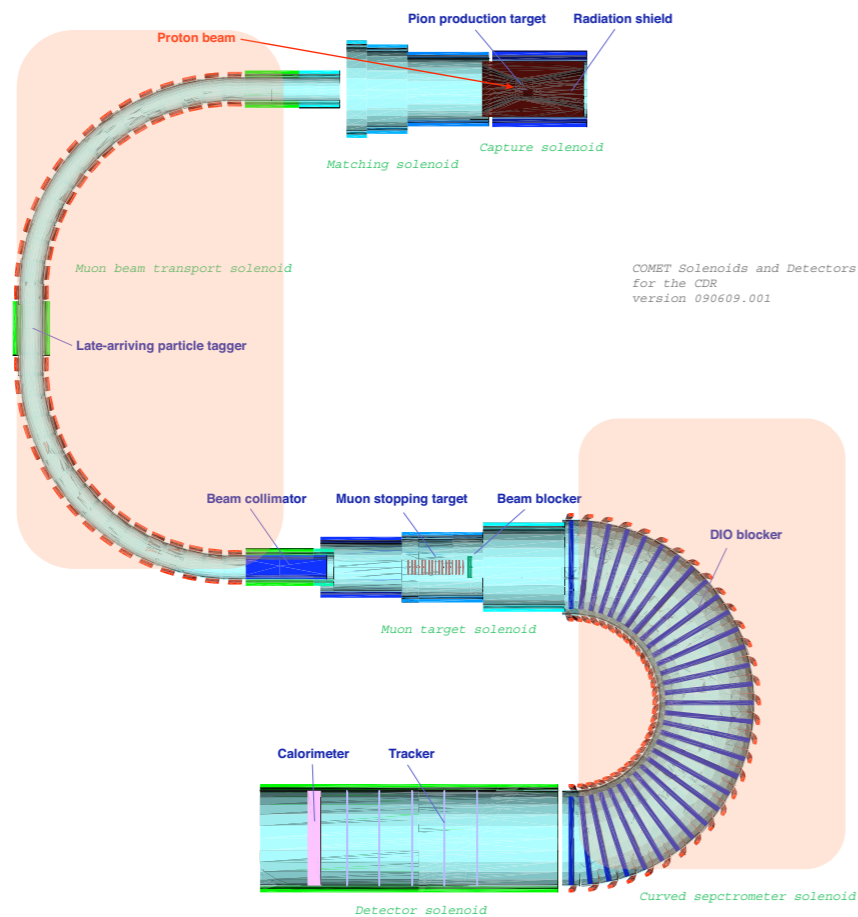
Selection of low momentum muons

- eliminate high energy electrons from muon decays in flight

momentum selection capability is proportional to bending angle

muon beam line	2x 90° bend (same direction)
electron spectrometer	180° bend curved solenoids

COMET Features



Selection of low momentum muons

- eliminate high energy electrons from muon decays in flight

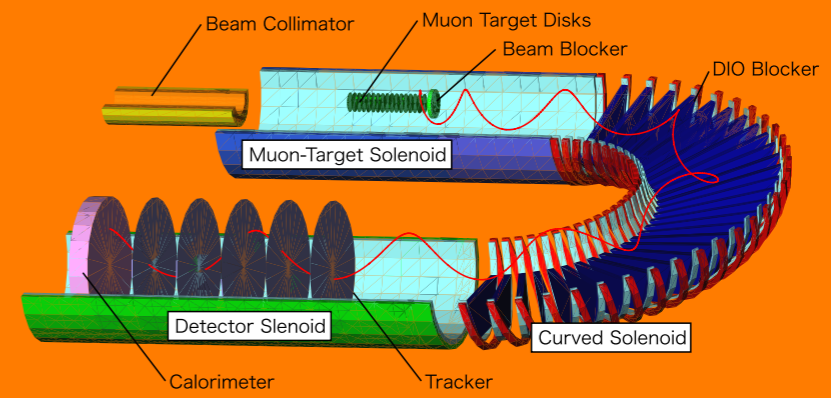
momentum selection capability is proportional to bending angle

Selection of 105 MeV signal electrons

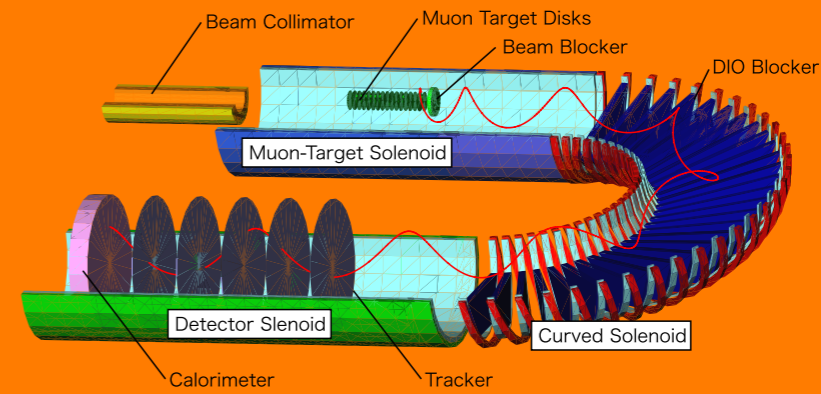
- eliminate neutrons and gamma-rays from muon target
- eliminate protons from muon target
- eliminate low energy DIO electrons from muon decays from muon target

muon beam line	2x 90° bend (same direction)
electron spectrometer	180° bend curved solenoids

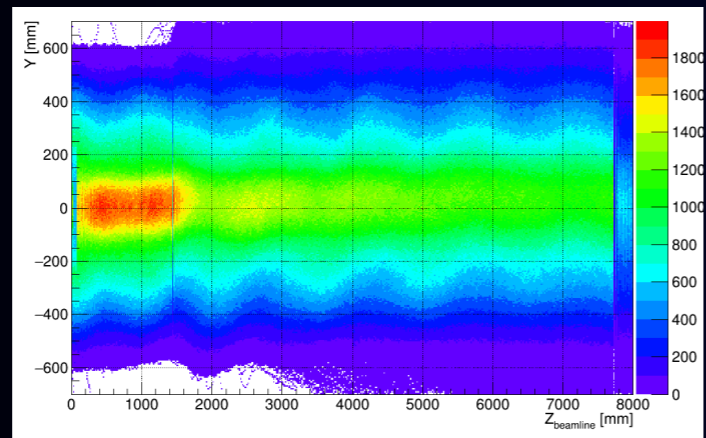
Electron Spectrometer in COMET Phase-II



Electron Spectrometer in COMET Phase-II

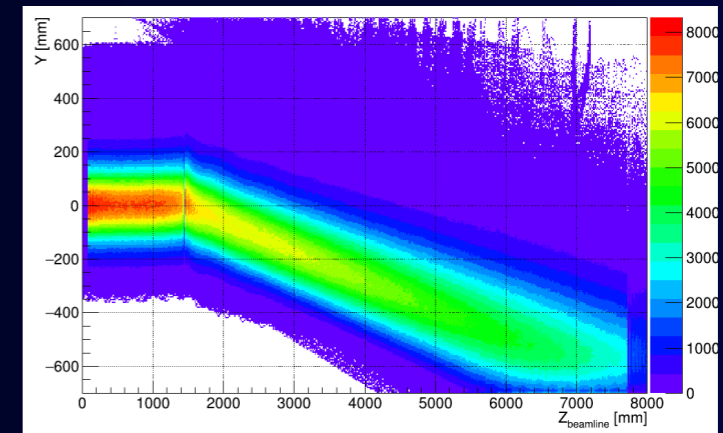


105 MeV/c signal electrons

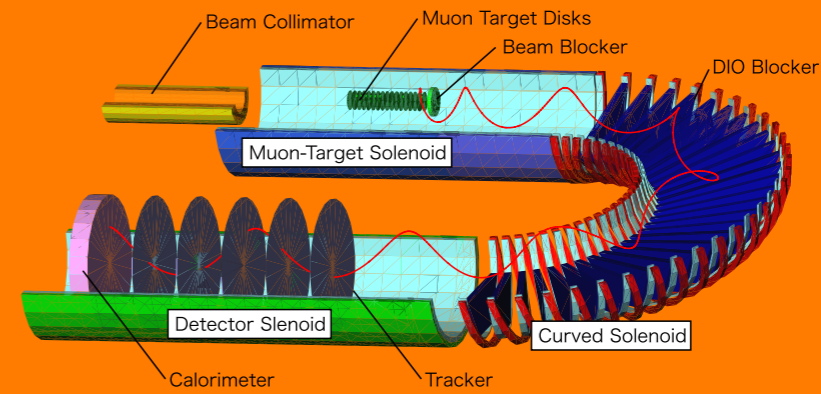


$B_{\text{dipole}} = -0.22\text{T}$

52 MeV/c DIO electrons



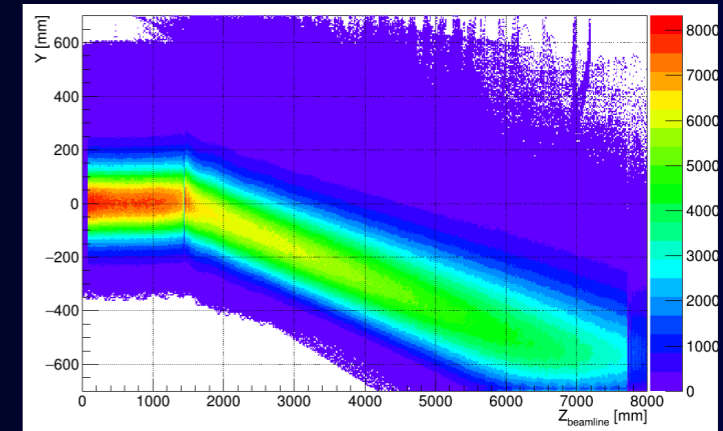
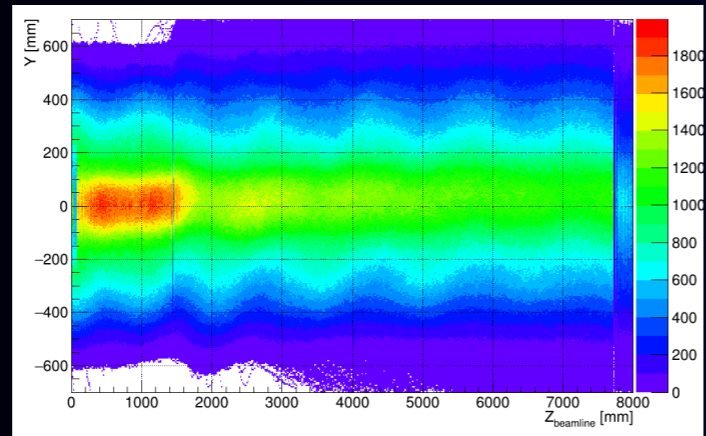
Electron Spectrometer in COMET Phase-II



105 MeV/c signal electrons

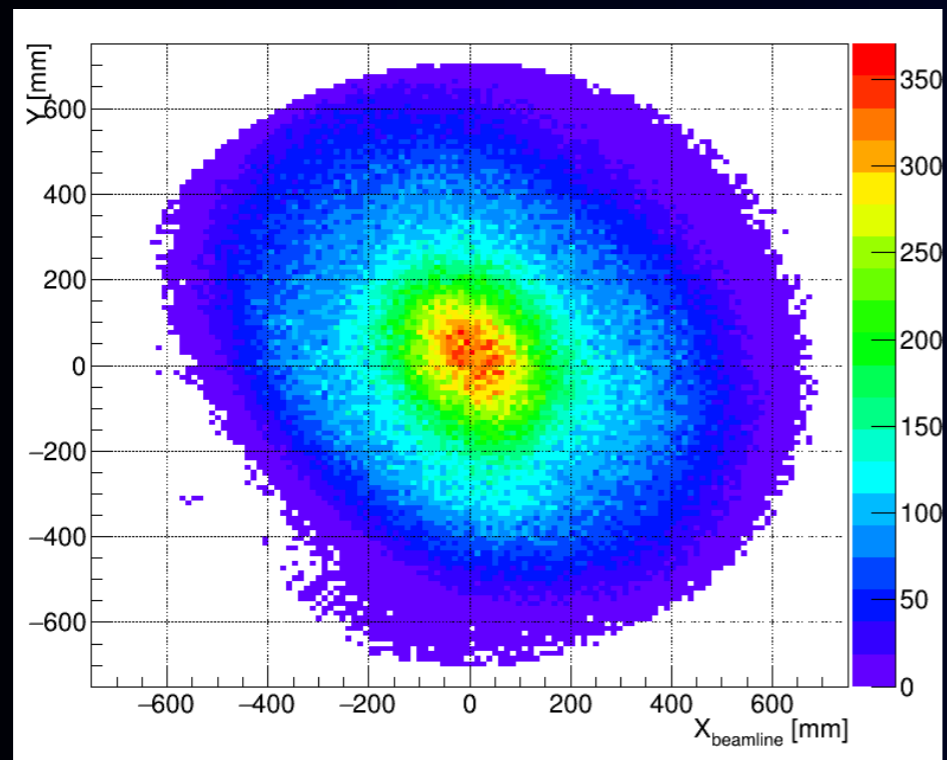
52 MeV/c DIO electrons

$B_{\text{dipole}} = -0.22\text{T}$



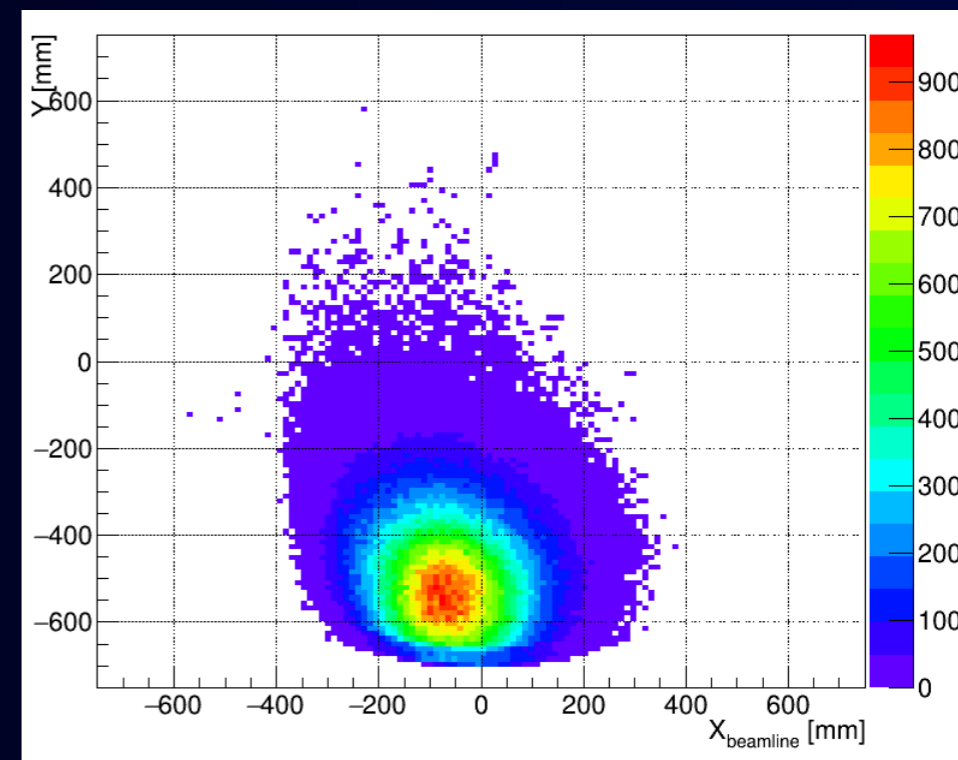
at the end of the electron spectrometer

vertical



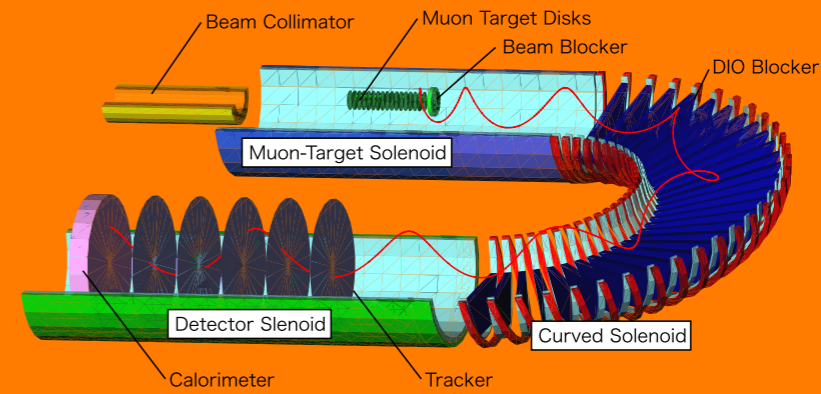
horizontal

vertical



horizontal

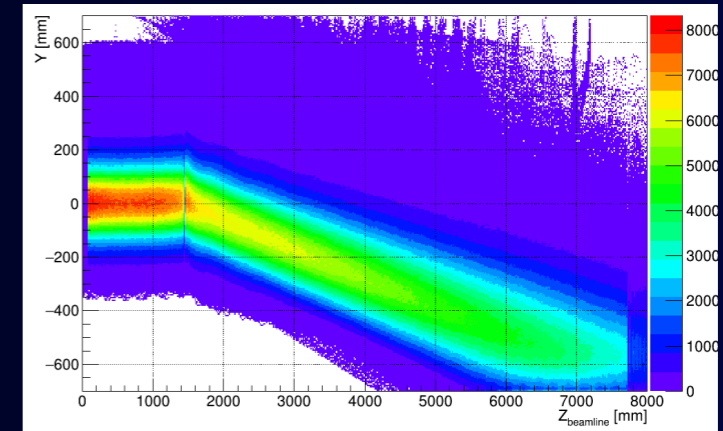
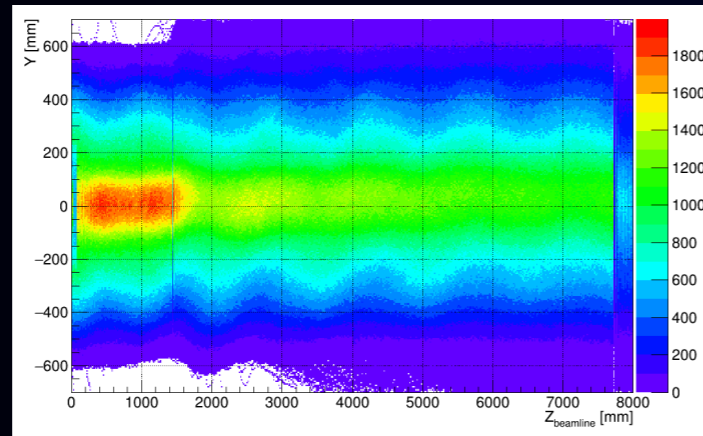
Electron Spectrometer in COMET Phase-II



105 MeV/c signal electrons

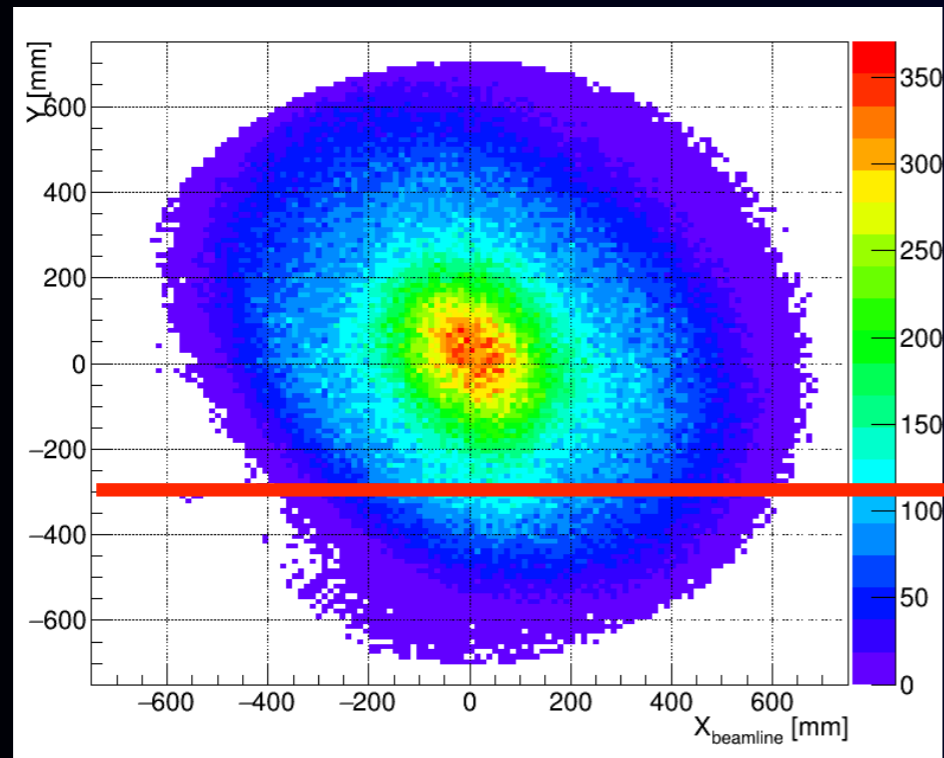
52 MeV/c DIO electrons

$B_{\text{dipole}} = -0.22\text{T}$

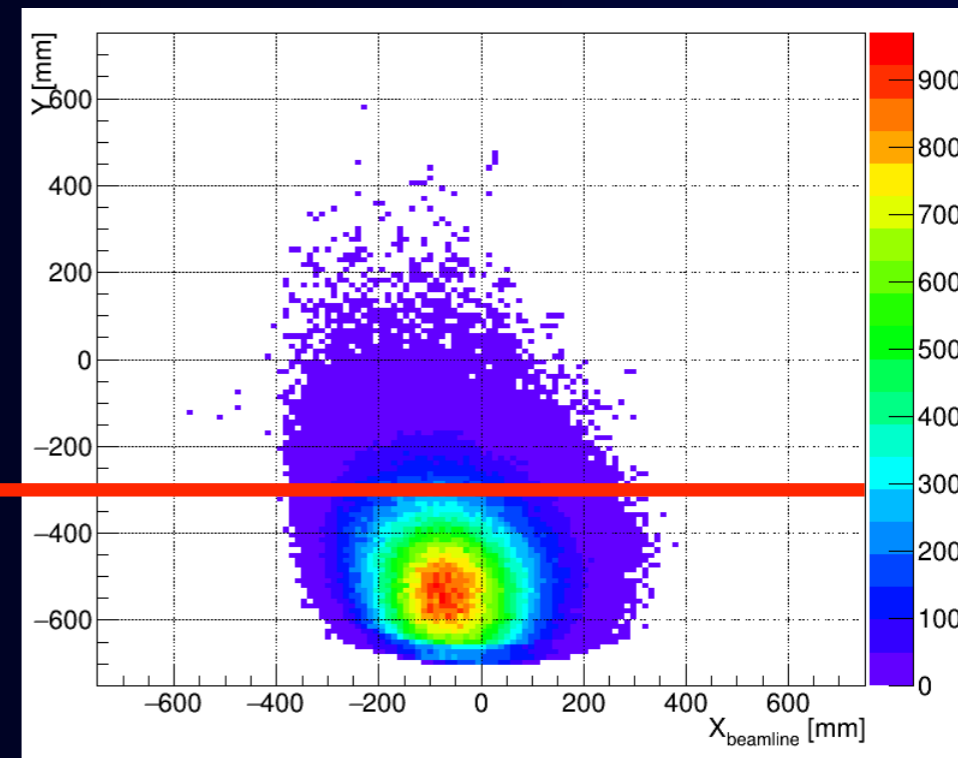


at the end of the electron spectrometer

vertical



vertical



removed

horizontal

horizontal

COMET Collaboration



COMET Collaboration



43 institutes, 17 countries

COMET Staged Approach

COMET Phase-I (2016 -)



COMET Phase-I (2016 -)



proton target

muon target

muon beamline

detector

only the first 90 degree curved solenoid + detector solenoid

COMET Phase-I (2016 -)

- Proton beam, 8 GeV, 3.2kW
- 2×10^9 stopped muons/s

- Single event sensitivity : 2×10^{-15}
- 90% CL limit : $< 5 \times 10^{-15}$
- x100 from SINDRUM-II
- Total background: 0.32 events
- Running time: 0.4 years (1.2×10^7 sec)

proton target

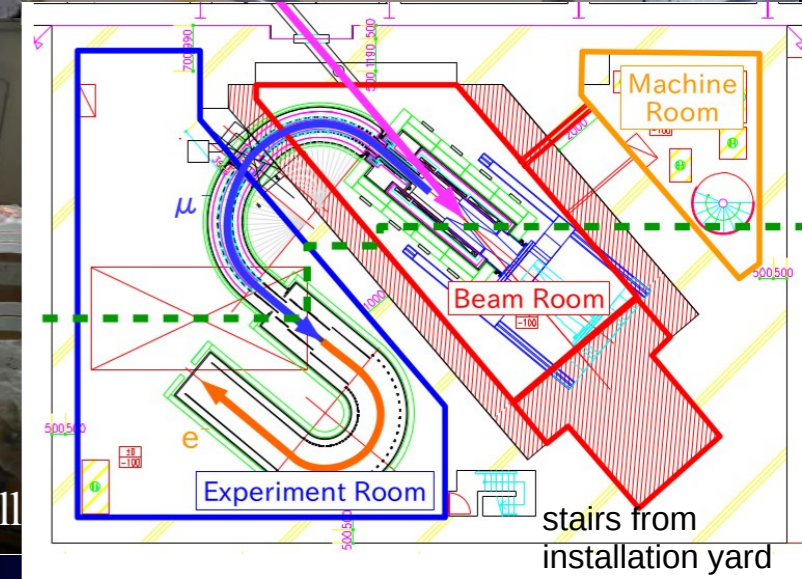
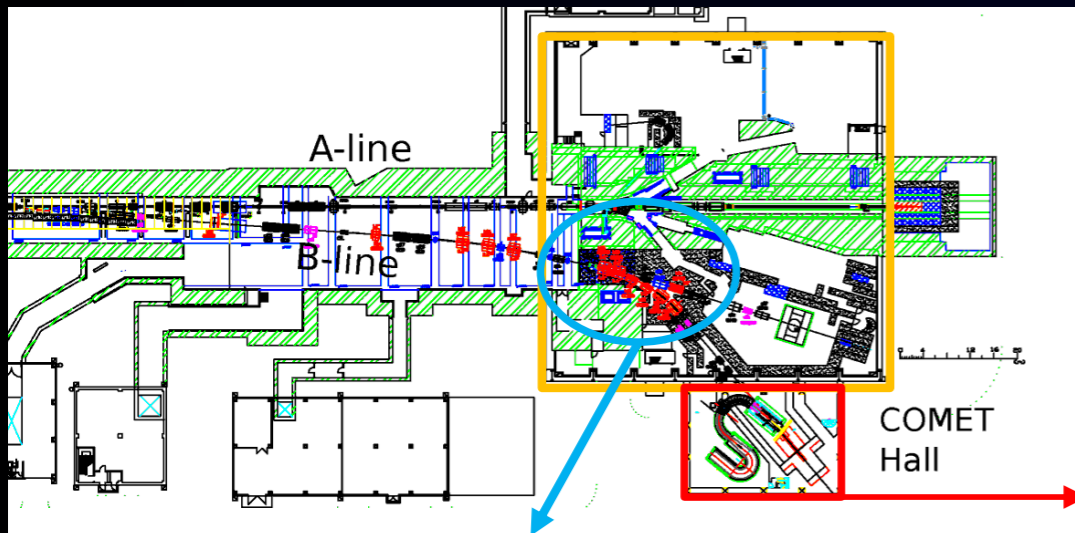
muon target

muon beamline

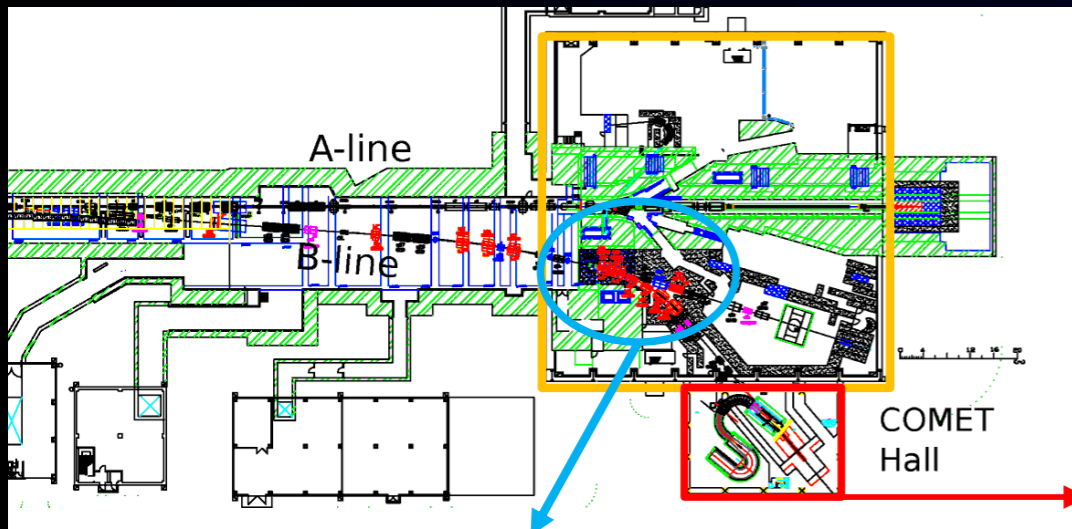
detector

only the first 90 degree curved solenoid + detector solenoid

COMET Facility at J-PARC



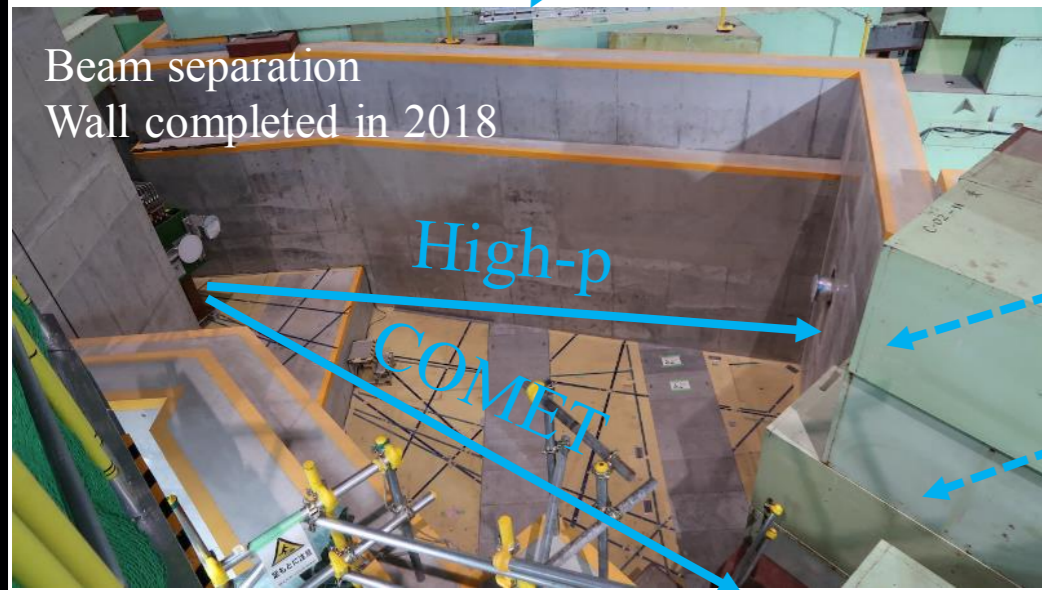
COMET Facility at J-PARC



COMET Experimental Hall
Constructed in 2015



Installation Yard in 2015

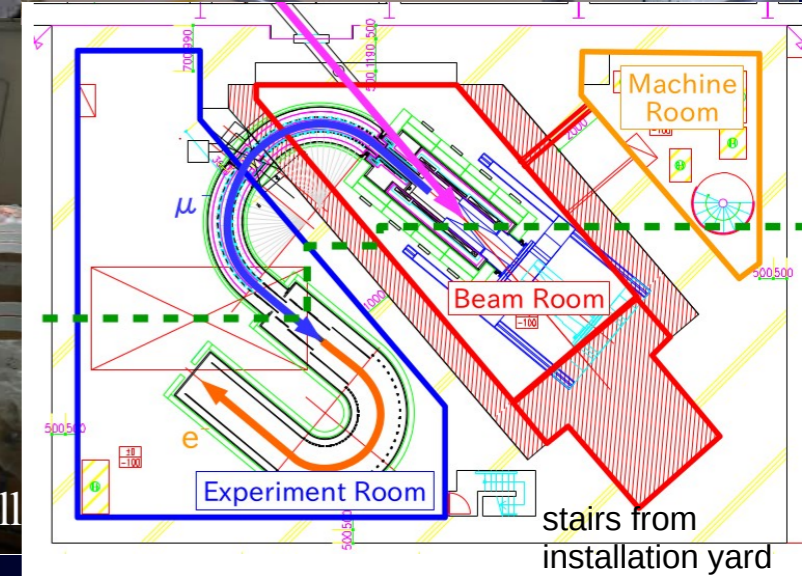


Beam separation
Wall completed in 2018

Experiment Room in 2019



2 magnets will be moved to Hadron Hall

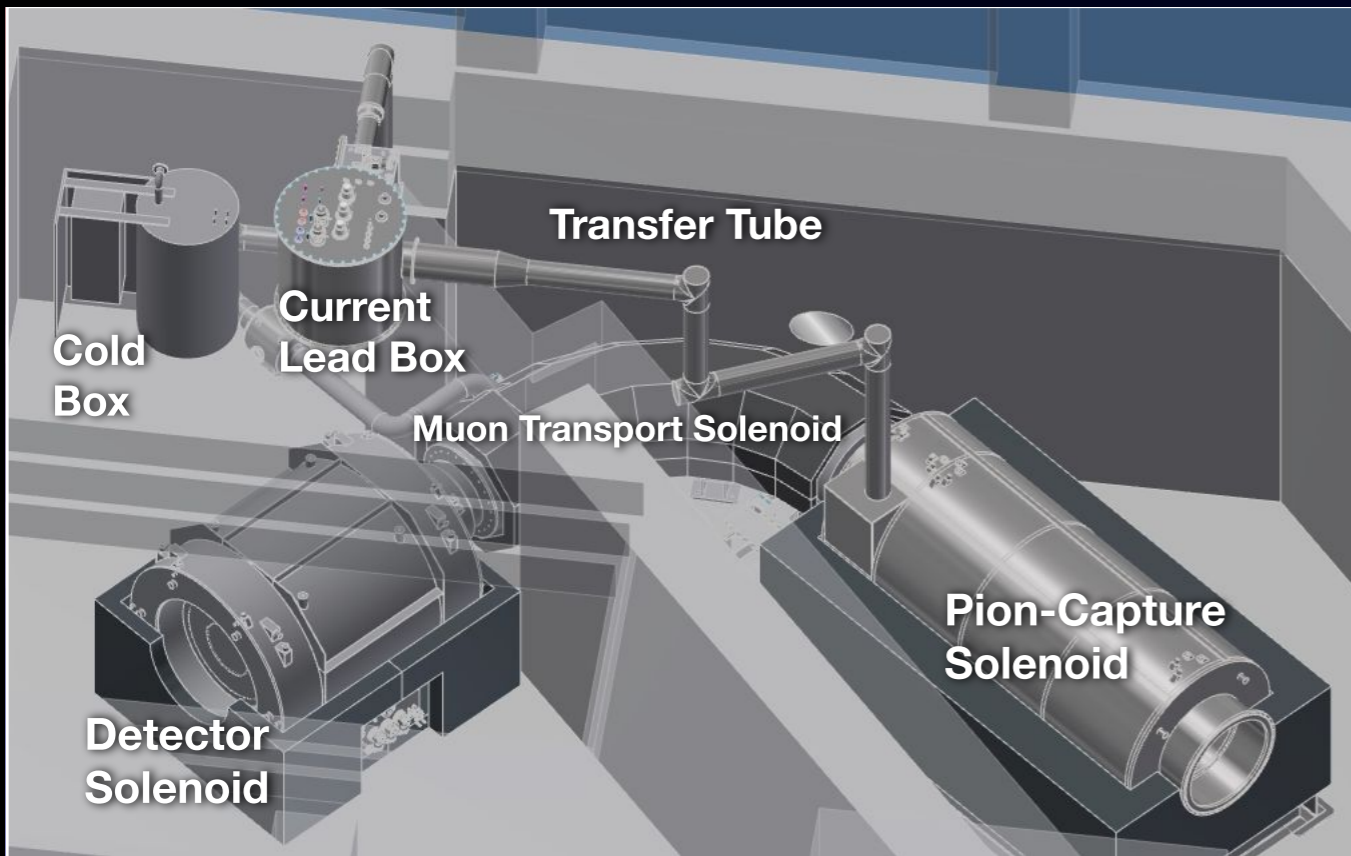


- COMET experimental hall building, completed in 2015
- Cryogenic system, completed in 2021
- New proton C line, completed in 2022

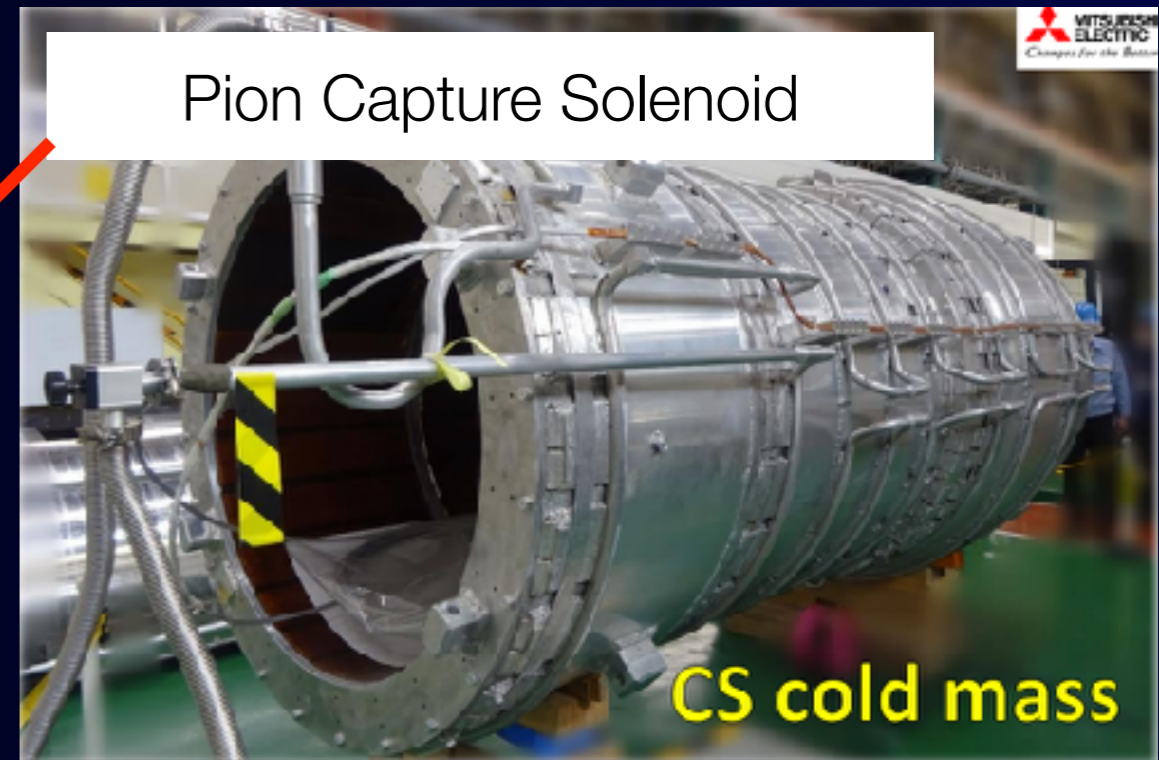
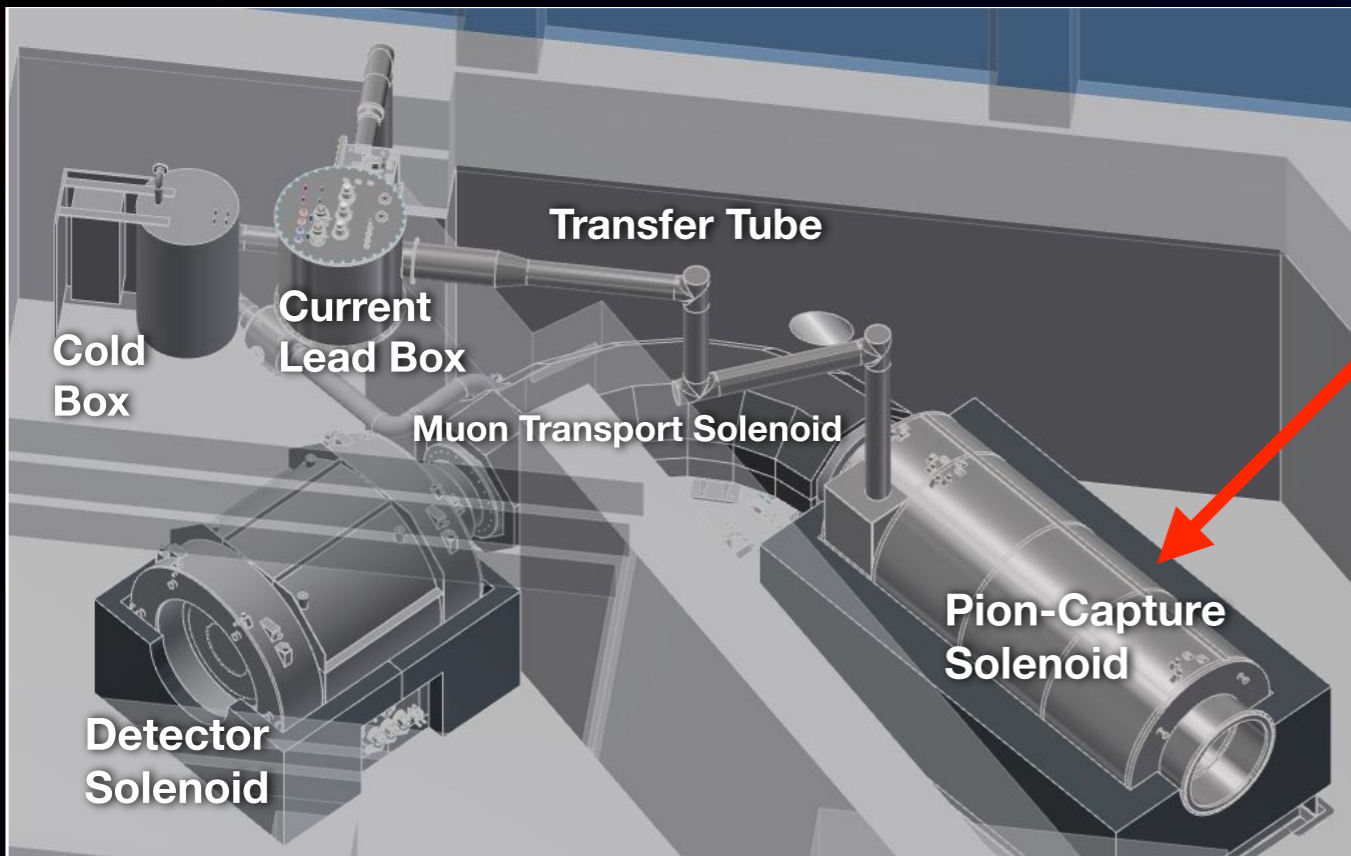
COMET Phase-I : Superconducting Solenoid Construction



COMET Phase-I : Superconducting Solenoid Construction

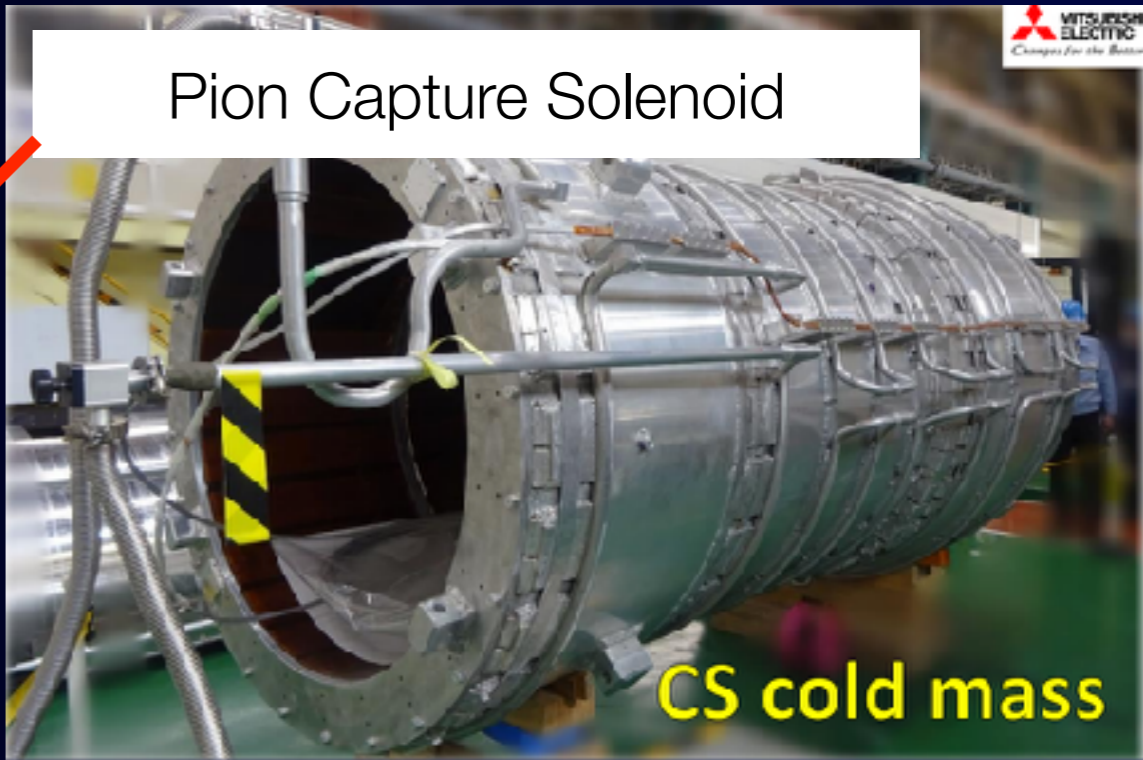
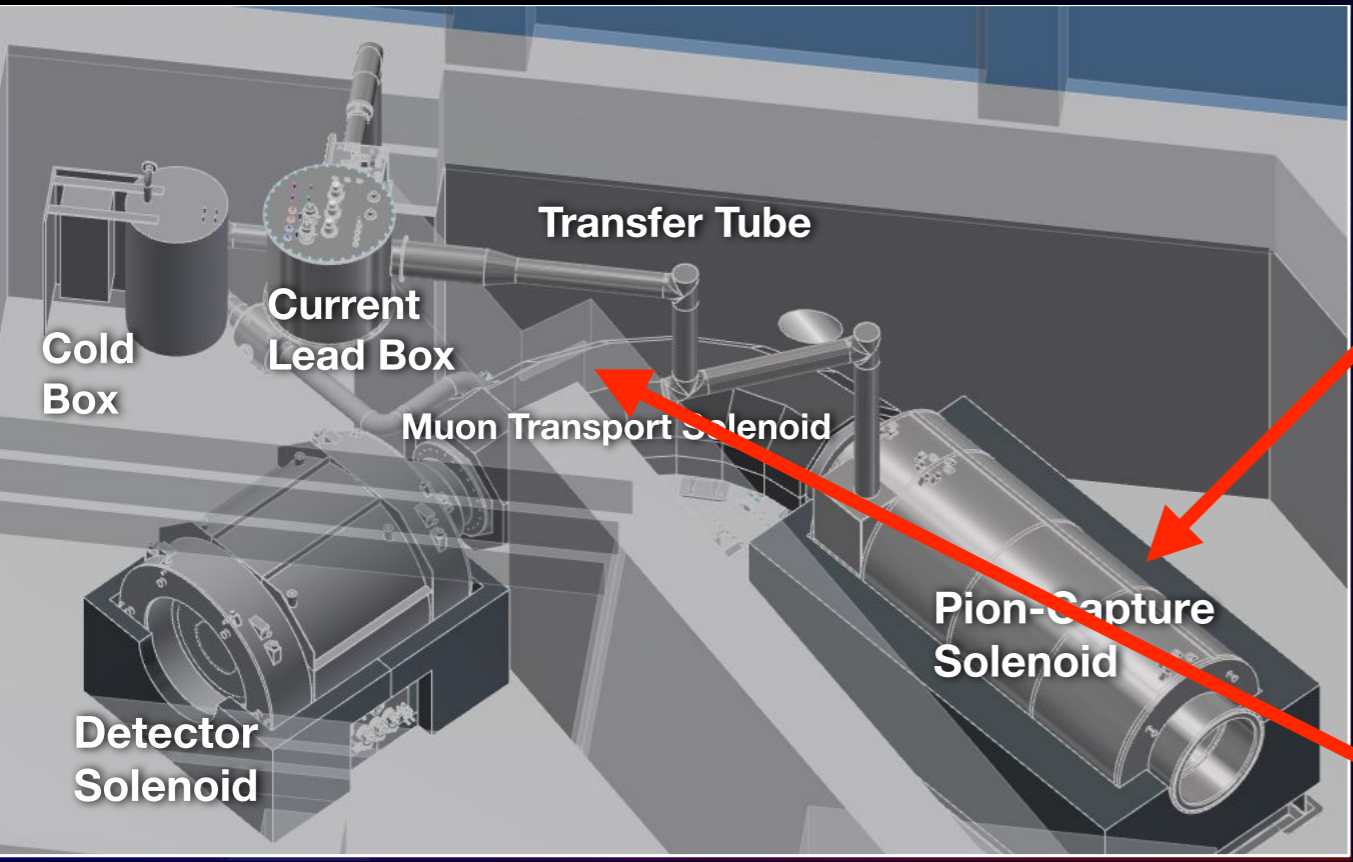


COMET Phase-I : Superconducting Solenoid Construction



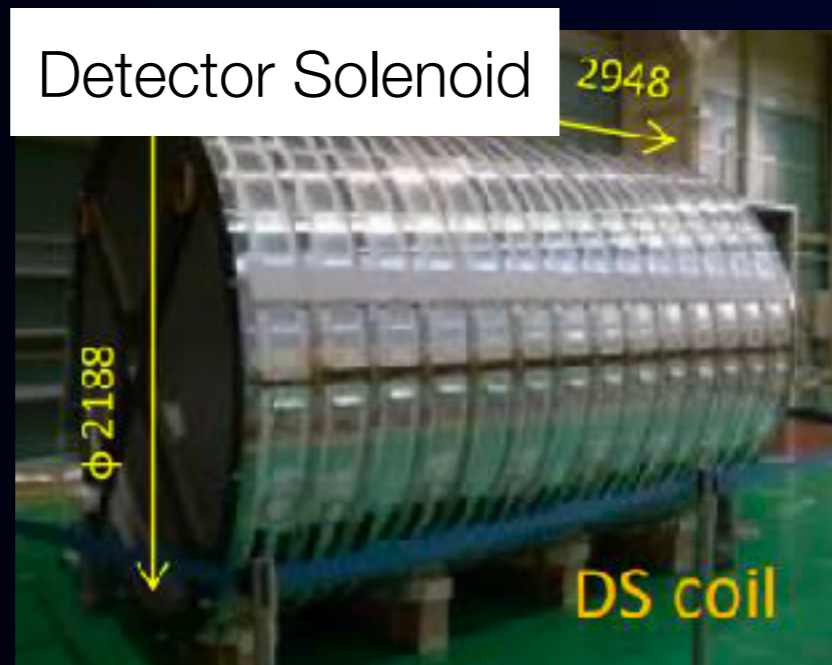
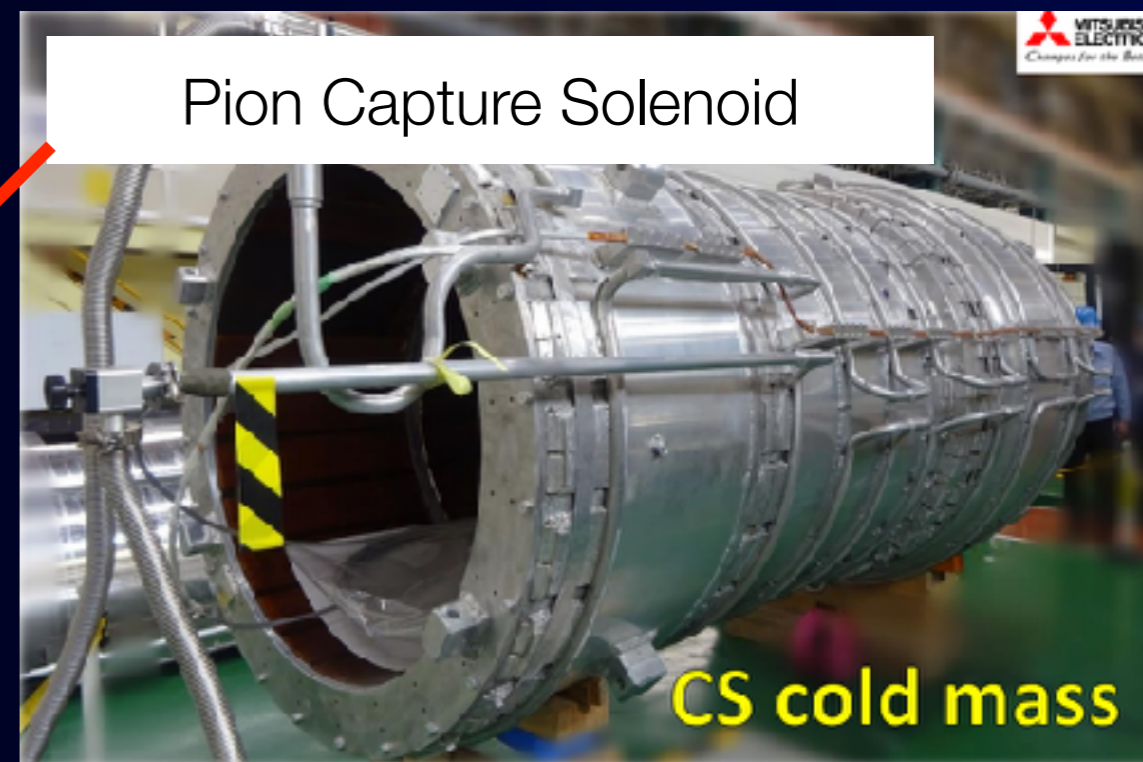
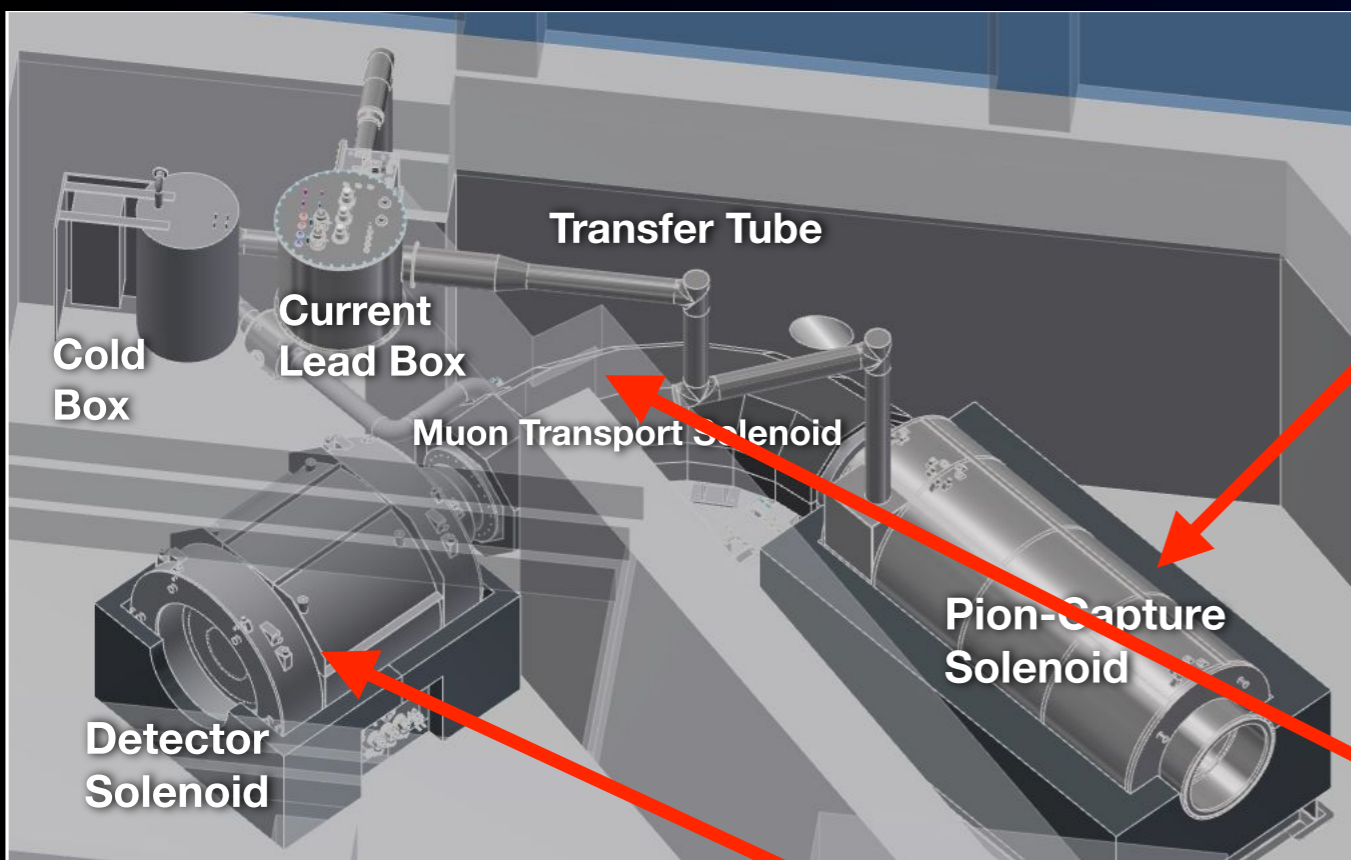
- PCS completed and commissioning will be made in 2025.

COMET Phase-I : Superconducting Solenoid Construction



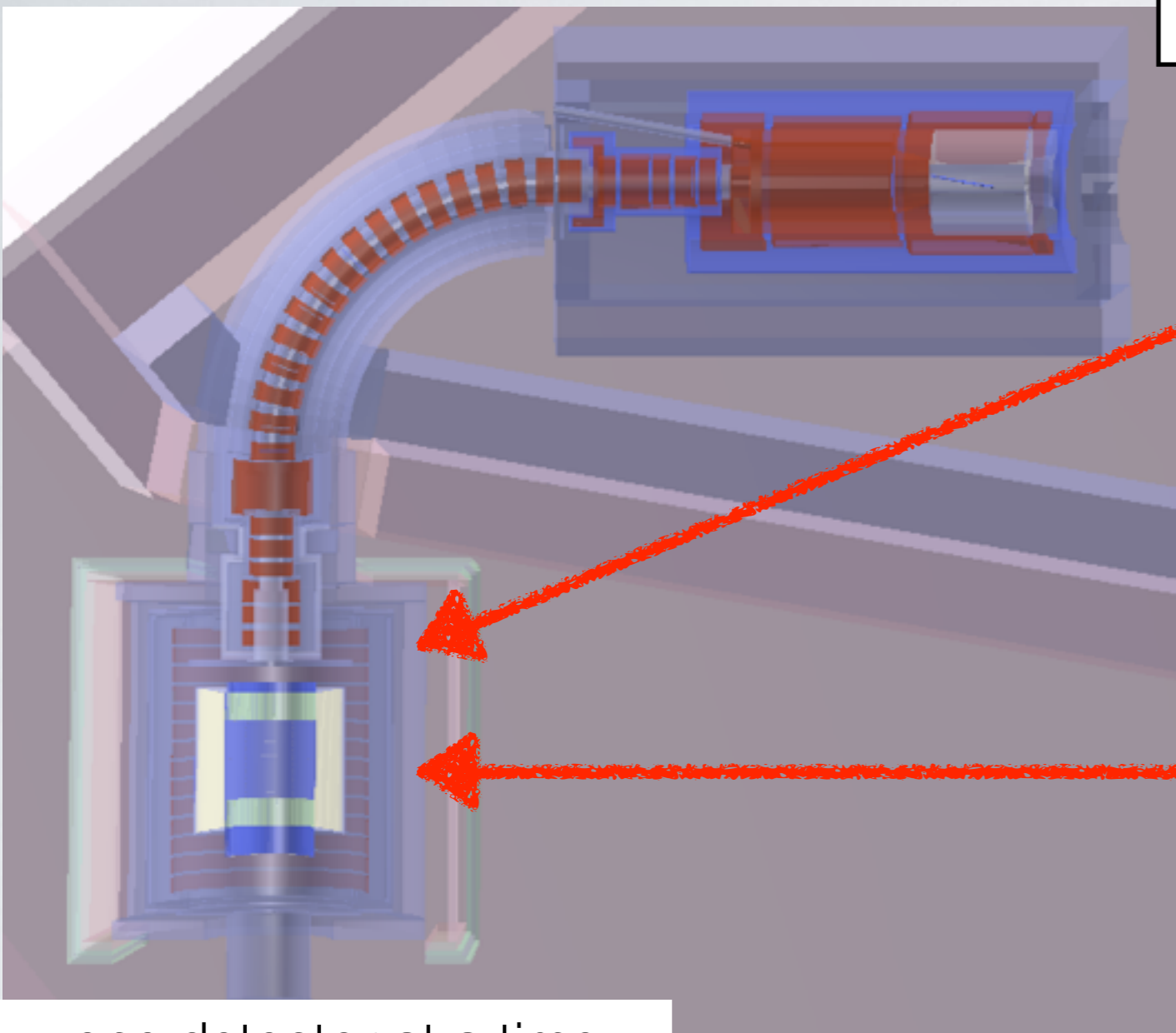
- PCS completed and commissioning will be made in 2025.
- MTS excitation complete in 2023.

COMET Phase-I : Superconducting Solenoid Construction

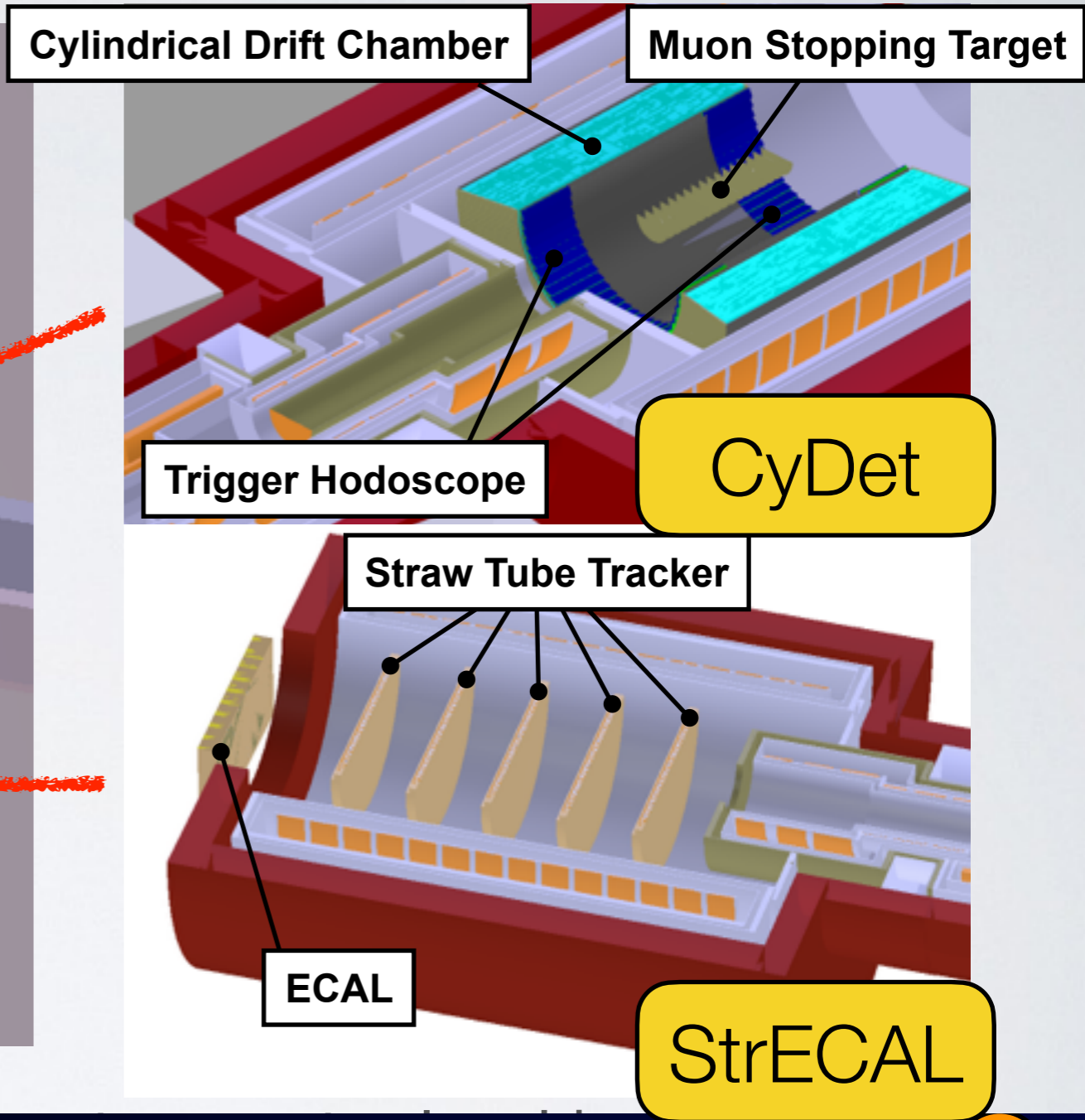


- PCS completed and commissioning will be made in 2025.
- MTS excitation complete in 2023.
- DS assembly will be complete in 2024.

Two Detectors, CyDet and StrECAL , for COMET Phase-I



one detector at a time



Two Detectors, CyDet and StrECAL , for COMET Phase-I



an apparatus to search for μ -e conversion at Phase-I

one detector at a time

Cylindrical Drift Chamber

Muon Stopping Target

Trigger Hodoscope

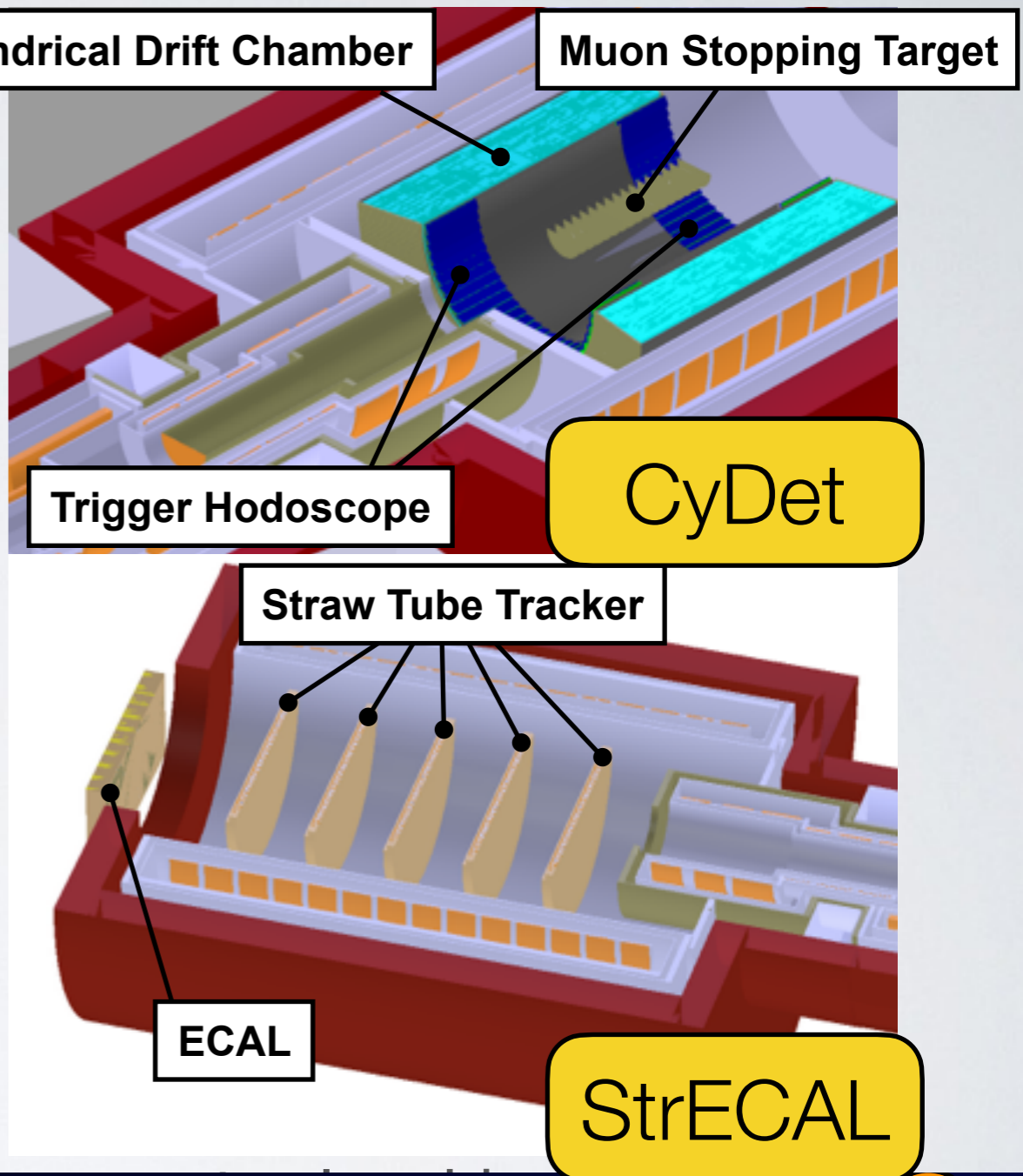
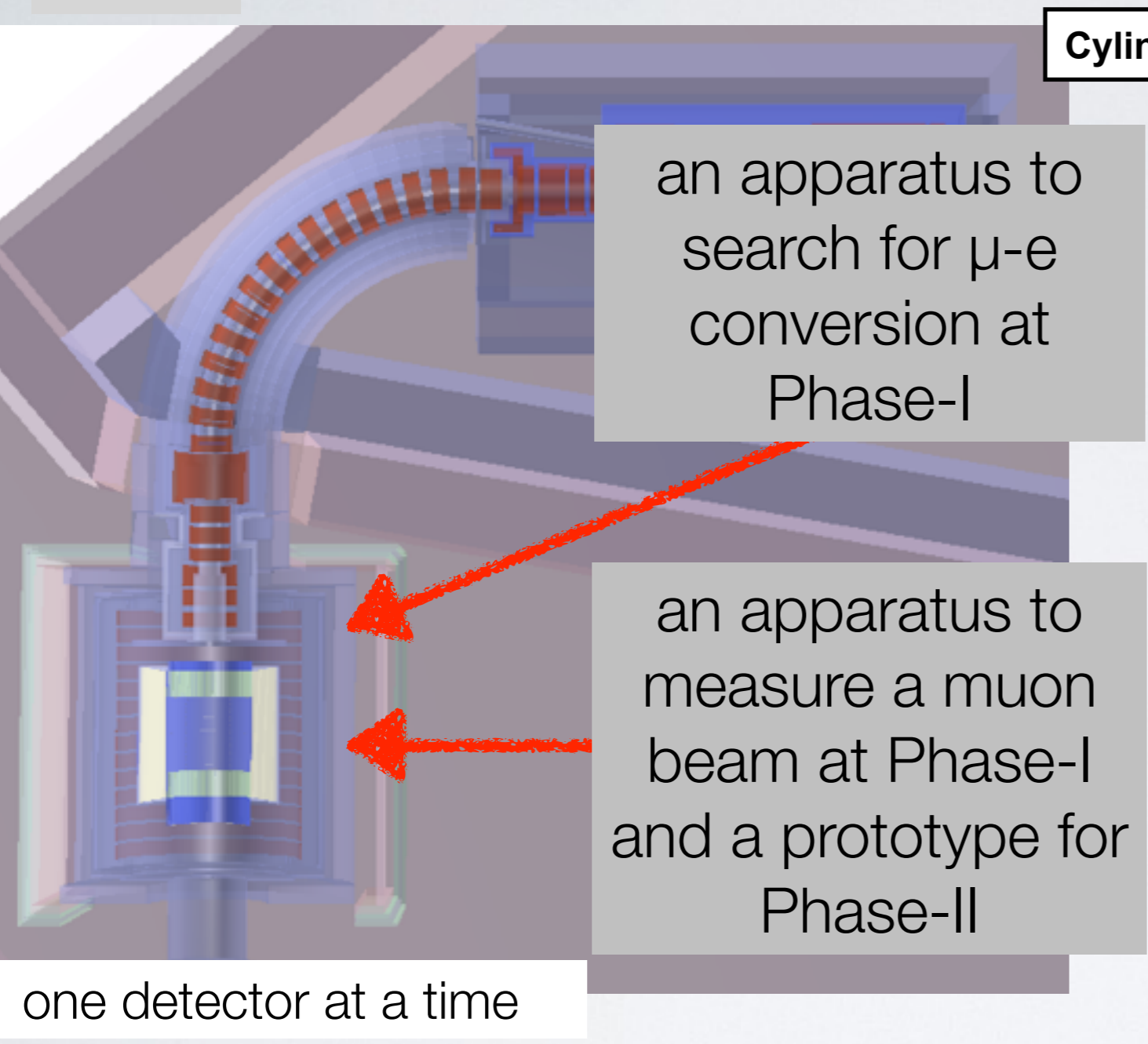
CyDet

Straw Tube Tracker

ECAL

StrECAL

Two Detectors, CyDet and StrECAL , for COMET Phase-I

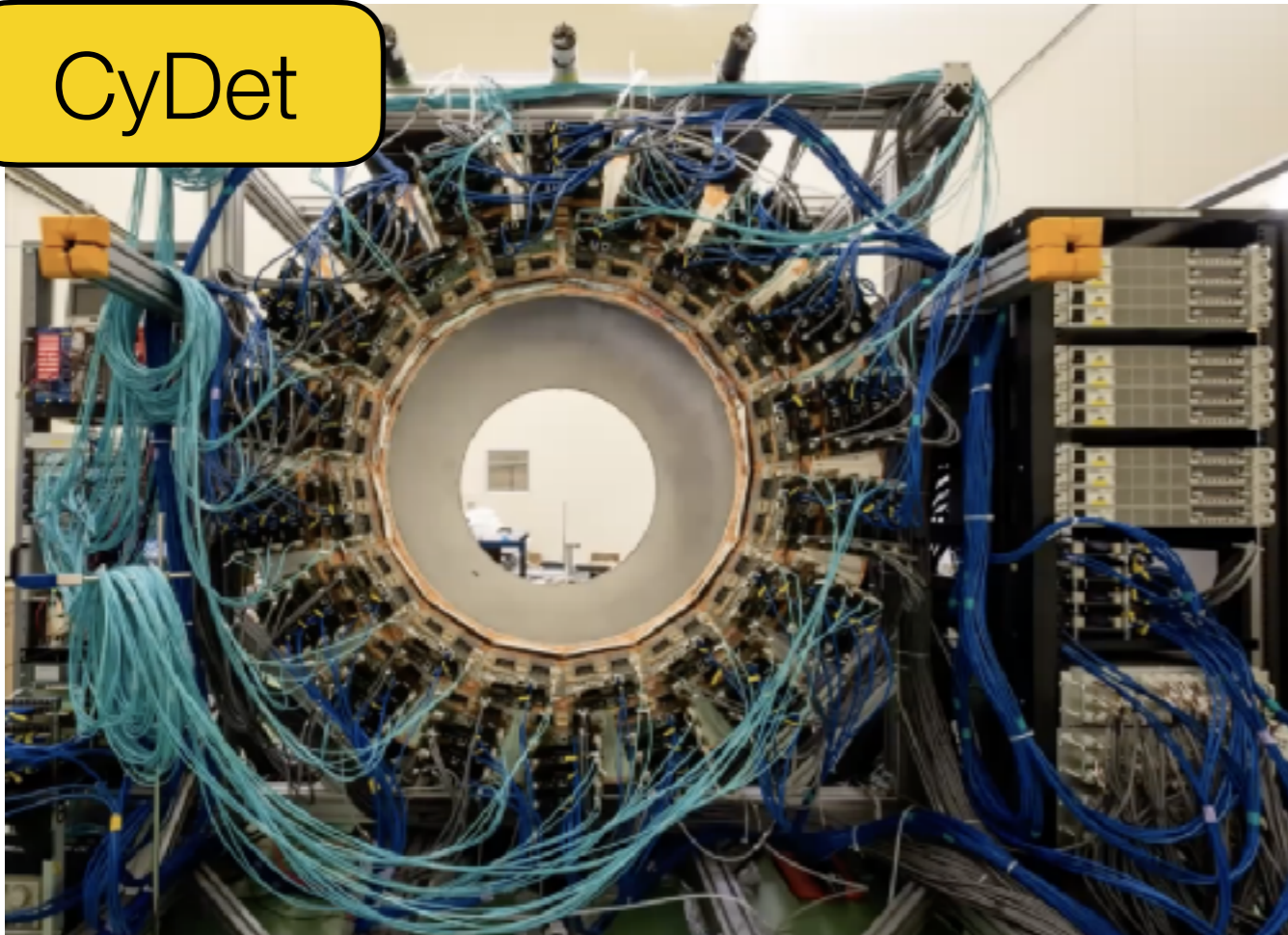




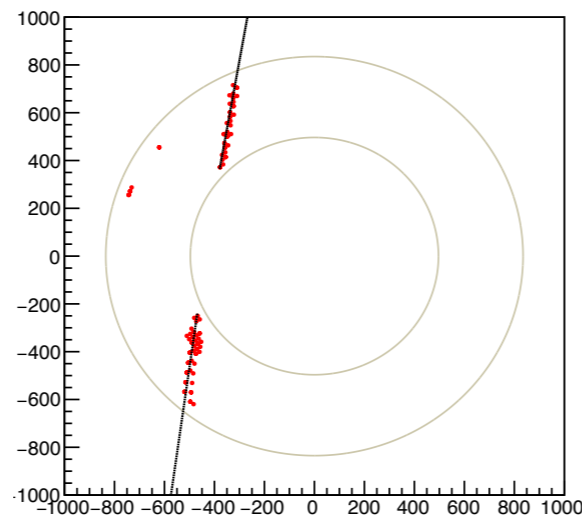
Construction of CyDet and StrECAL

Construction of CyDet and StrECAL

CyDet

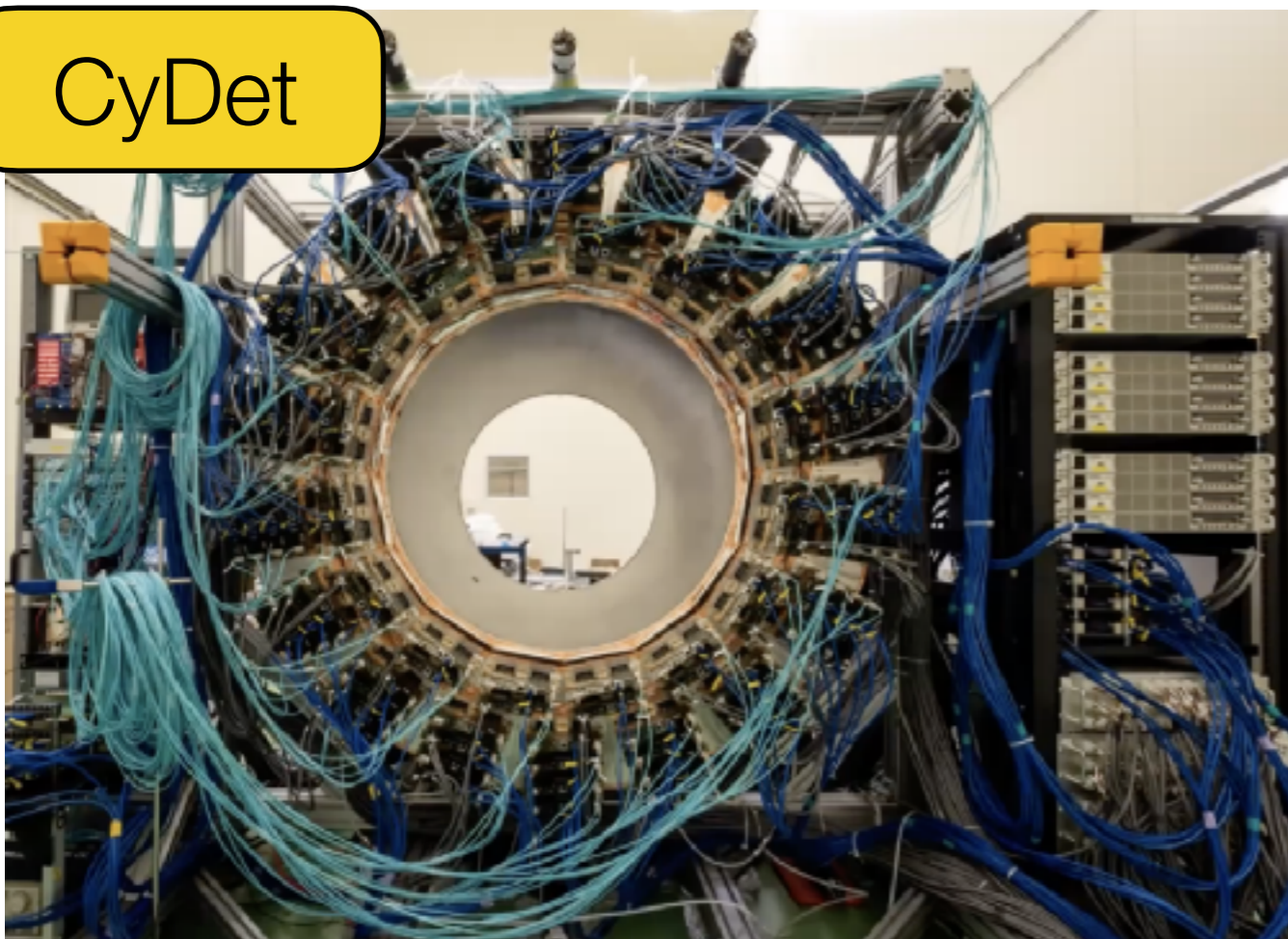


- CDC constructed at Osaka University.
- CDC readouts constructed at IHEP, China.



Construction of CyDet and StrECAL

CyDet

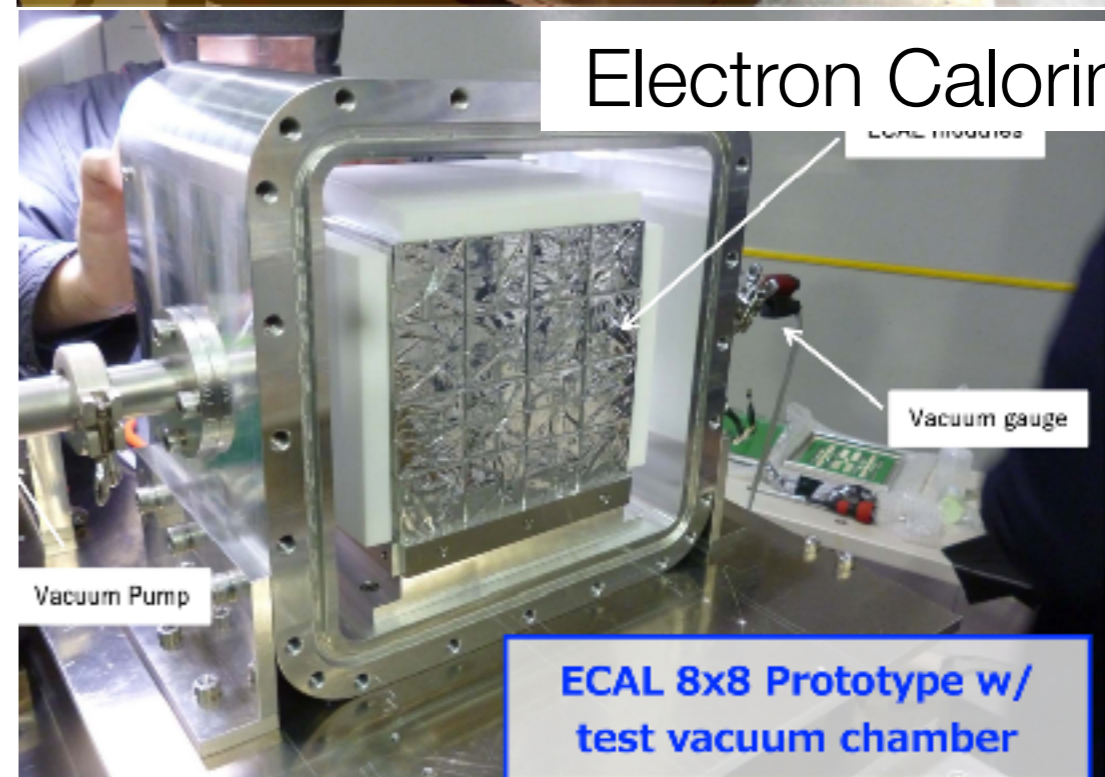


StrECAL

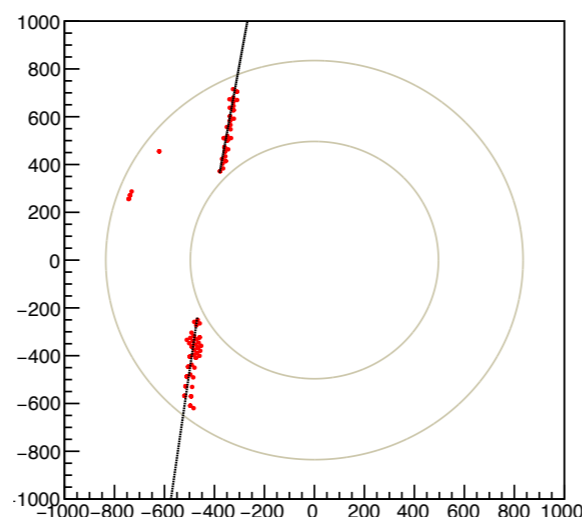


straw chamber

Electron Calorimeter



- CDC constructed at Osaka University.
- CDC readouts constructed at IHEP, China.



COMET Phase- α (Engineering Run)

COMET Phase α (2023)

Proton Beam Area



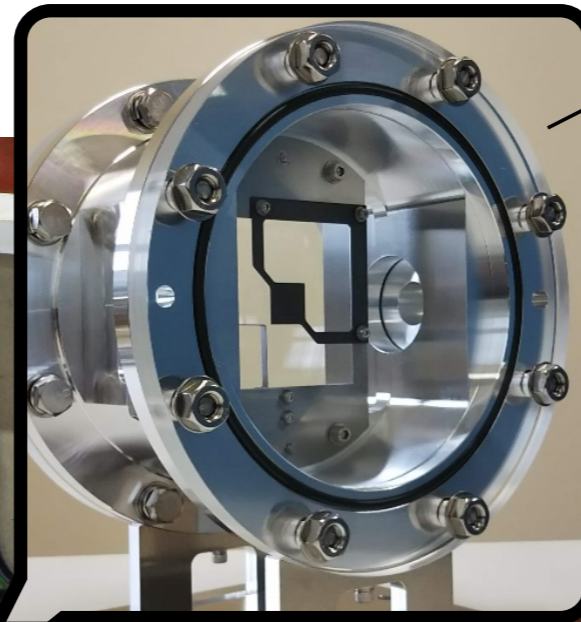
COMET Phase α (2023)

Proton Beam Area

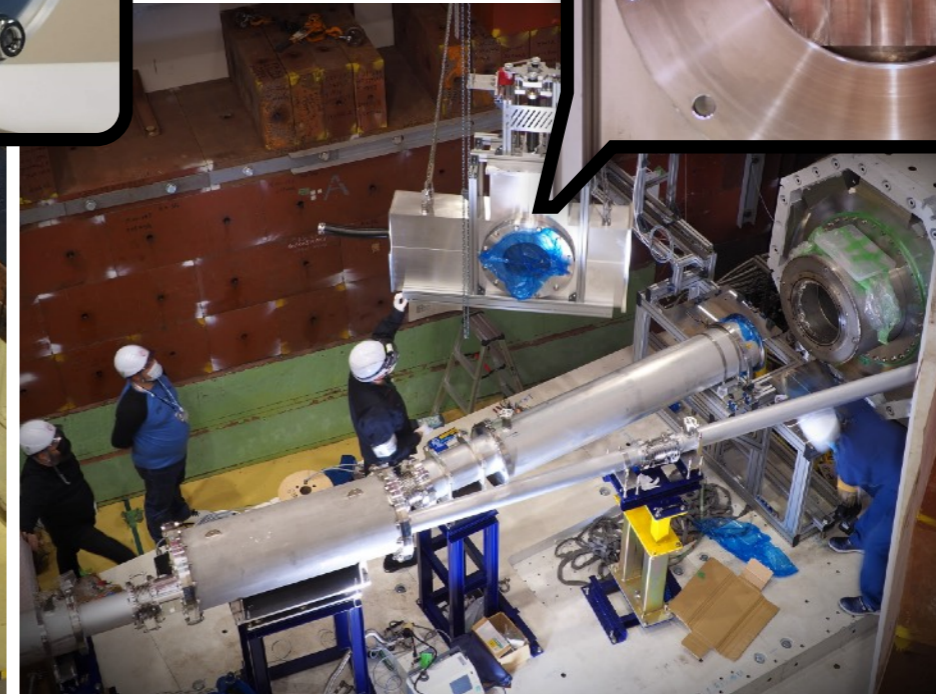
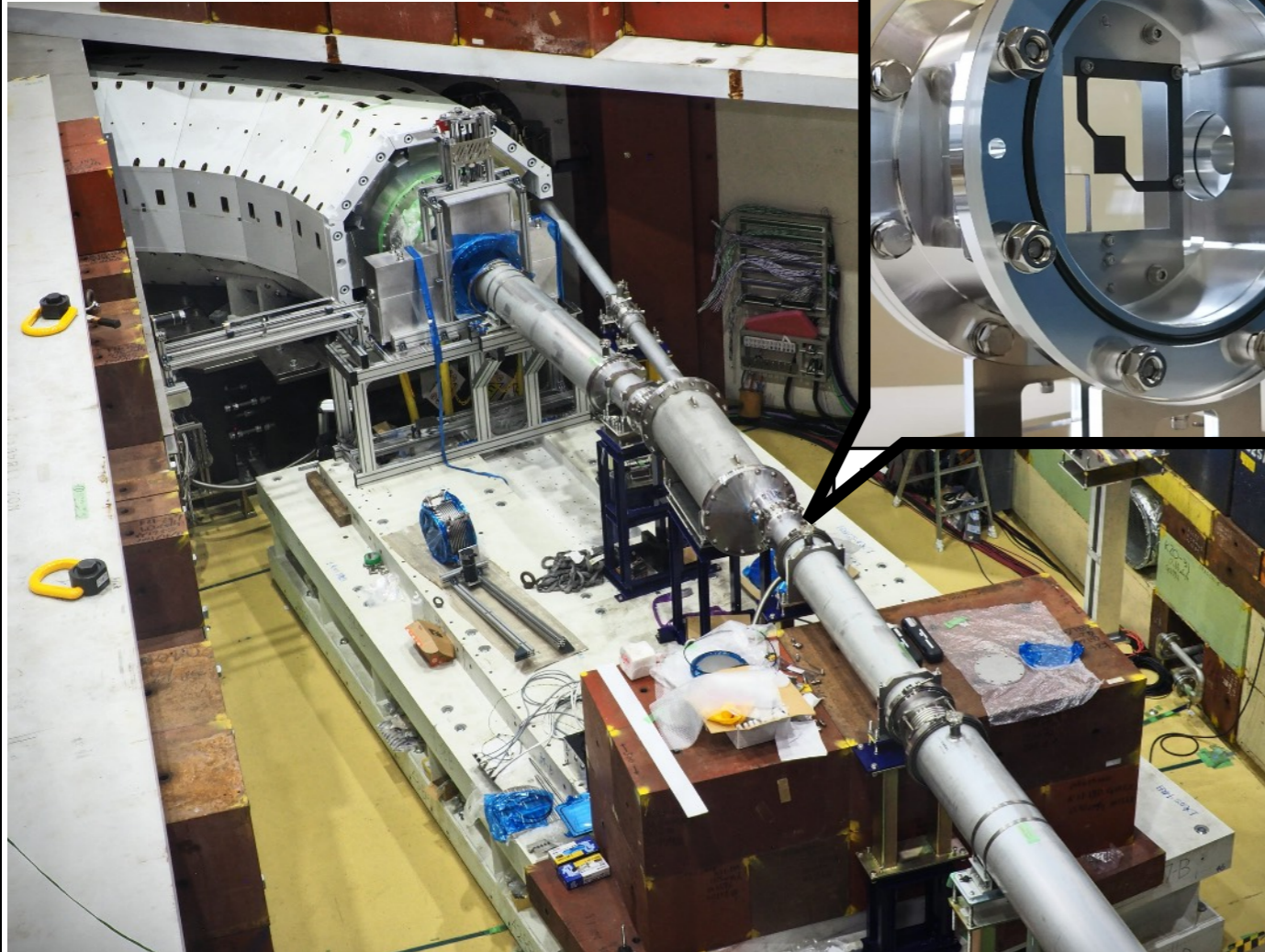
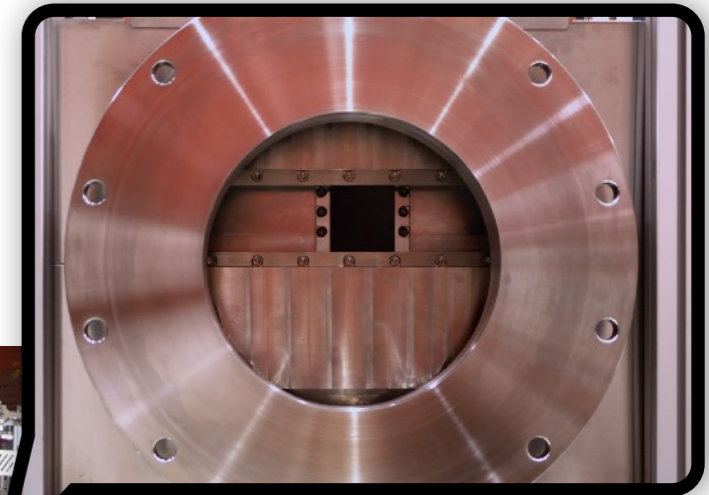


Beam commissioning: 0.26 kW beam power
Proton bunch time structure was the same as
COMET Phase-I.

1mm thick graphite target



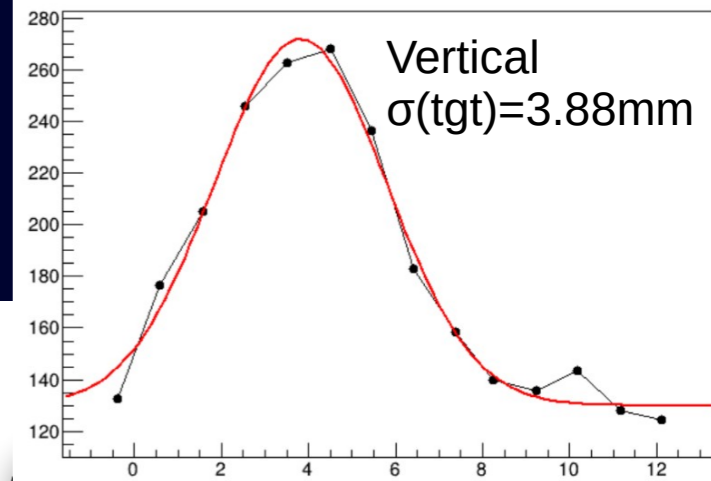
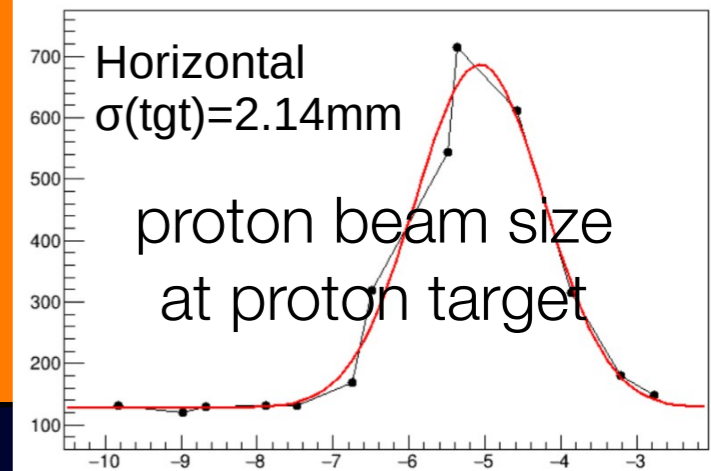
beam scanning slit



COMET Phase α (2023)

Proton Beam Area

Beam commissioning: **0.26 kW** beam power
Proton bunch time structure was the same as
COMET Phase-I.



1mm thick graphite target



COMET Phase α (2023)

Experimental Area



- Muon range distribution
- Beam time distribution
- Beam intensity distribution
- Beam xy distribution

Transport Solenoid Exit

Straw Tube Tracker

Muon Beam Monitor

Range Counter

K500 48.6MM X 2.4MM X 2,000MM

NBBOY12

COMET Phase α (2023)

First Muon Beam at COMET !



COMET Phase α (2023)

First Muon Beam at COMET !



Observation of the first muon beam on February 11th, 2023



COMET Phase α (2023)

First Muon Beam at COMET !



Observation of the first muon beam on February 11th, 2023

Upcoming schedule:

The engineering run is expected to start with a reduced beam intensity in late 2026 (or 2027), and gradually ramping up to its designed intensity thereafter.



Related Rare Physics Phenomena



$\mu^- \rightarrow e^+$ conversion in muonic atom

$\mu^- \rightarrow e^+$ conversion in muonic atom



$\mu^- \rightarrow e^+$ conversion in muonic atom



- Lepton number violation (LNV) and CLFV
- Sensitive to short ranged TeV LNV Physics

$\mu^- \rightarrow e^+$ conversion in muonic atom



- Lepton number violation (LNV) and CLFV
- Sensitive to short ranged TeV LNV Physics

Event Signature :

a single mono-energetic positron
(when the final nucleus is the ground state.)

$\mu^- \rightarrow e^+$ conversion in muonic atom



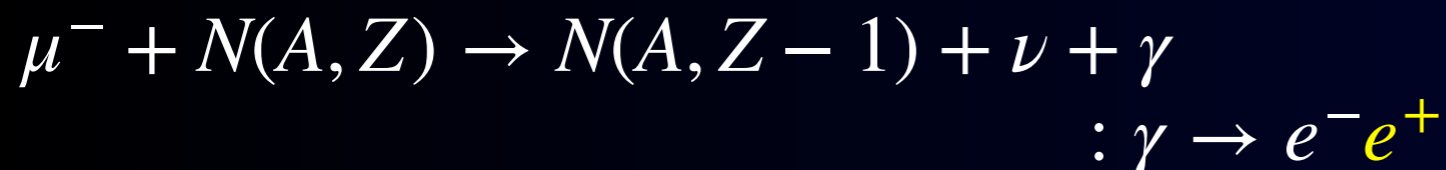
- Lepton number violation (LNV) and CLFV
- Sensitive to short ranged TeV LNV Physics

Event Signature :

a single mono-energetic positron (when the final nucleus is the ground state.)

Backgrounds:

radiative muon nuclear capture (RMC)



$\mu^- \rightarrow e^+$ conversion in muonic atom



- Lepton number violation (LNV) and CLFV
- Sensitive to short ranged TeV LNV Physics

Current limits

$$\mu^- + \text{Ti} \rightarrow e^+ + \text{Ca}(\text{gs}) \leq 1.7 \times 10^{-12}$$

$$\mu^- + \text{Ti} \rightarrow e^+ + \text{Ca}(\text{ex}) \leq 3.6 \times 10^{-11}$$

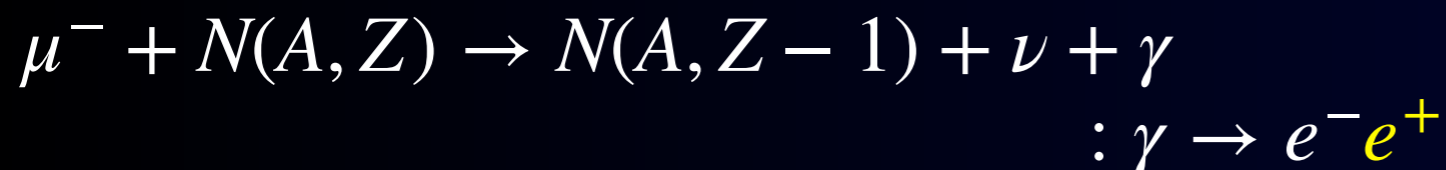
J. Kaulard et al. (SINDRUM-II), Phys. Lett. B422 (1998) 334

Event Signature :

a single mono-energetic positron (when the final nucleus is the ground state.)

Backgrounds:

radiative muon nuclear capture (RMC)



$\mu^- \rightarrow e^+$ conversion in muonic atom



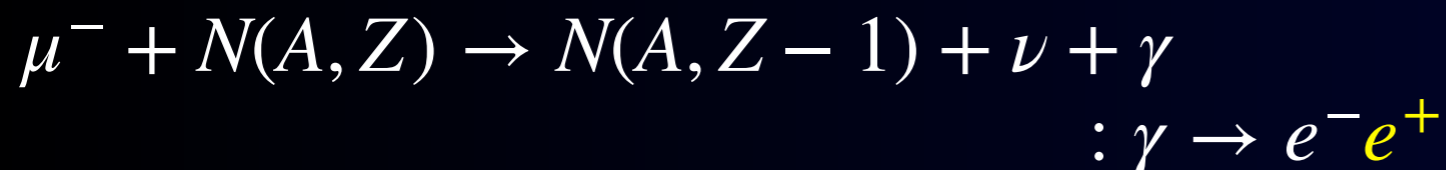
- Lepton number violation (LNV) and CLFV
- Sensitive to short ranged TeV LNV Physics

Event Signature :

a single mono-energetic positron (when the final nucleus is the ground state.)

Backgrounds:

radiative muon nuclear capture (RMC)



Current limits

$$\mu^- + \text{Ti} \rightarrow e^+ + \text{Ca}(\text{gs}) \leq 1.7 \times 10^{-12}$$

$$\mu^- + \text{Ti} \rightarrow e^+ + \text{Ca}(\text{ex}) \leq 3.6 \times 10^{-11}$$

J. Kaulard et al. (SINDRUM-II), Phys. Lett. B422 (1998) 334

COMET sensitivity

- Similar sensitivity to $\mu^- \rightarrow e^-$ conversion.

T.S. Wong, Ph.D. thesis (Osaka Univ.), 2020

$\mu^- \rightarrow e^+$ conversion in muonic atom



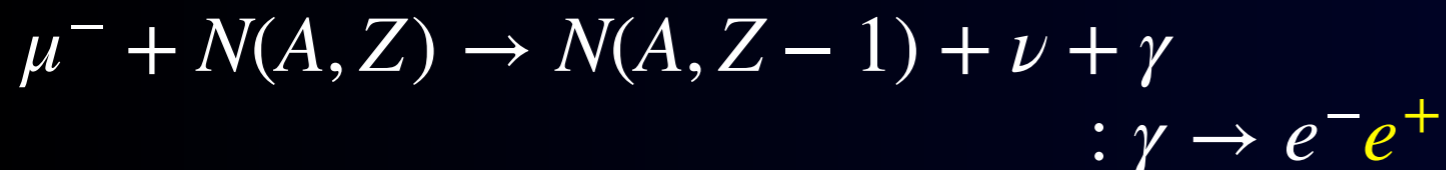
- Lepton number violation (LNV) and CLFV
- Sensitive to short ranged TeV LNV Physics

Event Signature :

a single mono-energetic positron (when the final nucleus is the ground state.)

Backgrounds:

radiative muon nuclear capture (RMC)



Current limits

$$\mu^- + \text{Ti} \rightarrow e^+ + \text{Ca}(\text{gs}) \leq 1.7 \times 10^{-12}$$

$$\mu^- + \text{Ti} \rightarrow e^+ + \text{Ca}(\text{ex}) \leq 3.6 \times 10^{-11}$$

J. Kaulard et al. (SINDRUM-II), Phys. Lett. B422 (1998) 334

COMET sensitivity

- Similar sensitivity to $\mu^- \rightarrow e^-$ conversion.

T.S. Wong, Ph.D. thesis (Osaka Univ.), 2020

- measurement of RMC by CDC

D. Pietres, Ph.D. thesis (Osaka Univ.), 2023

Bound $\mu^- \rightarrow e^- a$
in a muonic atom





Bound $\mu^- \rightarrow e^- a$
in a muonic atom

$$\mu \rightarrow ea$$

a is a light, invisible, neutral particle
with LFV coupling to leptons.

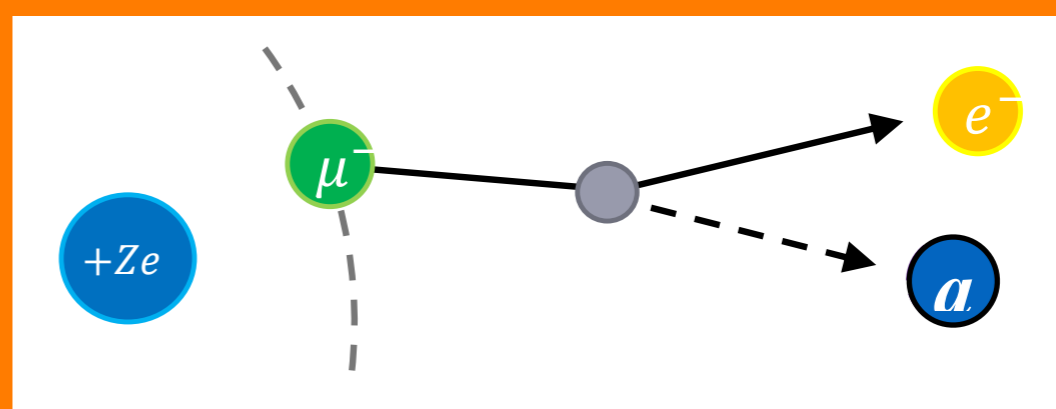
Bound $\mu^- \rightarrow e^- a$
in a muonic atom

$$\mu \rightarrow ea$$

a is a light, invisible, neutral particle
with LFV coupling to leptons.

$$\text{Bound } \mu^- \rightarrow e^- a$$

Bound $\mu^- \rightarrow e^- a$
in a muonic atom

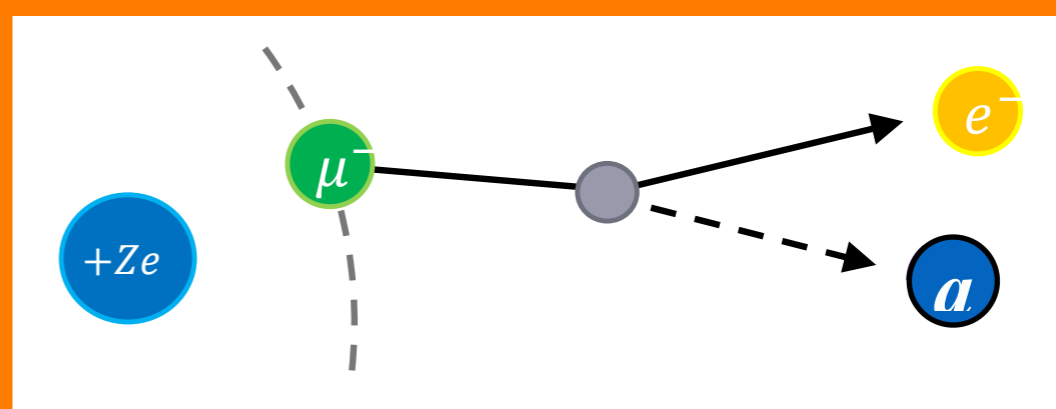


$$\mu \rightarrow ea$$

a is a light, invisible, neutral particle
with LFV coupling to leptons.

$$\text{Bound } \mu^- \rightarrow e^- a$$

Bound $\mu^- \rightarrow e^- a$ in a muonic atom



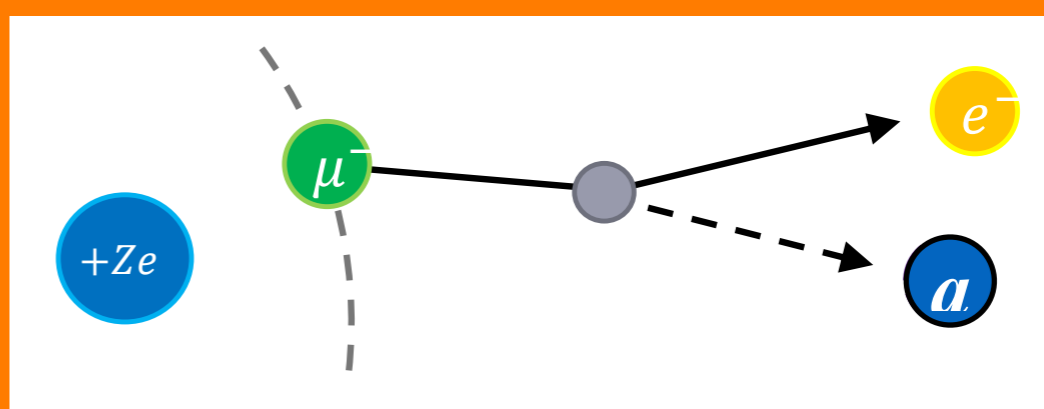
$$\mu \rightarrow ea$$

a is a light, invisible, neutral particle with LFV coupling to leptons.

$$\text{Bound } \mu^- \rightarrow e^- a$$

- Advantage
 - sensitive to even $m_a \sim 0$
 - different muon targets
- Disadvantage
 - Not mono-energetic.

Bound $\mu^- \rightarrow e^- a$ in a muonic atom



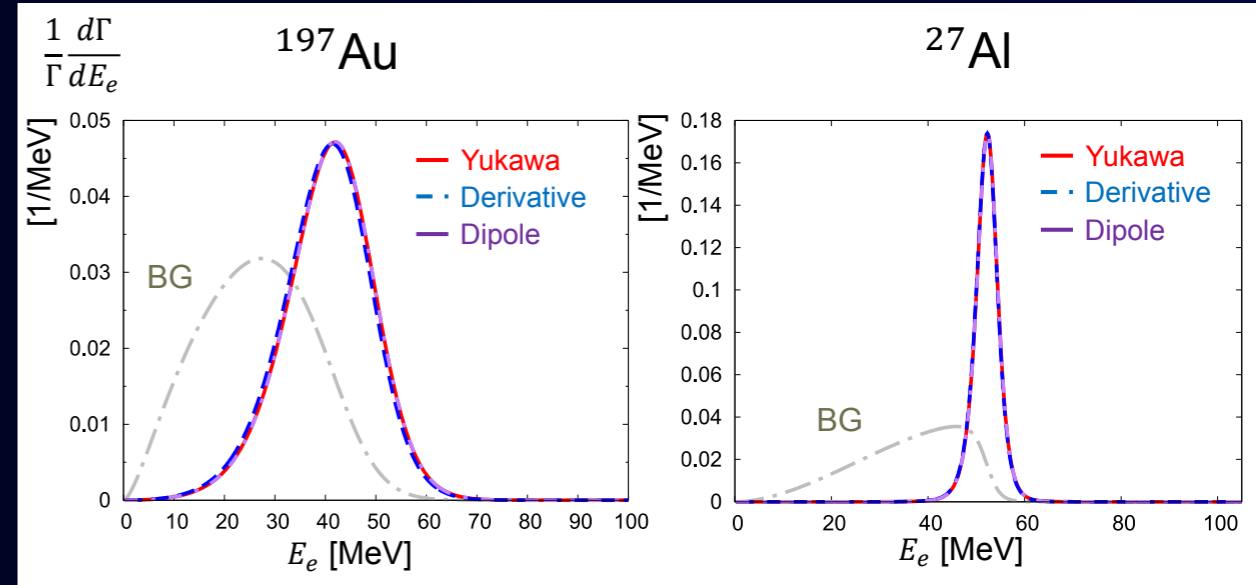
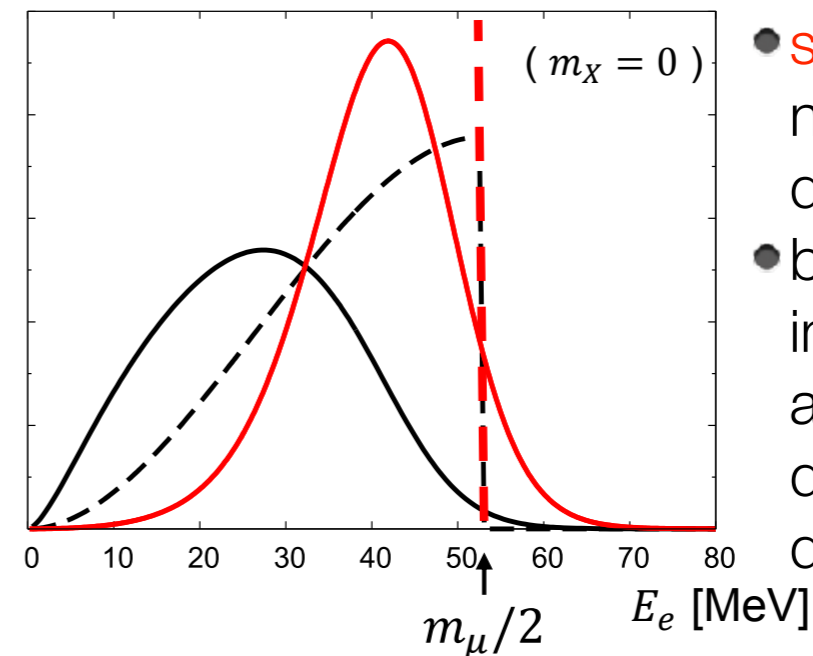
$$\mu \rightarrow ea$$

a is a light, invisible, neutral particle with LFV coupling to leptons.

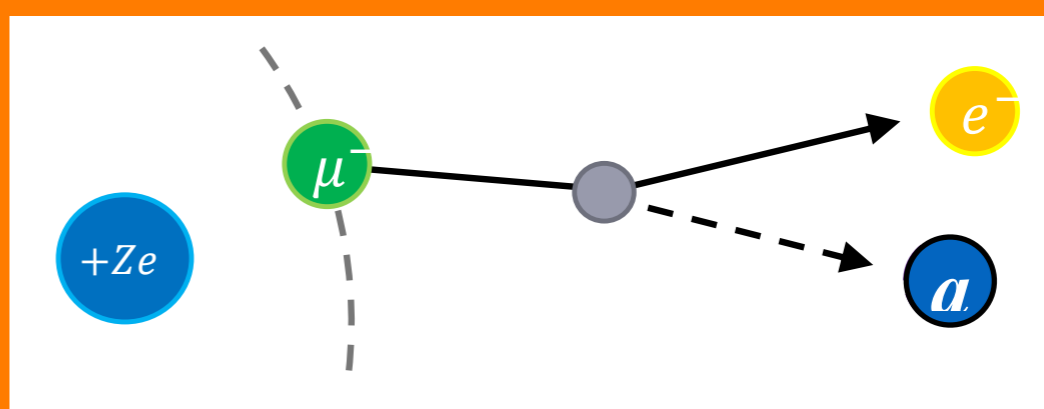
$$\text{Bound } \mu^- \rightarrow e^- a$$

- Advantage
 - sensitive to even $m_a \sim 0$
 - different muon targets
- Disadvantage
 - Not mono-energetic.

electron spectra (normalized by rate)



Bound $\mu^- \rightarrow e^- a$ in a muonic atom



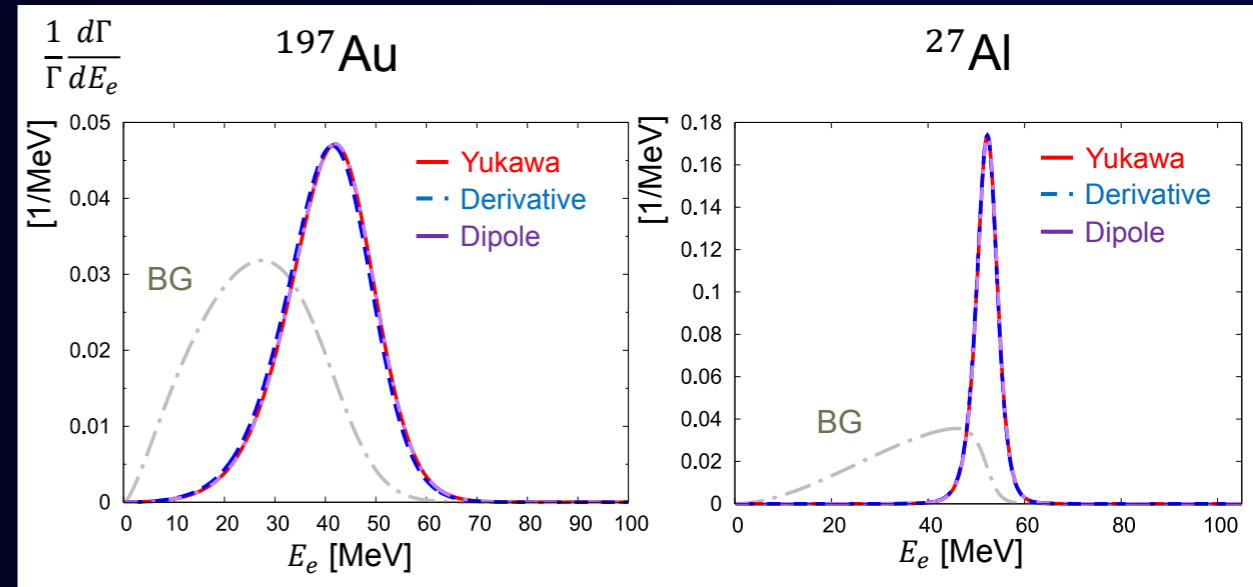
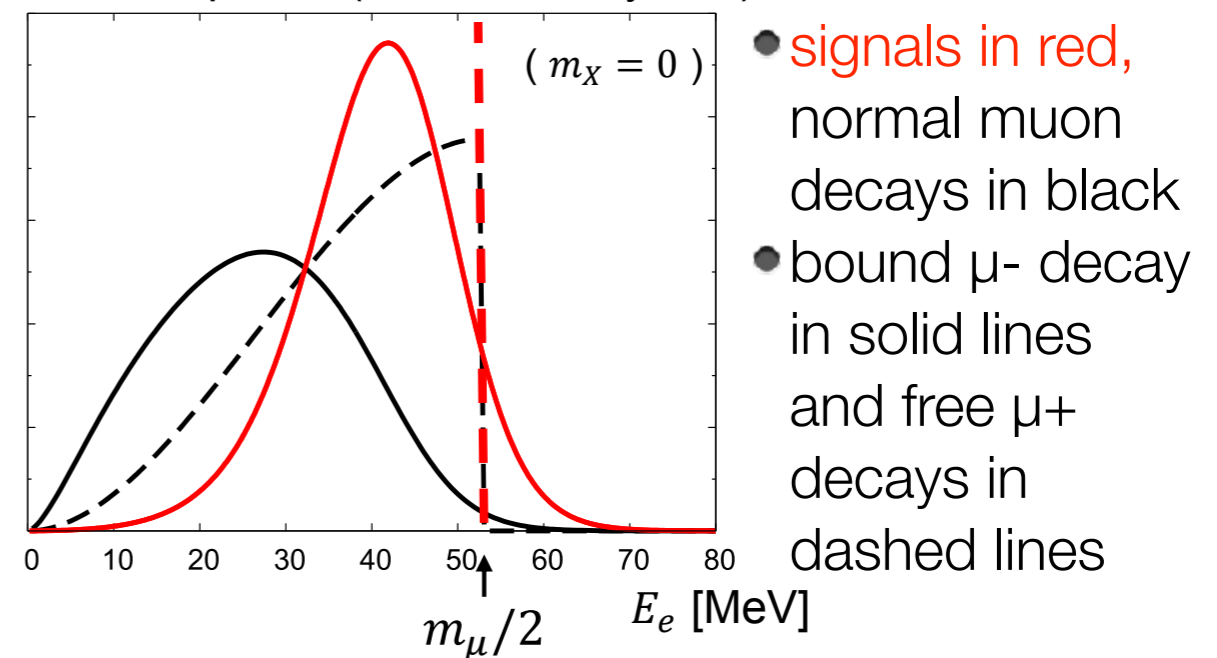
$$\mu \rightarrow ea$$

a is a light, invisible, neutral particle with LFV coupling to leptons.

$$\text{Bound } \mu^- \rightarrow e^- a$$

- Advantage
 - sensitive to even $m_a \sim 0$
 - different muon targets
- Disadvantage
 - Not mono-energetic.
- COMET Phase-II :
 - $B < O(10^{-9})$ $f_a > 10^{10-11}$ GeV

electron spectra (normalized by rate)



PRISM/PRIME

$$B(\mu N \rightarrow e N) \sim 10^{-19}$$

with a factor of 1000,000 improvement

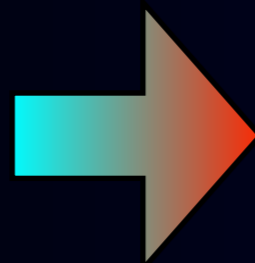
Requirements of Muon Beam for New $\mu \rightarrow e$ Conversion



Requirements of Muon Beam for New $\mu \rightarrow e$ Conversion



No pions



long muon beam-line

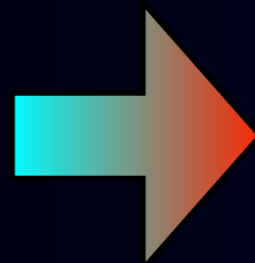
long beam flight
length (~100m)

allowing high-Z muon target

Requirements of Muon Beam for New $\mu \rightarrow e$ Conversion



No pions

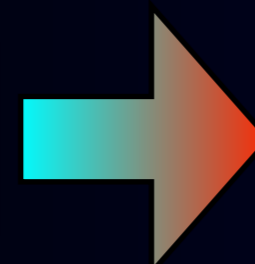


long muon beam-line

long beam flight
length (~100m)

allowing high-Z muon target

Better beam



narrow muon beam
spread

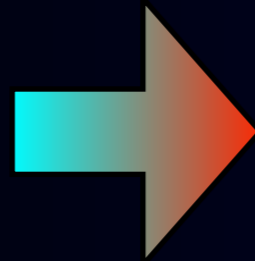
improvement of
resolution of
electron detection

allowing a thinner muon target

Requirements of Muon Beam for New $\mu \rightarrow e$ Conversion



No pions

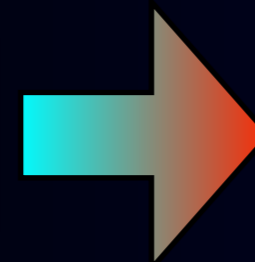


long muon beam-line

long beam flight length (~100m)

allowing high-Z muon target

Better beam

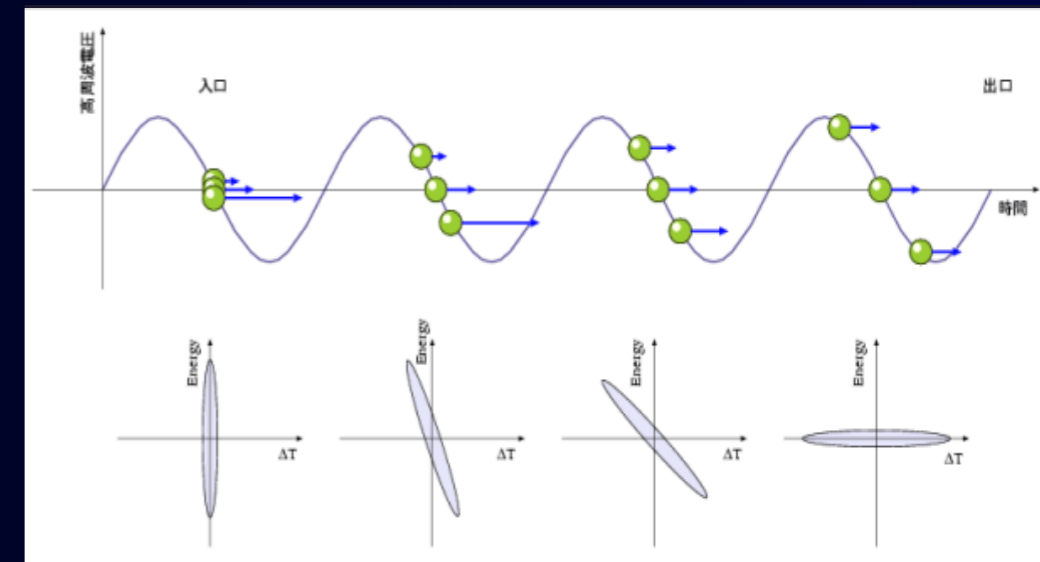
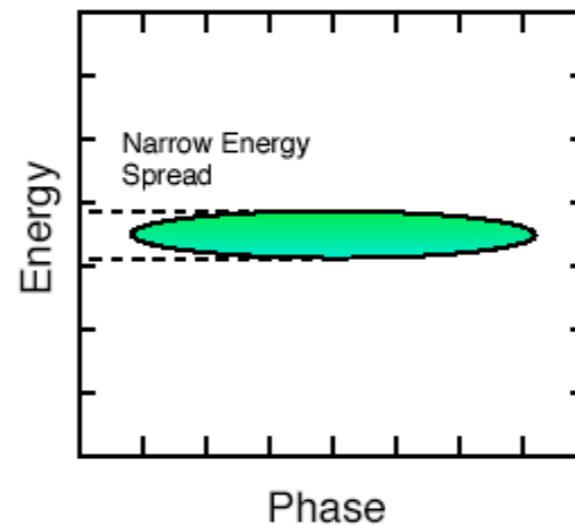
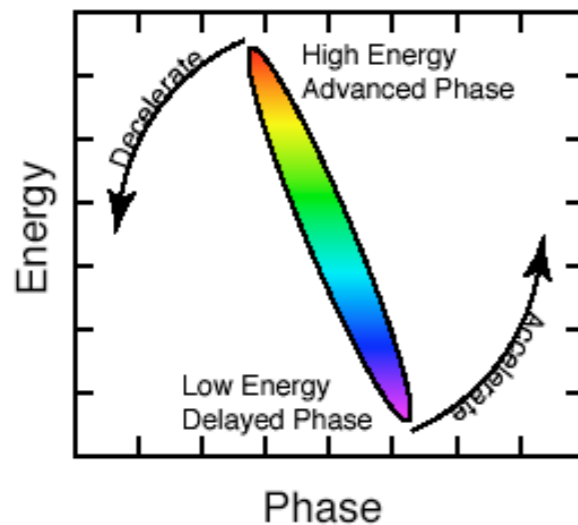


narrow muon beam spread

improvement of resolution of electron detection

allowing a thinner muon target

Phase rotation



PRISM/PRIME (2003)



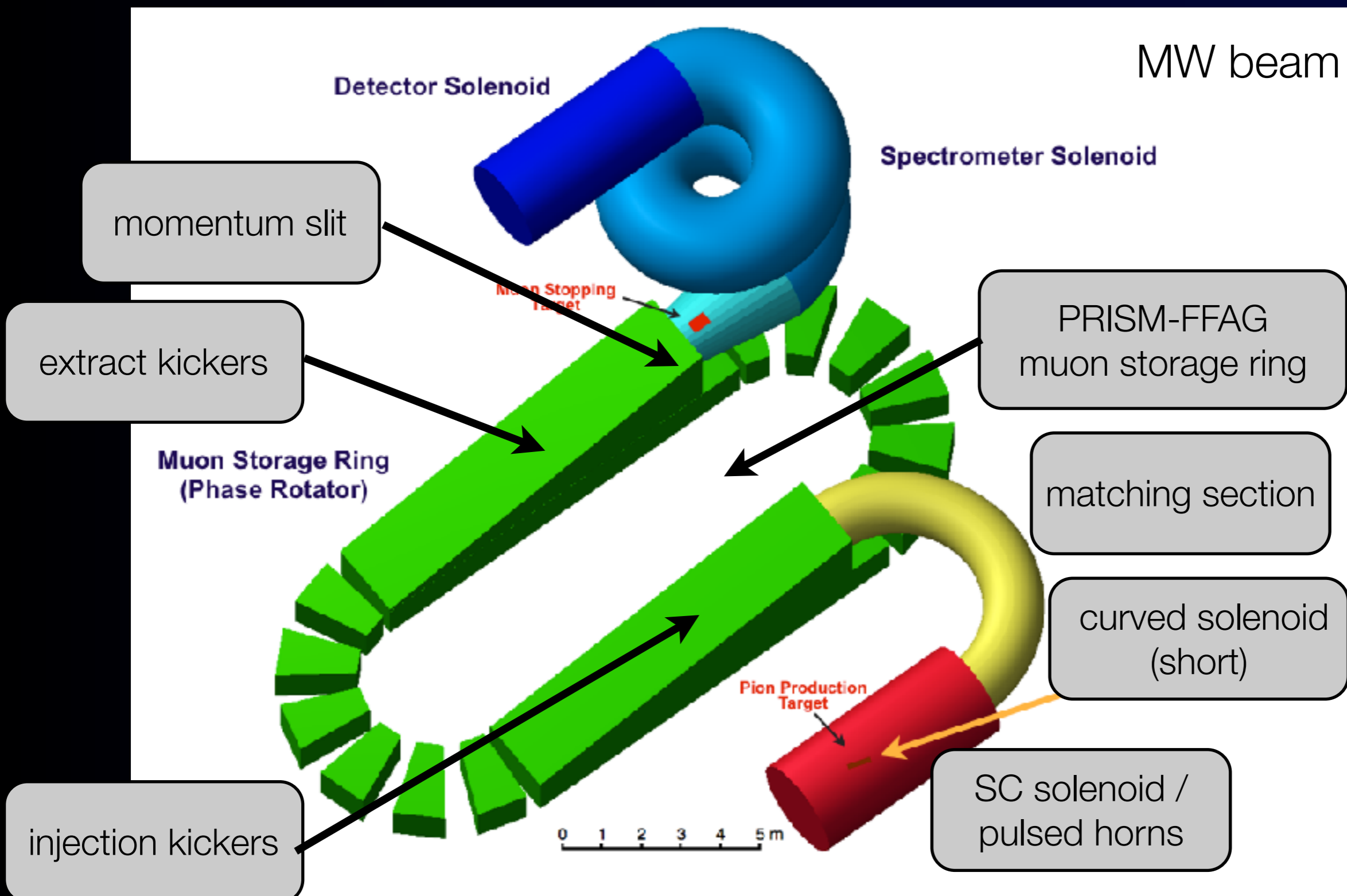
PRISM=Phase Rotated Intense Slow Muon source

PRISM/PRIME (2003)

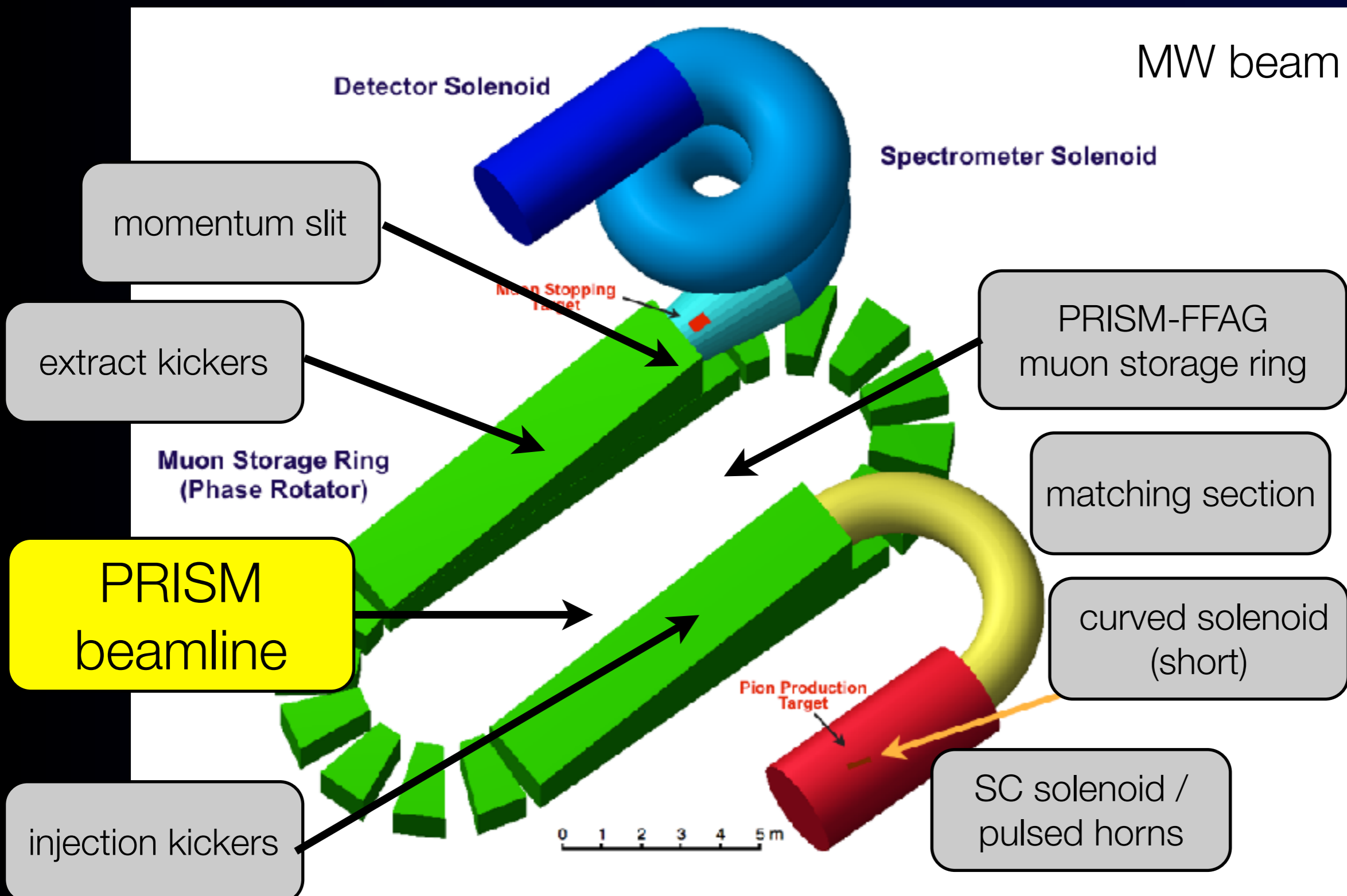


PRISM=Phase Rotated Intense Slow Muon source

PRISM/PRIME (2003)

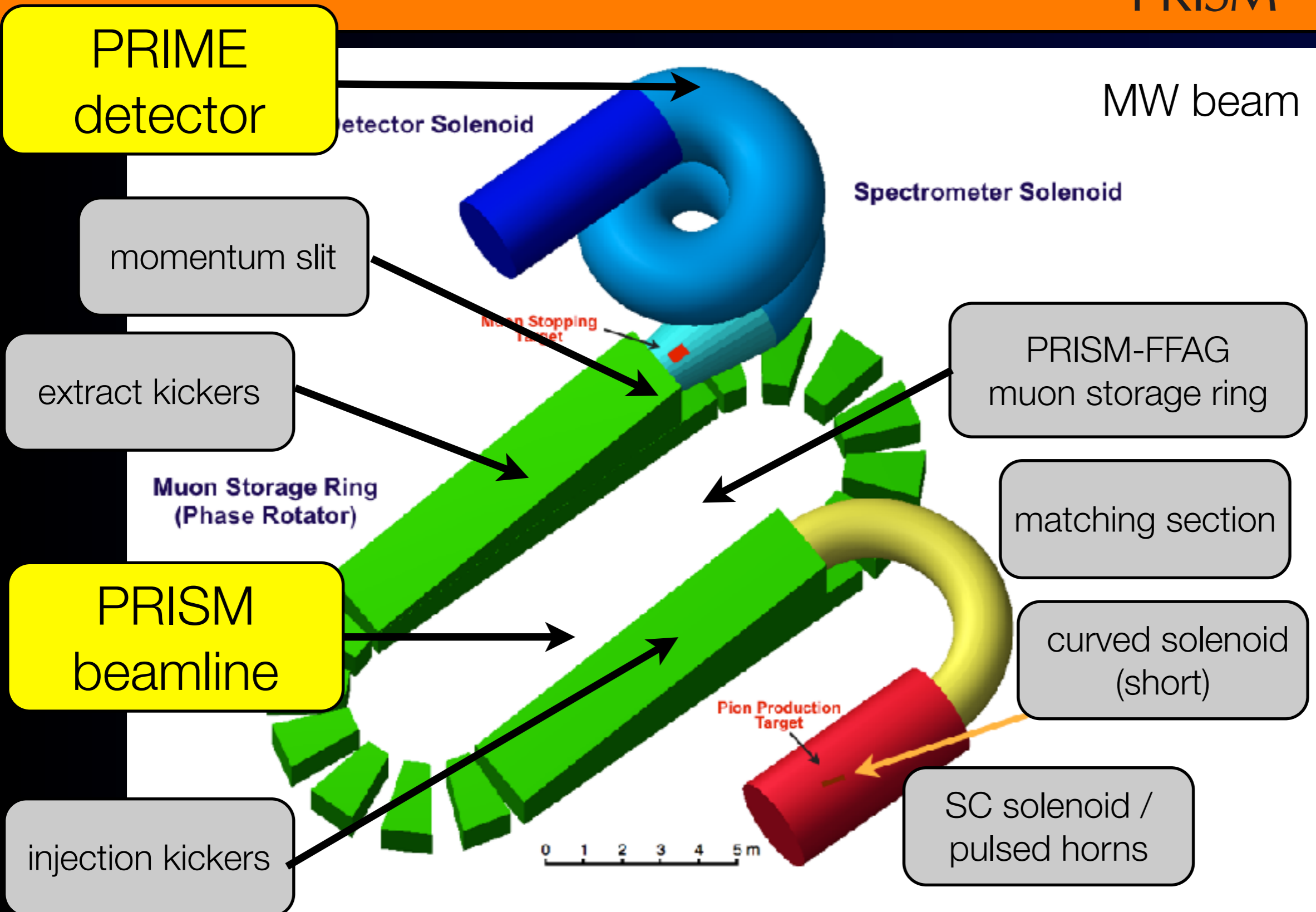


PRISM/PRIME (2003)



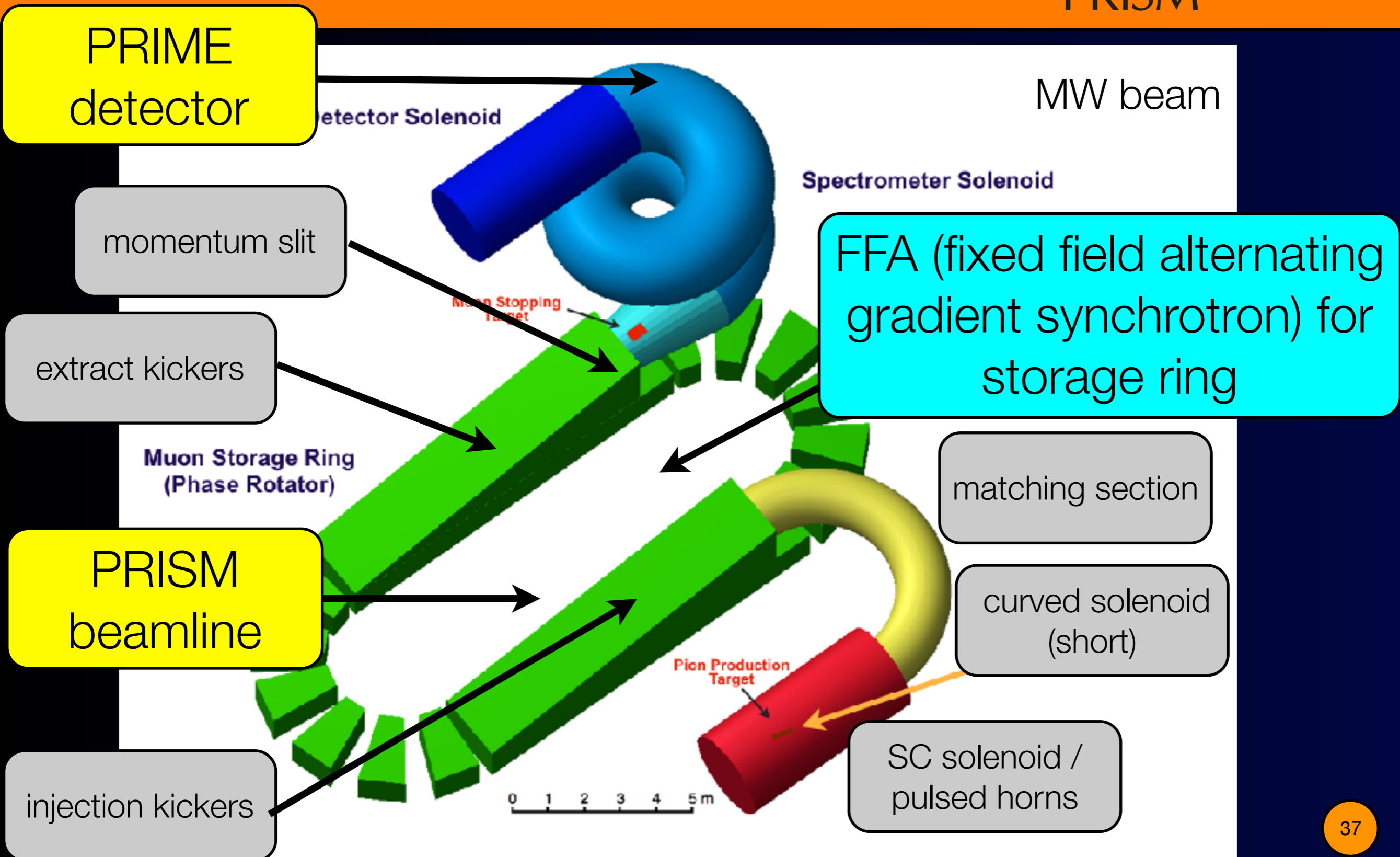


PRISM/PRIME (2003)





PRISM/PRIME (2003)



PRIME detector

momentum slit

extract kickers

PRISM beamline

injection kickers

FFA (fixed field alternating gradient synchrotron) for storage ring

matching section

curved solenoid (short)

SC solenoid / pulsed horns

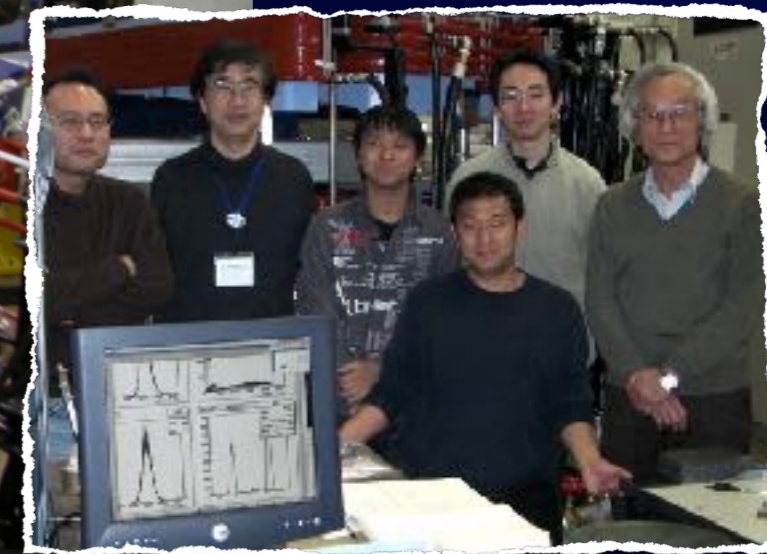
PRISM FFA Phase Rotation at Osaka University (2003 - 2007)



PRISM-FFAG (6 sectors) in RCNP, Osaka

Phase rotation at the PRISM FFA ring with α rays
successfully demonstrated at Osaka University (2007)

PRISM FFA Phase Rotation at Osaka University (2003 - 2007)

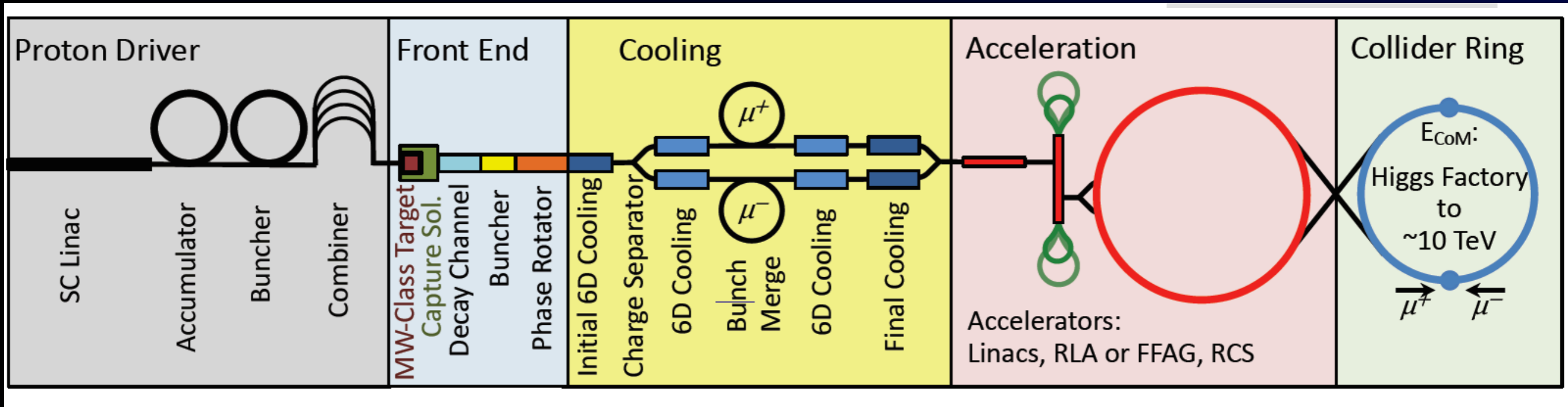


T. Nakanishi, Ms.thesis (2008)

Phase rotation at the PRISM FFA ring with α rays successfully demonstrated at Osaka University (2007)

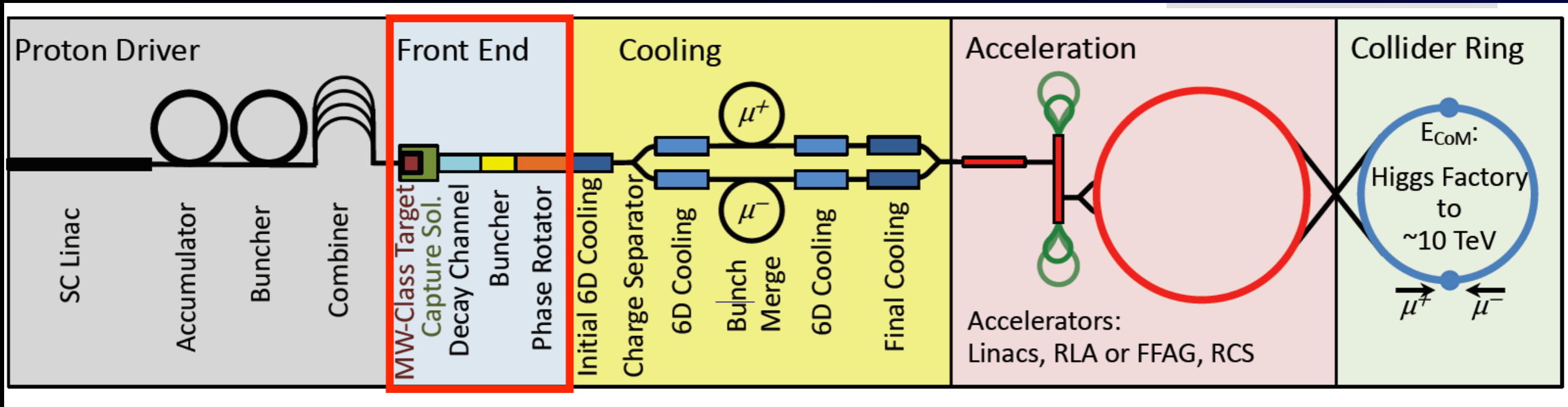
Synergy with Muon Collider R&D

Muon Acceleration Program (US)



Synergy with Muon Collider R&D

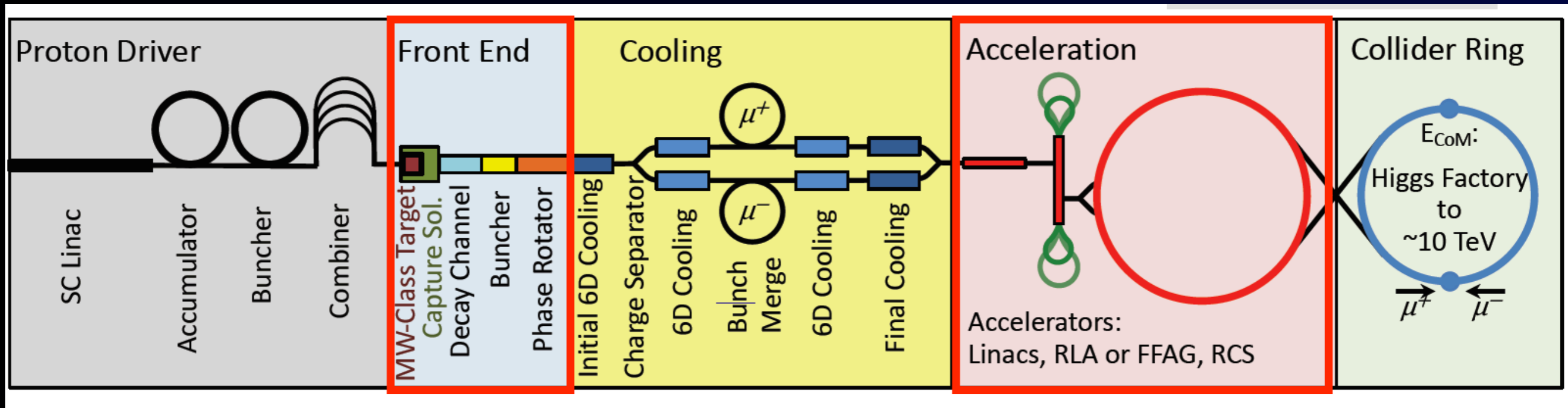
Muon Acceleration Program (US)



Pion capture solenoids
Phase Rotator

Synergy with Muon Collider R&D

Muon Acceleration Program (US)

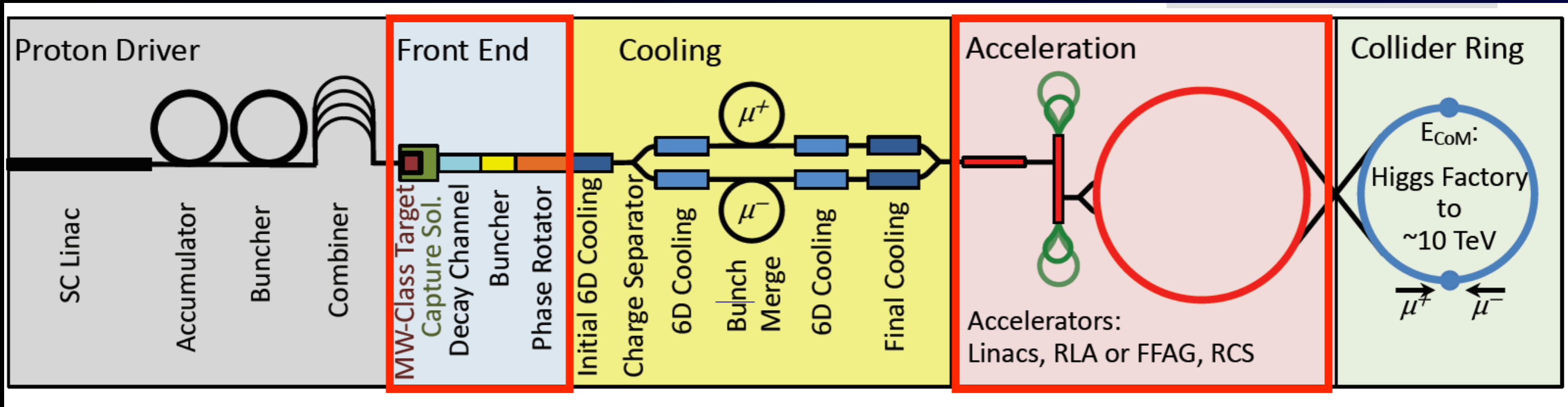


Pion capture solenoids
Phase Rotator

FFA accelerator
(at arc)

Synergy with Muon Collider R&D

Muon Acceleration Program (US)



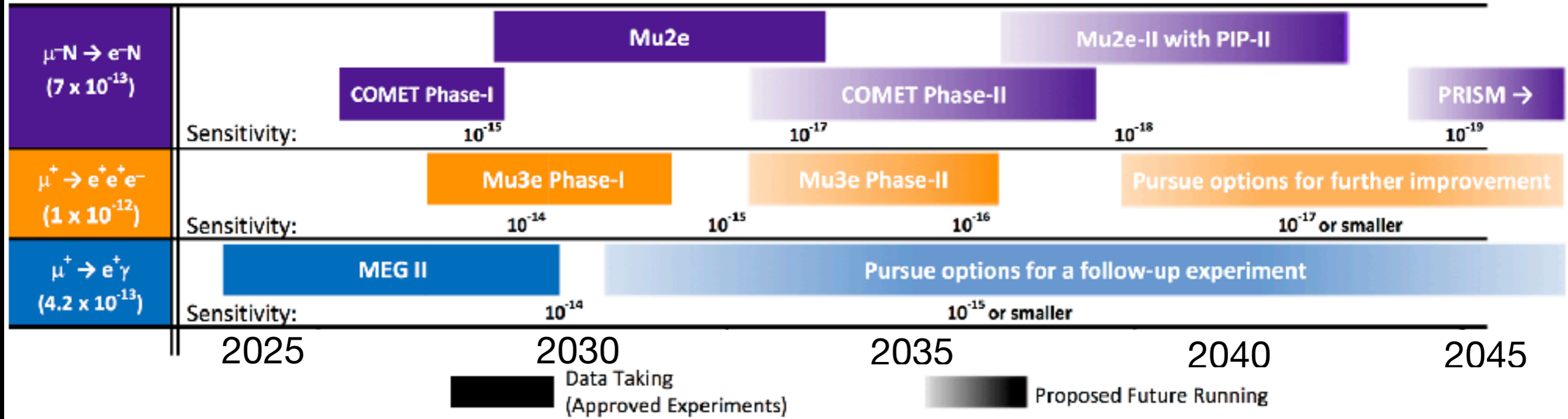
Pion capture solenoids
Phase Rotator

FFA accelerator
(at arc)

Developments of Highly intense muon sources would have strong synergy with muon collider R&D

“My” Wishful Timeline of Muon CLFV

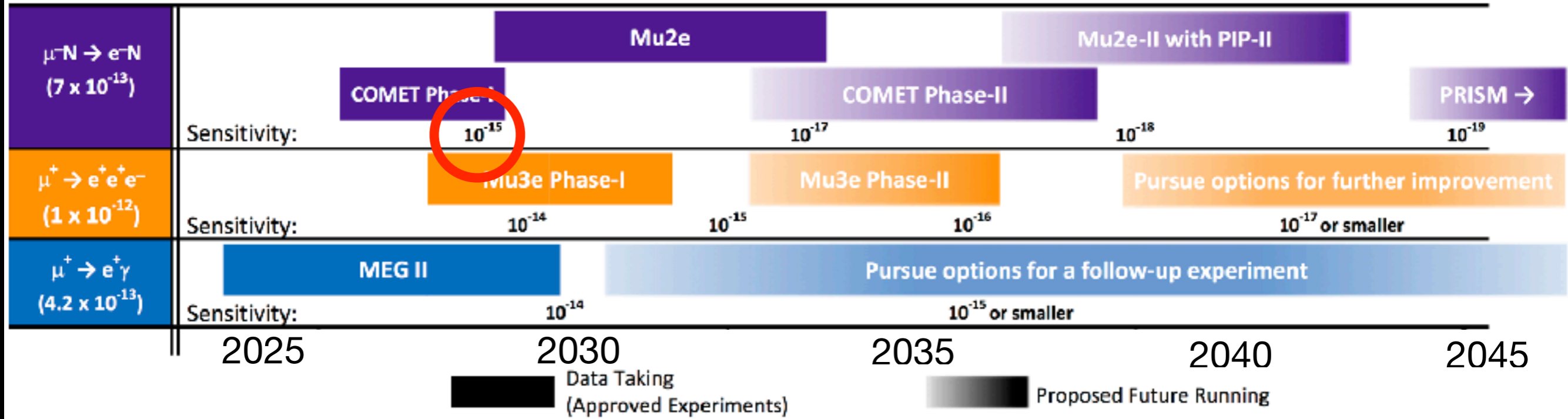
Searches for Charged-Lepton Flavor Violation in Experiments using Intense Muon Beams





“My” Wishful Timeline of Muon CLFV

Searches for Charged-Lepton Flavor Violation in Experiments using Intense Muon Beams

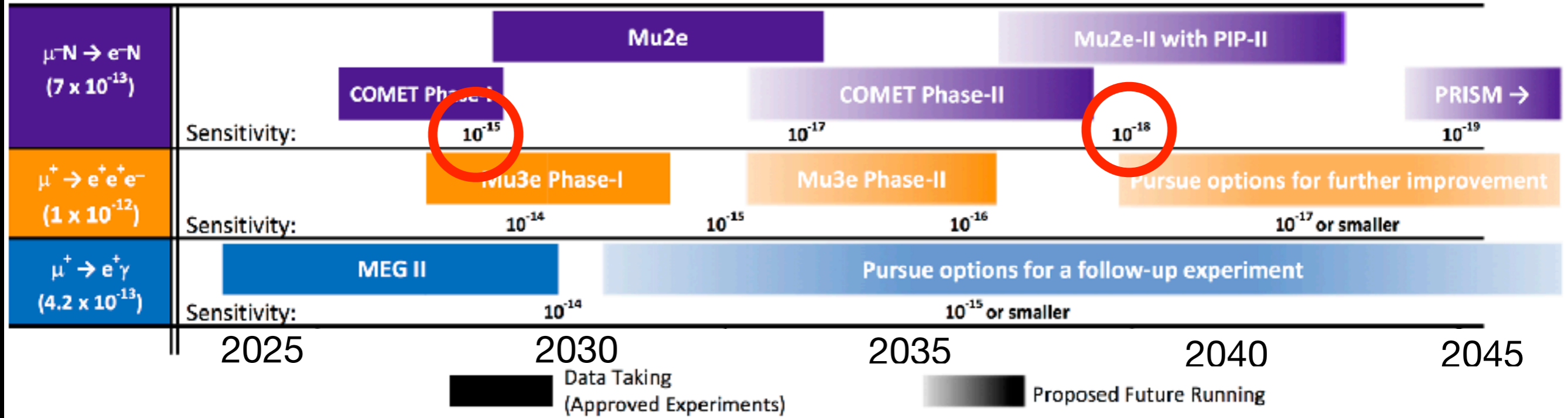


COMET Phase-I
× 100



“My” Wishful Timeline of Muon CLFV

Searches for Charged-Lepton Flavor Violation in Experiments using Intense Muon Beams



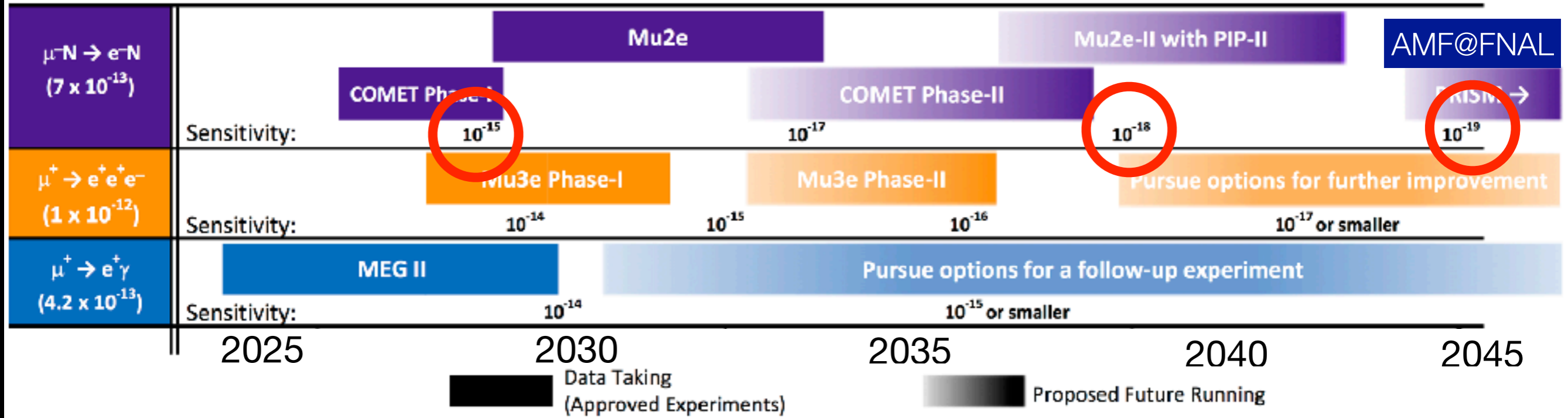
COMET Phase-I
× 100

COMET Phase-II
× 10,000
– × 100,000



“My” Wishful Timeline of Muon CLFV

Searches for Charged-Lepton Flavor Violation in Experiments using Intense Muon Beams



COMET Phase-I
× 100

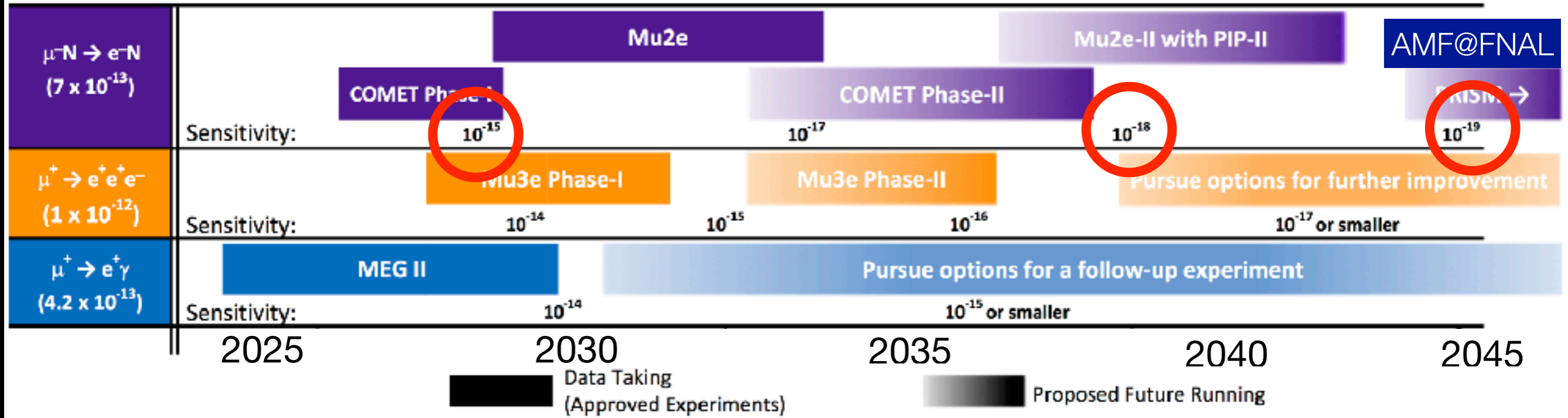
COMET Phase-II
× 10,000
– × 100,000

PRISM
× 1,000,000



“My” Wishful Timeline of Muon CLFV

Searches for Charged-Lepton Flavor Violation in Experiments using Intense Muon Beams



COMET Phase-I
× 100

COMET Phase-II
× 10,000
– × 100,000

PRISM
× 1,000,000

modified from the muon CLFV white paper for the 2020 update of European Strategy of Particle Physics

Summary





Summary

- CLFV serves as a crucial probe to search for BSM.
- $\mu \rightarrow e$ conversion is one of the most important muon CLFV processes.
- The latest experimental developments (like COMET) together with related physics topics are presented, mentioning future technical advancement (PRISM).
- It is hoped that exploration of CLFV will make implications in particle physics.

Summary

- CLFV serves as a crucial probe to search for BSM.
- $\mu \rightarrow e$ conversion is one of the most important muon CLFV processes.
- The latest experimental developments (like COMET) together with related physics topics are presented, mentioning future technical advancement (PRISM).
- It is hoped that exploration of CLFV will make implications in particle physics.



Summary

- CLFV serves as a crucial probe to search for BSM.
- $\mu \rightarrow e$ conversion is one of the most important muon CLFV processes.
- The latest experimental developments (like COMET) together with related physics topics are presented, mentioning future technical advancement (PRISM).
- It is hoped that exploration of CLFV will make implications in particle physics.



Summary

- CLFV serves as a crucial probe to search for BSM.
- $\mu \rightarrow e$ conversion is one of the most important muon CLFV processes.
- The latest experimental developments (like COMET) together with related physics topics are presented, mentioning future technical advancement (PRISM).
- It is hoped that exploration of CLFV will make implications in particle physics.



谢谢



Backup